Seismotectonic Study

for
Soldier Creek Dam,
Central Utah Project, Utah

U. S. DEPARTMENT OF THE INTERIOR
BUREAU OF RECLAMATION
SEISMOTECTONIC SECTION
DENVER, COLORADO

SEISMOTECTONIC STUDY FOR SOLDIER CREEK DAM, CENTRAL UTAH PROJECT

by

Alan R. Nelson
and
Richard A. Martin, Jr.

with assistance from
Edward M. Baltzer

SEISMOTECTONIC REPORT 82-1

Seismotectonic Section
Geologic Services Branch
Division of Geology
Engineering and Research Center
U.S. Bureau of Reclamation
Denver, Colorado

November 1982

Prepared by:

Alan R. Nelson
Geologist

Richard A. Martin, Jr.
Seismologist

Technical approval by:

Dean Ostenaa
Head, Seismotectonic Section

Louis R. Frei
Chief, Geologic Services Branch

Approved by:

Jerry S. Dodd
Chief, Division of Geology

12-14-87.
Date

CONTENTS

	Page
Summary of Conclusions	1
1 Introduction	3
1.1 Purpose and scope	3
1.2 Soldier Creek Dam	4
1.3 Acknowledgments	4
2 Regional geology and tectonics	6
2.1 Post-precambrian depositional history	6
2.2 Sevier Orogeny	6
2.3 Tertiary tectonics	7
2.4 Quaternary tectonics	8
2.4.1 Wasatch fault	9
2.4.2 The back valleys of the Wasatch Mountains	9
2.4.3 Uinta Basin	10
3 Historical seismicity	11
3.1 Regional seismicity	11
3.2 Local seismicity	13
3.2.1 Provo area	16
3.2.2 Heber Valley area	16
3.2.3 Moon Lake area	17
3.2.4 Price area	20
3.2.5 Strawberry Valley area	20
3.3 Focal depths	20
3.4 Focal mechanisms	21
3.5 Earthquake recurrence	21
4 Geology of the Strawberry Valley area	25
4.1 Strawberry and Soldier Creek Valleys	25
4.2 Stratigraphy	25
4.3 Structure	28
4.3.1 Stinking Springs fault	28
4.3.2 Strawberry fault	28
4.3.3 Structural origin of Strawberry Valley	29
4.4 Quaternary Geology	33
4.4.1 Chronology	33
4.4.2 Geomorphology	34
4.4.2.1 Fluvial	35
4.4.2.2 Structural influence on Strawberry River and Indian Creek Valleys	35
4.4.2.3 Pediments	36
4.5 Damsite geology	37
4.5.1 Geomorphology	37
4.5.2 Stratigraphy	37
4.5.3 Structure	38

CONTENTS - Continued

	Page
5 Seismotectonic investigations	40
5.1 Lineament mapping	40
5.1.1 Methods	40
5.1.2 Faults in the Soldier Creek area	41
5.1.2.1 Lower Currant Creek fault system	41
5.1.2.2 Middle Currant Creek fault system	41
5.1.2.3 Northern Stinking Springs fault system	41
5.1.2.4 Southern Stinking Springs fault system	42
5.1.2.5 Fault system south of Strawberry fault	42
5.1.2.6 Graben northwest of Willow Creek	42
5.1.2.7 Willow Creek fault	42
5.1.2.8 Strawberry normal fault system	42
5.1.2.9 Fault below Currant Creek landslide	43
5.1.2.10 Fault west of Currant Creek Reservoir	43
5.1.2.11 Strawberry thrust faults	43
5.1.2.12 Faults disclosed by the Water Hollow tunnel	44
5.1.2.13 Grabens southwest of Strawberry Reservoir	44
5.1.2.14 Indian Springs faults	44
5.1.2.15 Currant Creek Mountain faults	44
5.1.2.16 Timber Canyon graben	45
5.1.2.17 Additional faults	45
5.1.3 Lineament assessment summary	45
5.2 Stinking Springs fault	45
5.2.1 Colluvial wedge adjacent to the fault	45
5.2.2 Currant Creek terraces	48
5.2.3 Faulted pediment west of the fault	48
5.2.4 Assessment summary	48
5.3 Strawberry normal fault	48
5.3.1 Co-op Creek alluvial fan complex	51
5.3.1.1 Geomorphology	51
a. Drainage channel morphology	51
b. Fault scarp morphology	51
5.3.1.2 Scarp trenching	53
a. Co-op Creek trench 1	53
(1) Stratigraphic units	54
(a) Alluvial fan sediments	54
(b) Stream-reworked colluvium and alluvial fan sediments	54
(c) Colluvial sediment	57
(2) Estimated ages of units	59
(3) Sequence of events	60
b. Co-op Creek trench 2	62
(1) Stratigraphic units	62
(a) Alluvial fan sediments	62
(b) Colluvial sediments	62

CONTENTS - Continued

Page

(2) Estimated ages of units 64
(a) Soil relative dating 64
(b) Radiocarbon dating 64
(3) Sequence of events 70
c. Correlation of faulting events and displacements 71
5.3.2 Alluvial plain coring 72
5.3.2.1 Site geology 72
5.3.2.2 Radiocarbon dating 74
5.3.2.3 Amino acid age estimates 75
5.3.2.4 Estimated minimum slip rates 76
5.4 Fault activity summary 76

6 Maximum credible earthquakes and recurrence intervals 78
6.1 Regional seismicity considerations 78
6.2 Empirical earthquake magnitude-fault parameter relationships 78
6.2.1 Fault rupture length 78
6.2.2 Fault displacements 79
6.3 Fault recurrence 79
6.3.1 Scarp physiographic expression 79
6.3.2 Fault slip rates 82
6.3.3 Estimated recurrence intervals 82
6.4 Recommended maximum credible earthquakes 83
6.4.1 Wasatch fault 83
6.4.2 Strawberry fault 83
6.4.3 Stinking Springs fault 84

7 Conclusions 85
7.1 Design earthquakes for Soldier Creek Dam 85
7.2 Surface faulting 87
7.3 Reservoir-induced seismicity 87
7.4 Landsliding and landslide-induced water waves 88
7.5 Reservoir seiche 88
7.6 Liquefaction 88

8 References 90

9 Appendixes 103

A. Soil Profile Descriptions 103
B. Auger and Bore Hole Logs 111
C. Indian Creek Core Logs 115

TABLES

No.		Page
5.1	AIle/Ile amino acid ratios and estimated ages for gastropod samples from the Strawberry Valley area	47
5.2	Data summary for soil profiles from Strawberry Valley area	50
5.3	Lithologic description of stratigraphic units in Co-op Creek trench 1	55
5.4	Correlation of units, soils, and fault events in the Co-op Creek trenches	56
5.5	Lithologic description of stratigraphic units in Co-op Creek trench 2	63
5.6	Radiocarbon dates for samples from the Strawberry Valley area	68
6.1	Typical scarp parameters, recurrence intervals, and slip rates	80
6.2	Estimates of paleoearthquake magnitude calculated using fault parameters for faults of concern to Soldier Creek Dam	81
7.1	Design earthquakes for Soldier Creek Dam	85

FIGURES

Figure		Page
1.1	Soldier Creek Dam and Reservoir and the Stinking Springs fault	5
3.1	Epicenter map of the largest historical earthquakes in the Utah region, 1850-1978	12
3.2	Location map of the University of Utah telemetered seismic network as of June 1979	14
3.3	Wasatch Front earthquakes, October 1974 to June 1978	15
3.4	Intensity map for the September 30, 1977 magnitude 4.5 M_L earthquake near Moon Lake, Utah	19
3.5	Schematic summary of fault-plane solutions (lower-hemisphere projections) for the Utah region	22
3.6	Earthquake magnitude versus frequency of occurrence relationship for the Wasatch Front area	24
4.1	Stinking Springs fault scarp looking north from Solider Creek Dam	26
4.2	Scarp of the Strawberry fault where Indian Creek cuts across it south of Strawberry Reservoir	27
4.3	Strawberry alluvial fans and the Strawberry fault north of Strawberry Reservior	30
4.4	Sketch map of the Strawberry alluvial fans and associated faults	31
4.5	Sketch map of the area where Indian Creek flows across the Strawberry fault scarp	32

FIGURES

Figure		Page
5.1	Gully eroded in the colluvial wedge on the Stinking Springs fault scarp	46
5.2	Fluvial terrace remnants along Current Creek south of Water Hollow	49
5.3	Scarp angle vs. height for the Strawberry fan scarps and those studied by Bucknam and Anderson (1979) in Utah and Nevada	53
5.4	Fault zone 3 in Co-op Creek trench 1	58
5.5	Fault zone 2 in Co-op Creek trench 2	65
5.6	14C-dated burrow infilling at station 17 in Co-op Creek trench 2	67
5.7	Small sandy 14C-dated infillings at station 16 in Co-op Creek trench 2	69
5.8	Relationship of push-tube core locations, lithologies, and age data to the Strawberry fault scarp at Indian Creek	73
7.1	Earthquake magnitude versus frequency of occurrence relationships for the Wasatch fault and the Strawberry and Stinking Springs faults	86

PLATES

Plate	
1	Historical seismicity (1850 to 1980) and fault map of Strawberry Valley region
2	Fault map of Strawberry Reservoir area
3	Log of Co-op Creek trench 1
4	Log of Co-op Creek trench 2

SUMMARY OF CONCLUSIONS

This report presents the results of a Bureau of Reclamation seismotectonic study for Soldier Creek Dam, Central Utah Project, Utah. Fieldwork for this study was begun in September 1980 and was completed in October 1981.

Soldier Creek Dam is a zoned earth and rockfill structure 81 m high with a 404-m crest length. When water is impounded in the new, enlarged Strawberry Reservoir with about four times (1.36×10^9 m^3) the capacity of the existing Strawberry Reservoir, Strawberry Dam and Indian Creek Dike will be inundated.

The most likely sources of future large magnitude earthquakes producing strong ground motions at Soldier Creek Dam are the Wasatch fault, the Strawberry fault, and the Stinking Springs fault. Extensive studies by Woodward-Clyde Consultants on the Wasatch fault (45 km west of Soldier Creek Dam) have documented the high activity rate on this fault. These investigators found evidence of magnitude 6.5 to 7.5 events on the Wasatch fault, recurring every 500 to 5,200 years for four of six segments of the Wasatch fault. Recurrence of large events was estimated at 50 to 430 years for any point on the fault.

Although regional seismicity patterns do not provide conclusive evidence of fault activity near Soldier Creek Dam, the Strawberry fault (8 km west of Soldier Creek Dam) has experienced significant surface displacements during the Holocene [the last 10 Ka (thousand years)]. The Stinking Springs fault (180 m west of Soldier Creek Dam) is structurally and physiographically similar to the Strawberry fault, but its prominent topographic scarp is less than half as long as the scarp on the Strawberry fault. The only Quaternary deposits which might be used to assess the activity of the Stinking Springs fault lie under the present Soldier Creek Reservoir.

Estimates of paleoearthquake magnitudes for the Strawberry fault derived from displacement data from two exploratory trenches across a fault scarp range from 5.9 to 7.4. The larger magnitude estimates are based on displacements which were probably the result of more than one fault event; if so, magnitudes would be <7.0. However, these displacements were measured on a subsidiary fault parallel with the main fault which may have experienced larger displacements. Fault length-magnitude relationships suggest a magnitude 7.0 earthquake is credible, assuming the length of the Strawberry fault marked by its prominent topographic scarp ruptures in a single event. Stratigraphic units exposed in the trenches and age dating studies indicate recurrence intervals for the largest surface faulting events on the Strawberry fault are in the range 1,500 to 10 Ka.

Although we have no direct evidence to suggest that recent displacements on the Stinking Springs fault have been less than those on the Strawberry fault, geophysical data obtained during oil exploration in the area suggest displacements at a depth of 3000 m are less on the Stinking Springs fault than on the Strawberry fault. The topographic scarp of the Stinking Springs fault is also shorter than that of the Strawberry fault (11 km versus 28 km), suggesting the length of fault segments subject to repeated rupture are shorter. These differences in physiographic fault length and displacement at depth

suggest a somewhat smaller MCE (maximum credible earthquake) for the Stinking Springs fault than for the Strawberry fault. A magnitude of 6.5 derived from fault length-magnitude relationships corresponds with the physiographic length of the Stinking Springs fault.

The Richter magnitudes and hypocentral parameters of the design earthquakes for those faults capable of generating earthquakes hazardous to Soldier Creek Dam are listed below. The magnitudes of the 25-year and 100-year earthquakes were estimated from the magnitude versus frequency of occurrence curves shown in chapter 7.

Design earthquakes for Soldier Creek Dam

Seismogenic structure	MCE (M_L)	100-year (M_L)	25-year (M_L)	Epicentral distance (km)	Focal depth (km)
Wasatch fault	7.5	5.8	5.0	45	7
Strawberry fault	7.0	5.2	4.3	8	6
Stinking Springs fault	6.5	5.2	4.3	0	4.5

The Stinking Springs fault trends across the present Soldier Creek Reservoir 180 m (600 feet) west of the right abutment of Soldier Creek Dam. An MCE of 6.5 on the fault could produce a down-to-the-west displacement in the reservoir near the dam of 0.5 to 1 m based on empirical displacement-magnitude relationships. Thus, displacement on the fault would produce a relative increase in the height of the dam reducing any hazard to the dam due to reservoir seiche. Because our structural interpretation of the Stinking Springs fault includes eastward tilting of the downthrown block, the degree of tilting and net vertical displacement would decrease to the west away from the dam.

Our air photograph lineament study, general geologic mapping near the dam, and USBR construction engineering geology investigations did not reveal any faults with significant displacements extending under Soldier Creek Dam. However, the dam foundation, particularly the right abutment, is extensively jointed and a large earthquake on the Stinking Springs fault might produce some displacement along preexisting joints.

Based on our general geologic mapping near Soldier Creek Dam, the construction engineering geology report, and consultants reports, there do not appear to be significant landsliding, reservoir-induced seismicity, or foundation liquefaction hazards to the dam.

1. INTRODUCTION

1.1 Purpose and Scope

The construction of Soldier Creek Dam, Bonneville Unit, Central Utah Project, was completed in 1973, but earthquake hazards were not considered in the design of the dam (Wahler and Associates, 1977). In 1977, the consulting firm of W. A. Wahler and Associates reviewed the design, construction, and operation of Soldier Creek Dam and concluded "that there may be significant risk of serious distress and/or failure associated with filling the reservoir behind Soldier Creek Dam." Wahler and Associates (1977) made a number of recommendations including the following: "An evaluation should be made of regional and site seismicity to determine a design earthquake and develop attendant baserock motion criteria. As part of this evaluation, the recency of and potential for movement on the Stinking Springs fault should be determined."

This report summarizes the results of a USBR seismotectonic study designed to address these concerns. We have estimated MCE's and earthquake recurrence intervals for geologic structures in the vicinity of Soldier Creek Dam and have identified other potential seismically induced hazards to the dam. Analysis of ground motions (for example, Hays and others, 1980) from these design earthquakes is beyond the scope of this report.

Our study included:

a. Review of pertinent literature on the stratigraphy, structure, and tectonics of the Uinta Basin and Uinta and Wasatch mountains

b. Review of USBR engineering geology documents on the preconstruction and construction geology of Soldier Creek Dam

c. Interpretation of small- and large-scale aerial photographs for identification of suspected late Quaternary faults

d. Two low-sun-angle reconnaissance flights over the Strawberry Valley area

e. Review of historic seismicity

f. Limited regional reconnaissance geologic mapping within 15 to 20 km of Soldier Creek Dam

g. Detailed mapping, excavation of trenches across fault scarps, and coring adjacent to the most significant bedrock fault scarp including 14C and soil analysis of samples for dating

USBR geologists and seismologists spent approximately 15 man-months completing this study. Geologic fieldwork began in September 1980 and was completed in October 1981.

Van Arsdale (1979a) studied the structure, stratigraphy, and geomorphology of the Strawberry Valley in detail. Because his thesis is recent, concise, and

deals with many of the problems addressed in this study, we quote extensively from it in sections 2 and 4 (quotes indicate his original text). Additional regional geologic data are discussed in Sullivan and others (1983) (Central Utah Project Regional Seismotectonic Study, which is available in draft).

1.2 Soldier Creek Dam

Soldier Creek Dam (fig. 1.1) is located on the Strawberry River about 50 km southeast of Heber, Utah, and 53 km west of Duchesne, Utah. It is in sec. 16, T. 4 S., R. 10 W., about 11 km downstream from the existing Strawberry Dam and Reservoir. Soldier Creek Dam will replace Strawberry Dam when water is impounded in the new enlarged Strawberry Reservoir some time after 1990. The new reservoir will hold 1.36×10^9 m^3, about four times the existing capacity, and inundate both Strawberry Dam and Indian Creek Dike. The active conservation level of the enlarged reservoir will be 2319 m (7602 ft) (Wahler and Associates, 1977).

The reservoir will provide principal storage for the Bonneville Unit's Strawberry Aqueduct. The aqueduct, which consists of dams, tunnels, and pipelines, will transport waters diverted from Rock Creek and other tributaries of the Strawberry and Duchesne Rivers. Water from this unit will be conveyed by the Wasatch Aqueduct to the Bonneville Basin for municipal, industrial, and irrigation purposes.

Soldier Creek Dam is a zoned earth and rockfill structure 81 m high and 404 m long. Its construction required 2.6×10^6 m^3 of embankment materials. It contains two outlet works tunnels, the upper 44 m above the lower. The higher tunnel will release high oxygen content water for downstream fish. Both tunnels can be used for the release of reservoir water (Randolph, 1974).

1.3 Acknowledgments

We would like to extend our appreciation to the staffs of the Uinta Basin Project Office, Bonneville Construction Office, and Salt Lake City Regional Office, Upper Colorado Region, for providing right-of-way, environmental clearances, and considerable logistical support. In particular, Jim Rogers, Mike Deming, Gary Robinson, and their staffs in Duchesne made most of the arrangements for and excavated the Co-op Creek trenches, and Dennis Logue, Dennis Williams, and his staff directed the coring along Indian Creek. We thank the Strawberry Valley Water Users Association for permission to excavate on their property. Able field assistance was provided by Ed Baltzer, Karen Janowitz, Carol Krinsky, and Becky Stoneman. Ed Baltzer did the air photography lineament study for the Soldier Creek area, including field checking. Discussions with Dean Ostenaa and Tim Sullivan, Seismotectonic Section, throughout the study were very helpful. We thank Roy Van Arsdale for permission to quote extensively from his thesis (1979a).

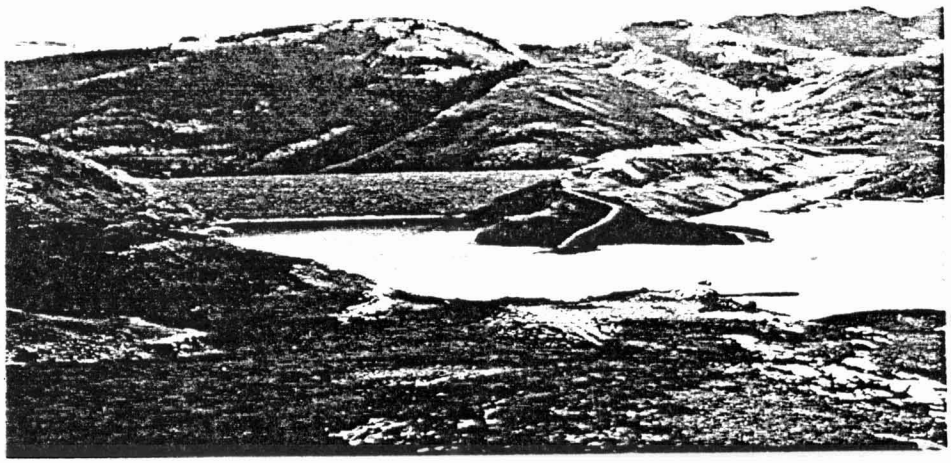

Figure 1.1. Soldier Creek Dam and Reservoir. The scarp of the Stinking Springs fault runs from the left foreground, across the reservoir, along the slope parallel with the road leaving the right abutment, and through the notch in the ridge on the skyline.

2. REGIONAL GEOLOGY AND TECTONICS

Soldier Creek Dam is located on the western margin of the Uinta Basin in the transition area between the Basin and Range and Colorado Plateau physiographic and tectonic provinces. The Uinta Mountains lie 45 km to the north and the Wasatch Mountains 35 km to the west (pl.1).

2.1 Post-Precambrian Depositional History

Van Arsdale (1979a) provides a concise summary of the geologic history of the Basin and Range - Colorado Plateau transition zone:

> "The * * * [transition area in Central Utah] was a slowly subsiding miogeosyncline from Lower Cambrian through Upper Triassic time (Armstrong, 1968; Stokes, 1976). During subsidence, what would later become the Great Basin, divided into a mosaic of local basins with large portions of the shelf having been uplifted above sea level (Armstrong, 1968). The major basin was the Pennsylvanian to Early Permian Oquirrh basin, whose southern lobe coincided with the westerly projection of the present Uinta Basin axis (Roberts and others, 1965). Late Precambrian to Permian age sediments, [15 000 m] 50,000 feet thick in the geosyncline, thin greatly where they cross the Wasatch Front which marks the boundary between the Cordilleran geosyncline and the stable platform to the east (Burchfiel and Hickcox, 1972). Sedimentation terminated in the miogeosyncline with the onset of the Sevier Orogeny during the latest Jurassic time (Roberts and others, 1958; Armstrong, 1968). Accompanying this uplift was the development of an extensive foredeep basin to the east of the Wasatch Front (Armstrong, 1968). [Six thousand meters] 19,000 feet of syntectonic sediments accumulated in the foredeep basin in Cretaceous time. Sedimentation continued into Tertiary time with the Uinta Basin accumulating a maximum thickness of [4 000 m] 13 000 feet of Paleocene to Eocene fluviatile and lacustrine sediments (Hintze, 1973)."

2.2 Sevier Orogeny

> "The Sevier Orogeny in Utah was typified by uplift of the Sevier Orogenic Belt in excess of [14 000 m] 45 000 feet and eastward thrusting during latest Jurassic to Late Cretaceous time (Roberts and others, 1958; Armstrong, 1968). A [15 000 m] 50 000 feet thickness of Late Precambrian and Paleozoic miogeosynclinal sediments of predominantly marine carbonates was thrust over a [5 000-m] 15 000-foot platform sequence near Provo, Utah (Baker, 1959). Apparently the miogeosynclinal sequence was detached from the crystalline basement whose upper surface acted as a regional decollement surface (Burchfiel and Hickcox, 1972). Eastward displacement has been estimated to be [64 km] 40 miles in the Charleston-Strawberry-Nebo thrust (Crittenden, 1961). Concurrent with thrusting was the development of many large folds (Eardley, 1934; Burchfield and Hickcox, 1972). Large easterly-overturned folds in the Stansbury, Oquirrh, and Lake Mountains, and in the southern Wasatch Range, have curving axial traces which form an arc

convex to the east (Proctor, 1959; Burchfield and Hickcox, 1972; Crittenden, 1976). Most of these folds lie in the area of the Late Paleozoic Oquirrh Basin and it is believed that the abnormally thick section in this basin influenced their formation (Armstrong, 1968; Burchfield and Hickcox, 1972). The Oquirrh Basin may also be responsible for the more easterly translation of the Charleston-Strawberry-Nebo thrust sheet (Crittenden, 1964; Burchfield and Hickcox, 1972).

"Thrust structures of the Idaho-Wyoming thrust belt are well documented in the subsurface. The dominant features of the thrust belt north of the Uinta Mountains are low-angle, west-dipping, reverse faults that lie above an essentially undisturbed westward sloping surface at the top of the crystalline Precambrian basement (Royse and others, 1975). Folding is also prevalent with many of the folds being overturned to the east. Beutner (1977) modeled deformation of the Idaho-Wyoming thrust belt by compressing a gelatin slab against an irregular clay foreland to generate visible stress trajectories. The stress trajectories are chiefly affected by the 'Southwestern Montana Recess' and the 'Uinta Recess,' deep-rooted buttresses around which the eastward moving thrust sheets were deformed. Such a model is supported by paleomagnetic studies of Triassic redbeds (Grubbs and van der Voo, 1976). Farther south, the Uinta Mountains and the northwest corner of the Colorado Plateau may have acted like buttresses, thereby allowing more easterly thrusting along the axis of the Uinta Basin (Crittenden, 1976; Stokes, 1976). Periods of uplift of the Uinta Mountains alternated with easterly thrusting in the Salt Lake City area, so a buttress effect is considered probable (Crittenden, 1976).

"Whether the easterly convex axial traces of the folds and the leading edge of the Charleston-Strawberry-Nebo thrust sheet are a consequence of an anomalously thick sedimentary section or due to buttressing, the result was more easterly extending Mesozoic deformation along the Uinta Basin Axis and the formation of an arcuate structural grain."

2.3 Tertiary Tectonics

"Uplift of the Uinta Mountains and concurrent subsidence of the Uinta Basin continued sporadically from mid-Eocene into the Oligocene (Osmond, 1964). The Oligocene epoch was a period of volcanism throughout much of the area * * *, with volcanic centers at Bingham and Tintic (Hintze, 1973).

"Gentle Miocene folding may have been related to minor reactivation of the Sevier thrusts (Walton, 1959); however, the next major tectonic event was the Basin and Range Orogeny with normal faulting continuing to the present. The time of initiation of Basin and Range faulting in the Wasatch Front area has been placed from late Eocene (Crosby, 1972) to early Miocene (Armstrong, 1968; Hintze, 1973). During segmentation of the Sevier uplift, the eastern edge

of the fold belt was uplifted while subsidence of the Basin and Range occurred (Stokes, 1976). The total relative vertical movement between the two provinces is estimated to have been [21 000 m] 70,000 feet (Crosby, 1972).

"The geometry and mechanics of Basin and Range structures have been the subject of numerous studies (Gilbert, 1928, Nolan, 1943; Osmond, 1960; Atwater, 1970; Stewart, 1971; Scholz and others, 1971; Proffett, 1977; and Stewart, 1978) to name a few. Four principal hypotheses for the origin of the Basin and Range Province variously invoke subduction of the East Pacific Rise, mantle plumes, wrench faulting, and back-arc spreading (Stewart, 1978). Subsurface depictions of Basin and Range structures range from nearly vertical faults bounding horsts and grabens to tilted blocks bounded by downward-flattening (listric) faults (Stewart, 1978). * * * eastward tilting of the Stansbury, Oquirrh, Wasatch, and West Tintic Mountains and Thorpe Hills has been noted (Gilbert, 1890; Moore, 1960; Stewart, 1978). Gilbert (1890) depicts the mountain range and basin immediately to its east as a single tectonic block. That is, Stansbury Mountain-Rush Valley, Oquirrh Mountains-Jordan Valley, and the Wasatch Mountains are three separate easterly-tilted blocks. A very similar subsurface interpretation of the Great Salt Lake basin is given by Jones and Marsell (1955).

"The dips of Basin and Range normal faults has been a point of controversy (Nolan, 1943; Crosby, 1972). Variation in reported dips may be explained in part by fault planes that decrease in dip with depth (Longwell, 1936; Hamblin, 1965). If downdip flattening of normal faults occurs, then the dip of the fault would vary as a function of depth of exposure. Downdip flattening of normal faults is well documented north and south of the area * * * in the Idaho-Wyoming thrust belt (Royse and others, 1975), in the Sevier desert of central Utah (McDonald, 1976), and in the southwestern Colorado Plateau (Hamblin, 1965)."

2.4 Quaternary Tectonics

Seismic and other geophysical data (Smith and Sbar, 1974; Smith, 1978; Stewart, 1978) and Quaternary fault scarps (Cluff and others, 1975; Hamblin, 1976; Anderson, 1979; Anderson and Miller, 1979; Hamblin and others, 1981) demonstrate continuing Quaternary faulting in the Great Basin-Colorado Plateau transition zone. Moment rate studies using geologic data show the historical seismicity reflects the long-term seismicity with the exception of the Wasatch fault zone (Doser and Smith, 1982). Detailed studies of fault recurrence intervals and estimated paleoearthquake magnitudes have been made on the Wasatch fault (Swan and others, 1980; Hansen and others, 1981; Swan and others, 1981), the most active structure in the region. Less extensive attempts to assess fault recurrence in the area have been made by Sullivan and others (1983) in the back valleys of the Wasatch Mountains and by Martin and others (1983) in the northwestern Uinta Basin. Van Arsdale (1979a, 1979b) suggested the latest movement on the Strawberry fault (8 km west of Soldier Creek Dam) occurred as recently as 12,000 years ago (discussed in section 5.3).

2.4.1 Wasatch Fault

The Wasatch fault is a major, down-to-the-west, normal fault extending 370 km from Gunnison, Utah, north into Idaho with an estimated displacement of 4500 m. The fault trace is near the base of the west-facing triangular facets forming the west face of the Wasatch Mountains. Along almost its entire length, vegetation lineaments and scarps in Lake Bonneville lacustrine sediment, moraines, and Holocene alluvial and colluvial deposits indicate late Quaternary fault displacement (Cluff and others, 1975; Swan and others, 1980; 1981). Swan and others (1980; 1981) and Hanson and others (1981) reach the following conclusions based on interpretation of 13 trenches at 4 sites (Kaysville, Hobble Creek, Little Cottonwood, and North Creek) along the Wasatch fault zone: (1) cumulative net vertical tectonic displacement since the middle Holocene is 10 to 11 m, (2) repeated displacements of 0.8 to 3.7 m producing earthquakes of M = 6.5 to 7.5 have occurred during Holocene time, (3) the recurrence interval of surface faulting events on segments at the localities trenched is 500 to 5,200 years, (4) Holocene slip rates are 0.6 to 1.9 mm/yr, and (5) if the Wasatch fault is assumed to consist of 6 to 10 segments, the recurrence interval for major earthquakes on the entire fault is 50 to 430 years.

Attention has also focused on the displacement history of the Wasatch fault as revealed by the physiographic features of the bedrock fault scarp (Hamblin, 1976; Anderson, 1977; Osborne, 1978). Remnants of bedrock pediment surfaces have been correlated along the face of the bedrock fault scarp and interpreted as representing periods of quiescence in its displacement history. Osborne (1978) concludes that differences of correlative scarp heights in the Ogden-Salt Lake City portion of the fault scarp may be the result of pivotal- or scissors-type movement on the Wasatch fault.

2.4.2 The Back Valleys of the Wasatch Mountains

A reconnaisance study (Sullivan, 1982; Nelson and Krinsky, 1982; Sullivan and others, 1983) of the back valleys (Gilbert, 1928, p. 58) demonstrates that many of the valley bounding faults have had recurrent Quaternary displacement. However, no post-Bonneville [<20 ka (thousand years)] displacement has been documented (except for the Strawberry fault discussed in section 5.3). A few faults may have had displacements only slightly predating the last high stand of Lake Bonneville. A suspected Quaternary fault scarp on the south edge of Heber Valley (Anderson and Miller, 1979) has been shown to have a nontectonic origin (Sullivan and others, 1983).

2.4.3 Cache Valley

No systematic neotectonic study of Cache Valley has been made. Cluff and others (1974) mapped a large number of lineaments from air photographs, many of which they feel could be fault scarps along both margins of Cache Valley. Lake Bonneville deposits in the Paradise area are unfaulted (Mullens and Izett, 1964), but displaced Bonneville gravels on the East Cache fault were clearly visible at one time at the mouth of Logan Canyon (W. Scott, oral communication, 1981). Temporary exposures in several other areas along the East Cache fault have revealed post-Bonneville displacements (B. N. Kaliser, oral communication, 1981), and these undocumented reports of displacement

have been confirmed near Logan in excavations by Woodward-Clyde Consultants (D. P. Schwartz, oral communication, 1982).

2.4.4 Uinta Basin and Uinta Mountains

Martin and others (1983) have shown that recurrence intervals on the Towanta Flat faults north of Duchesne are in the range of at least 50 Ka. Seismicity data suggest other faults on the south flank of the Uintas may be active, but no conclusive evidence of Quaternary displacement has been found. In particular, the South flank fault does not show evidence of late Quaternary displacement.

2.4.5 Wasatch Plateau

Spieker and Billings (1940) recognized only one period of glaciation (Wisconsin; the equivalent of "Pinedale") on the Wasatch Plateau. Most faulting was considered to predate glaciation, but these authors found some evidence for postglacial faulting. Based on offset moraines, alluvial fans, and mudflow deposits, Kucera (1954) concluded recurrent fault movement on the Joes Valley fault zone totaling hundreds of feet had taken place between his glacial stages II and III (probably early and late "Pinedale") with displacements of 4 to 6 m on even younger deposits. Late Quaternary fault scarps about 4 m high have been reported near Joes Valley Reservoir by R. C. Bucknam (written communication to A. Viksne, 1976) and a number of other scarps in relatively recent deposits have been noted by Bucknam, J. T. Sullivan, and others. The neotectonics of the Wasatch Plateau will be the focus of future seismotectonic studies for Joes Valley and Scofield Dams.

3. HISTORIC SEISMICITY

3.1 Regional Seismicity

The historic record of earthquake occurrence in Utah dates back to 1847 when Mormon settlers first moved to the Salt Lake City area. Prior to the installation of a seismograph station at the University of Utah in 1907, the only locatable earthquakes were those occurring near populated areas, primarily along the Wasatch Front. Instrumental epicenter determinations for earthquakes occurring in Utah after 1907 were still not very accurate, and felt reports of ground shaking were relied on heavily through 1949 (Arabasz, 1979).

In 1950, the U.S. Coast and Geodetic Survey initiated routine epicentral determinations for moderate size earthquakes (Richter magnitude, M_L, greater than 3) in the Intermountain area using data from widely spaced regional seismographs. A skeletal statewide network was installed in 1962 providing sufficient coverage and data within the next 12 years to define a prominent zone of diffuse but locally intense seismicity at least 100 km wide, roughly centered along the major north-south Wasatch fault zone (Smith and Sbar, 1974).

The ISB (Intermountain Seismic Belt), the adopted name of this zone of intraplate seismicity, has subsequently been shown to approach 200 km in width and over 1300 km in length. It extends from the Arizona-Nevada border through Utah, Idaho, and Wyoming into Montana (Arabasz and others, 1979). It is considered to have one of the highest levels of earthquake risk in the contiguous United States outside of California and Nevada (Arabasz and Smith, 1979). More than 15 events with magnitudes greater than or equal to 6 have occurred within the ISB since the mid-1800's, the largest being the 1959 Hebgen Lake earthquake of magnitude 7.1 (Smith and Sbar, 1974). Eight of the magnitude 6+ earthquakes have occurred within Utah and include the 1901 magnitude 6.5 M_L Richfield and 1934 magnitude 6.6 M_L Hansel Valley earthquakes. The Hansel Valley event is the only earthquake in Utah that has produced surface displacement (0.5 m) during historic times.

Epicenters of the largest earthquakes ($M_L \geq 4$) occurring in Utah since 1850 are shown with zones of major faulting in figure 3.1. The distribution of epicenters and faulting indicates there is a broad, north-south zone of ongoing crustal deformation in Utah that coincides with the transition between the Basin-Range province to the west and the Colorado Plateau and Middle Rocky Mountains provinces to the east. The most prominent feature within this zone in central and northern Utah is the 370-km-long Wasatch fault, a segmented geologic break along which young mountain blocks have been uplifted to form a steep, west-facing scarp (Arabasz and Smith, 1979).

Only two of the historic earthquakes of magnitude greater than 4 are suspected of occurring directly on the Wasatch fault, the 1910 earthquake ($M_L = 5.5$) near Salt Lake City and the 1914 event ($M_L = 5.5$) near Ogden (Arabasz and Smith, 1979). There has been abundant and persistent small magnitude activity associated with Wasatch fault. This activity is mainly concentrated along specific sections of the fault that are separated from each other by segments of nonactivity (i.e., seismic gaps). The great majority of historic earthquake

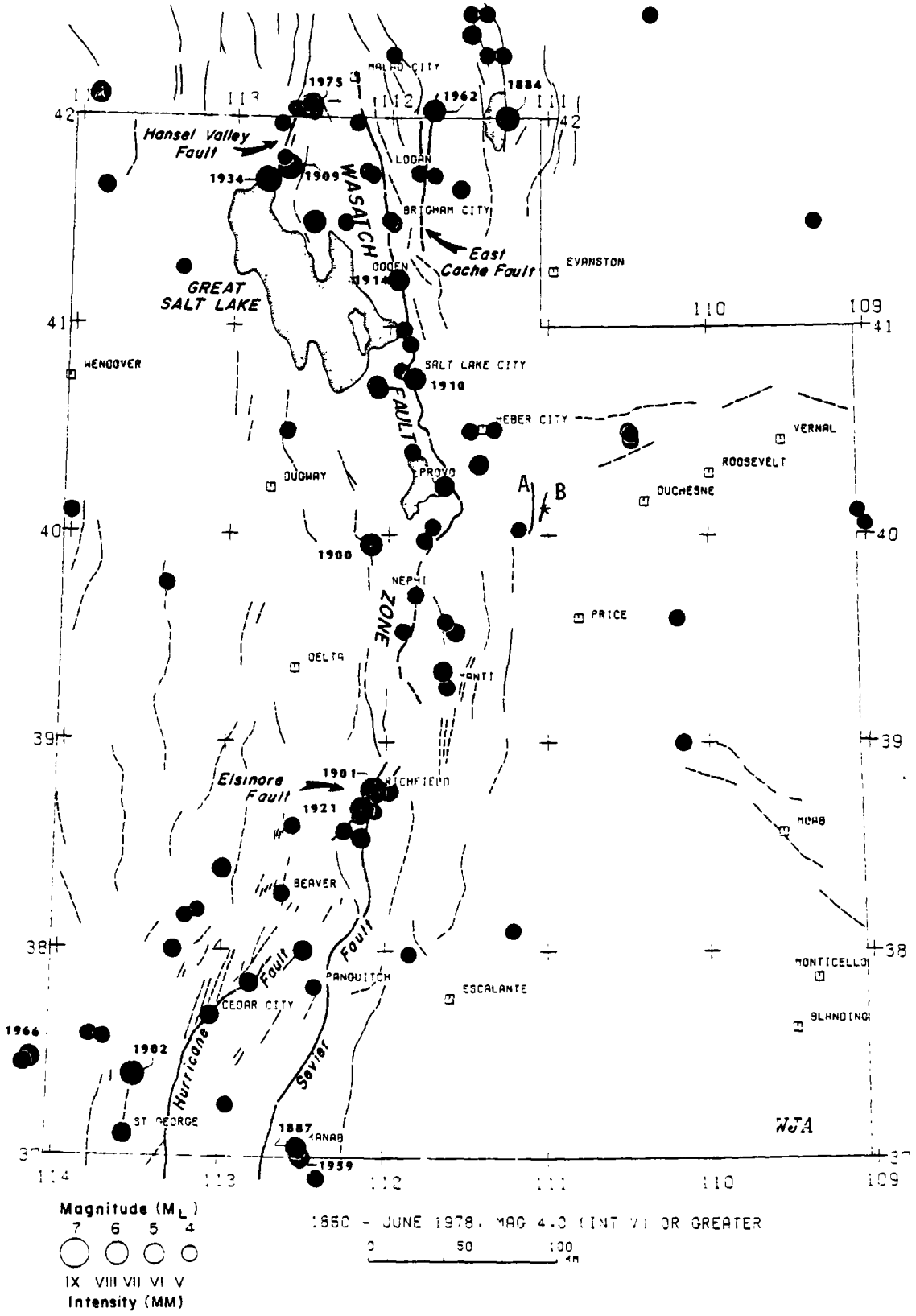

Figure 3.1 Epicenter map of the largest historical earthquakes in the Utah region, 1850-1978. For coincident epicenters, only the largest event is shown. Earthquakes of magnitude 5.5 or greater are dated by year. "A", "B", and "*" indicate Strawberry fault, Stinking Springs fault and Soldier Creek Dam, respectively. (From Arabasz and Smith, 1979).

activity within the ISB in central and northern Utah has been east and west of the Wasatch fault and, in general, does not coincide with known Cenozoic faulting.

Current knowledge of the present-day nature of the ISB in Utah is due to the installation of regional arrays of relatively dense, high-gain, short-period, telemetry seismograph stations in October 1974 by the University of Utah for the purpose of studying seismicity and associated hazards along the Wasatch fault. The station distribution, as of June 1979, is illustrated in figure 3.2. The dashed line encloses the area covered in figure 3.3, an epicentral map of earthquakes recorded by the telemetered network through June 1978. The occurrence of earthquake activity east and west of the Wasatch fault is well illustrated in figure 3.3 as is the lack of activity within the seismic gaps along the Wasatch fault, here enclosed by dashed lines north and south of Salt Lake City.

Although the seismic network is concentrated and in the Wasatch fault region, the ability to locate earthquakes accurately in the mountains and valleys east of the Wasatch fault has improved significantly from that which was possible prior to October 1974. There can be, however, considerable error involved in computing hypocenters in this region. This location error can exceed 5 km, depending on the distance to the closest seismograph station recording the event as well as the size of the earthquake. Thus, it is not possible to make a direct correlation between earthquakes recorded by the regional array either before or after October 1974 and known faulting east of the Wasatch fault.

The historic record, especially the better located post-October 1974 data (fig. 3.3), demonstrate that there is an obvious increase in earthquake activity to the east where the geologic evidence suggests rates of Cenozoic fault displacement are less than those on the Wasatch fault. This is particularly true along a zone a few tens of kilometers east of the Wasatch fault that extends for about 200 km from north of the Idaho-Utah border south to about the latitude of Salt Lake City (40.8° N.). From this latitude south to Heber City, the activity becomes diffuse. At Heber City, the linear trend begins again and continues south to at least Joes Valley (30 km due east of Manti) although it is less pronounced and is offset to the east an additional 20 to 30 km. Soldier Creek Dam is located along the eastern margin of this southern linear trend of seismicity.

3.2 Local Seismicity

Plate 1 is an epicentral plot of all seismicity known to have occurred within the area bounded by 39.6 to 40.6° N. latitude and 110.4 to 111.7° W. longitude between 1850 and 1981 (University of Utah, 1982). A total of 395 earthquakes, ranging in Richter magnitude (M_L) from -0.2 to 5.0 are shown along with major faults (compiled by Stokes and Madsen, 1961). The much improved ability to detect and locate earthquakes east of the Wasatch fault since the installation of the dense regional array of telemetered stations in October 1974 is well illustrated. Only 110 of the earthquakes shown in plate 1 occurred during the 125 years of record prior to October 1974. The remaining 285 earthquakes were detected and located by the telemetered array during the remaining 7 years of historic record. This apparent increase in seismic

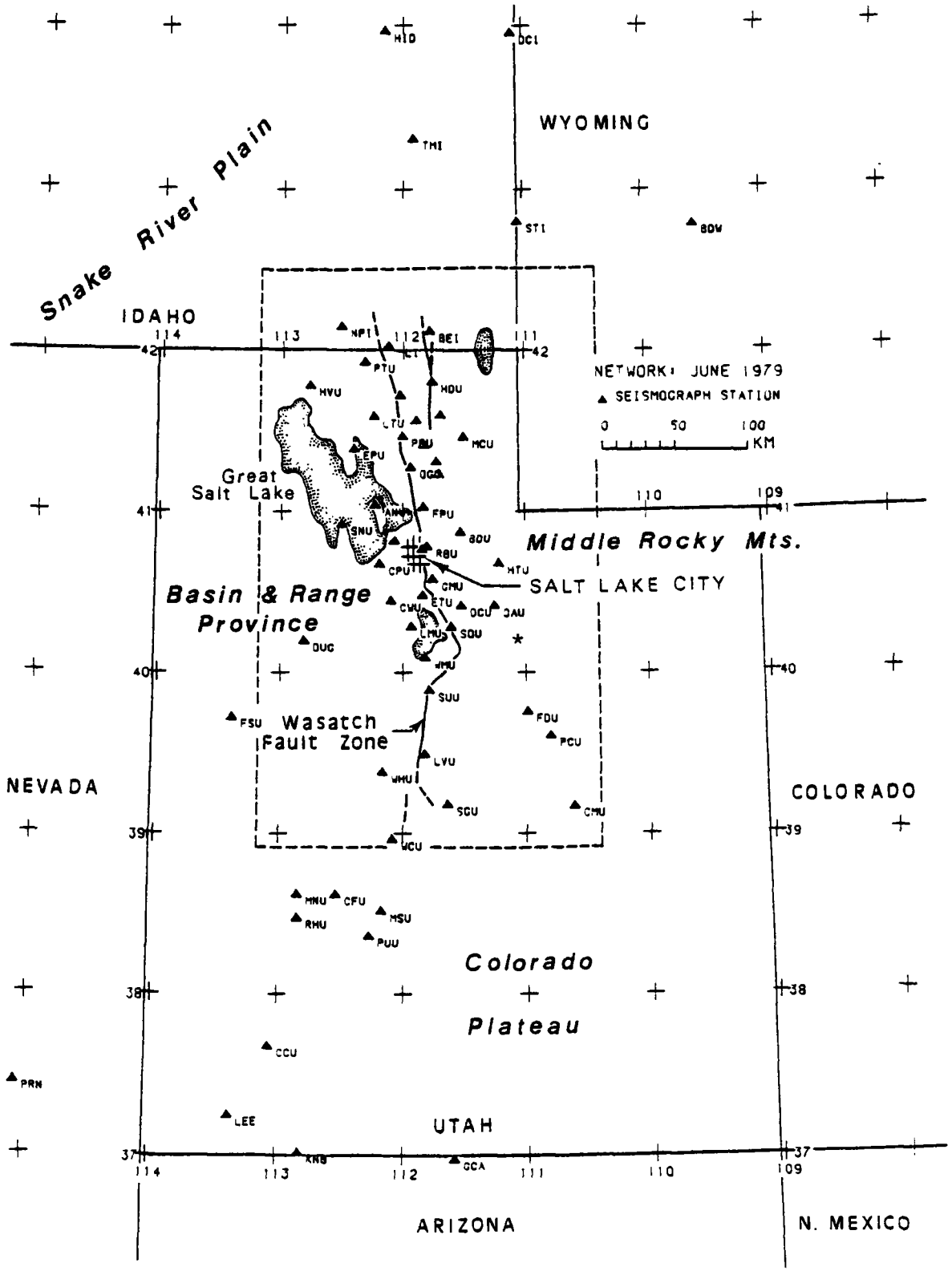

Figure 3.2 Location map of the University of Utah telemetered seismic network as of June, 1979. Dashed line outlines the area illustrated in figure 3.3. Soldier Creek Dam is indicated by a "*". (From Arabasz and others, 1979)

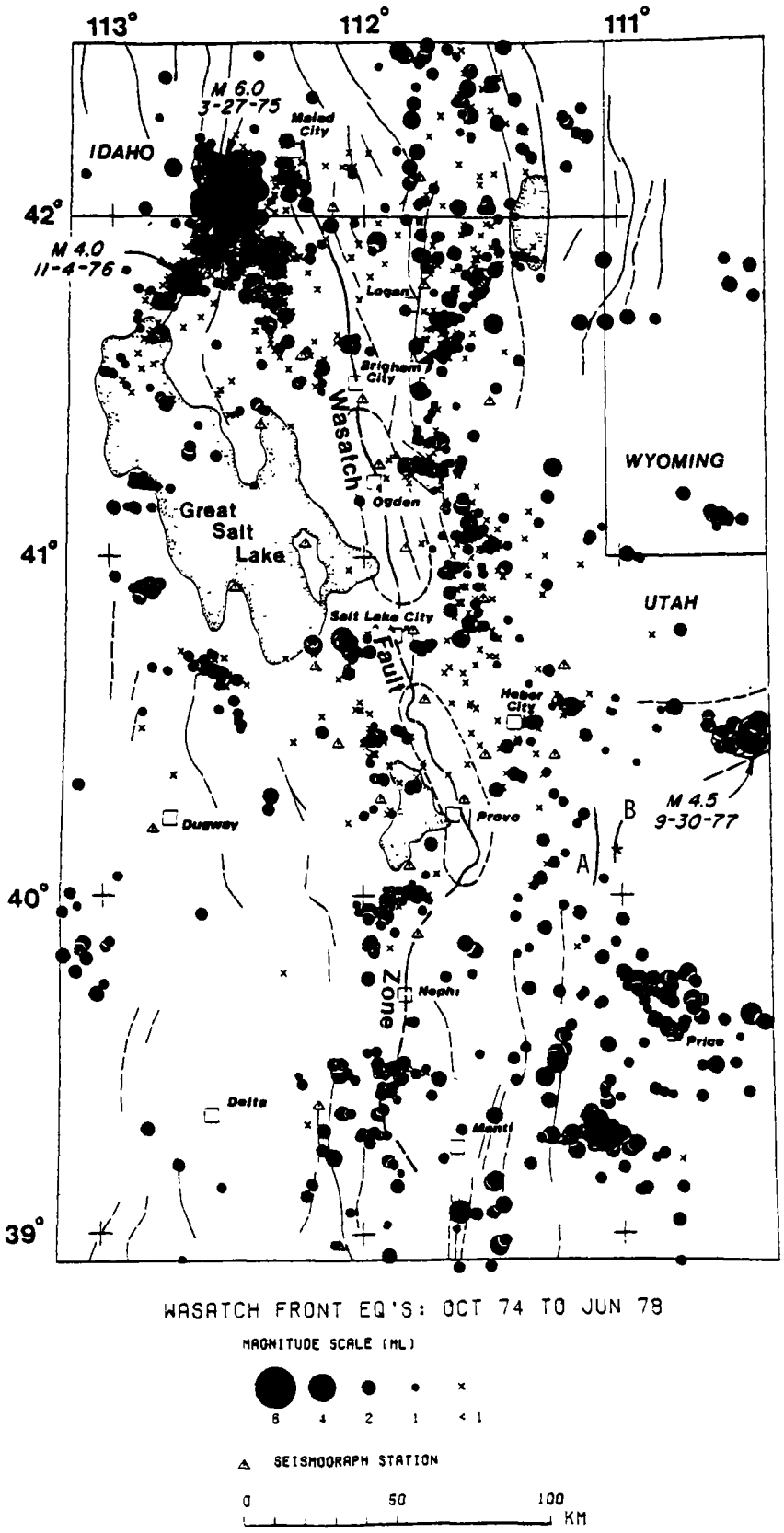

Fig. 3.3. Wasatch Front Earthquakes, October 1974 to June 1978. "A", "B", and "*" indicate Strawberry fault, Stinking Springs fault and Soldier Creek Dam, respectively. (From Arabasz and others, 1979).

activity is a direct result of increased station coverage and lower magnitude detection thresholds and not,in itself, an indication of a change in seismicity characteristics of the Soldier Creek Dam region.

The spatially diffuse occurrence of seismicity in the mountains and back valleys east of the Wasatch fault is apparent in this plate, as is the general lack of correlation between epicenters and mapped faults. Locally intense clustering, however, can be observed east and northeast of Heber City in the northeast corner of the plate, south of Wallsburg, north of Price, and at Provo.

3.2.1 Provo Area

The concentric pattern of epicenters at Provo represents the assumed location of four earthquakes that were felt in the area prior to adequate instrumental control. As with all noninstrumentally located events, the epicenters are assumed to be at the center of the region of maximum observed intensity. This assumption is heavily dependent on population distribution and, therefore, not very accurate. The epicenters of these felt events could be in error by 20 km or more; thus, little significance should be attributed to their coincident clustering at Provo. The estimated magnitudes of noninstrumental earthquakes are also subject to considerable error because they too are based on maximum observed intensities. In an evaluation of the historic record, more significance should be placed on the more recently occurring earthquakes for which more reliable data are available.

The largest earthquakes presumed to have occurred within the limits of plate 1 are two magnitude 5.0 events, one at Provo in 1915 and the other near Wallsburg in 1958. The magnitudes of both these earthquakes are based on maximum observed intensities (Modified Mercalli, MM) of VI in the epicentral regions. Additional better located smaller magnitude events clustering near Wallsburg indicate an active structure is present in this locale.

3.2.2 Heber Valley Area

Three km east of Heber City is one area of dense epicenter occurrence. Most of these earthquakes have occurred since and, therefore, are probably aftershocks of the Richter magnitude 4.3 (body wave magnitude, m_b, 4.7) earthquake of October 1, 1972. The main shock produced a maximum intensity of MM VI at the town of Midway west of Heber City and was felt over an area of 6500 km^2 (Langer and others, 1979), producing minor damage at many nearby towns. There is evidence to suggest the main shock actually consisted of two shocks, the first earthquake being followed by another one of slightly smaller magnitude approximately 90 seconds later (Langer and others, 1979). An aftershock study conducted by NOAA and the University of Utah recorded 28 earthquakes between October 3 and October 12, 1972. Nineteen of these aftershocks were large enough to be located by the nine-station, high-gain-portable array. The epicenters of these well-located aftershocks (not shown on pl. 1) cluster 5 km east of Heber City in a northwesterly trend. The focal depths range from 4.9 to 13.6 km, and their depth distribution combined with the composite fault plane solution suggest the causative structure is a normal fault trending northwest dipping 64° NE. Geologic mapping, however, has not revealed Quaternary faulting in this area (Baker, 1959; Bromfield,

and others, 1970; Bromfield and Crittenden, 1971: cited in Langer and others, 1979), although the physiography of Heber Valley suggests a west-dipping normal fault may bound this margin of the valley (Sullivan and others, 1983).

Approximately 16 km northeast of Heber City is another area of relatively dense epicenter distribution consisting of 17 small-magnitude earthquakes. Eleven of these earthquakes occurred during a 42-hour period on October 10 and 11, 1975, followed by four earthquakes on October 26, and two earthquakes on November 2, 1975. The Richter magnitudes of all earthquakes in this sequence are less than 2.0 with the exception of one earthquake of magnitude 2.7 that occurred on October 11, 1975. Spatially, these epicenters follow a west-northwest trend along and just west of the western exposure of the South Flank fault, and it has been suggested this swarmlike earthquake sequence may be related to subsurface westerly extension of that fault (Langer and others, 1979).

3.2.3 Moon Lake Area

Another area of high epicenter density is in the northeast corner of plate 1 near 40.5° N. latitude 110.5° W. longitude. This is the isoseismically determined epicenter of an earthquake that occurred January 17, 1950. Intensity data indicate only MM IV ground shaking was reported in the epicentral area; whereas, the greatest ground shaking reportedly occurred at Grand Junction, Colorado, 225 km to the southeast where the maximum intensity was MM V. Apparently, this discrepancy between epicenter location and region of maximum reported intensity results from a combination of local site amplification and population concentration in Grand Junction. The magnitude of this earthquake is uncertain. The maximum intensity versus magnitude relation of Gutenburg and Richter (1956), $M_L = 1 + 2/3I$, yields a magnitude estimate of 4.3 M_L. The magnitude reported by the California Institute of Technology as determined from seismograms recorded at their observatory in Pasadena is 5.25 (NOAA, 1980). Based on the locally observed intensity of IV in the epicentral area, the magnitude estimate of 5.25 appears high. The actual magnitude is probably less than 5.0, perhaps even less than 4.5. Because the epicenter was reported only to the nearest half degree, the implied accuracy is about 25 km.

The rest of the earthquakes clustered near the 1950 event are associated with an earthquake sequence that commenced with the main shock on September 30, 1977. The USGS (U.S. Geological Survey) determined parameters for this event include Richter magnitude 5.1 ($m_b = 5.0$), focal depth 5 km, and epicentral location 6 km southeast of Moon Lake (USGS, 1977). The University of Utah estimated the Richter magnitude, focal depth, and epicentral location at 4.5, 7 km, and 11 km south of Moon Lake, respectively. This large discrepancy in reported magnitudes results, apparently, from the USGS using seismograms recorded as far away as Albuquerque, New Mexico ($\Delta > 700$ km), to compute the magnitude while the University of Utah used only data from their regional array. The USGS has recently recomputed the magnitude neglecting the extreme far-field data and now report it as 4.5 M_L in agreement with the University of Utah (D. Carver, personal communication, July 20, 1981). The epicenter of the main shock is shown at the University of Utah-determined location in plate 1.

The maximum ground shaking experienced during the September 30, 1977 event reportedly occurred in Grand Junction, Colorado (USGS, 1977), thus making this event similar to the earthquake of January 19, 1950 (fig. 3.4). This maximum intensity MM VI was also reported in the immediate epicentral area and may be due, in part, to an apparent increase in population density near the epicenter since 1950 and/or a general deterioration in the structural stability of local dwellings during the recurrence interval. The only evidence supporting MM VI near the epicenter was reported in Mountain Home, Utah, 10 km to the southeast where a septic system drain was reported broken, old mortar of a log house was cracked at the corners, and some furniture shifted position (USGS, 1977). Intensity V ground shaking was reported throughout the epicentral area in contrast to reports of intensity IV shaking during the 1950 event, thus indicating the magnitude of this earthquake was greater than the 1950 event. These data further support the assignment of a magnitude less than 5.0 M_L to the January 19, 1950 earthquake.

In a combined effort, the USGS and the University of Utah conducted an aftershock study from October 1 through October 15, 1977, using 12 high-gain portable seismographs (Carver and others, 1978). Hundreds of aftershocks were recorded during the 14-day study, the largest being the Richter magnitude 4.0 earthquake of October 11. Epicenters of the larger aftershocks, as listed in the University of Utah earthquake catalog, are shown in plate 1. This data set includes all epicenters clustered near the January 19, 1950 and September 30, 1977 events, as well as the nine events located west of 110.5° W. longitude, here indicated by solid octagons.

One gains a false impression of the spatial distribution of seismicity from considering only the epicenter plot without noting the temporal significance of these earthquakes relative to the installation of the portable array. All nine events occurred either immediately after the main shock and before installation of the local stations, or after the aftershock study was terminated on October 15. The solution quality of these epicenter determinations, as listed in the earthquake catalog, is generally poor and results from insufficient station coverage. Because the University of Utah station distribution is entirely to the west of the epicentral area, the solutions are biased in this direction. The subsurface velocity structure has probably been underestimated, thus resulting in the systematic mislocation of the epicenters to the west toward the points of observation (i.e., the seismograph stations).

Uniform station coverage alleviates this bias in the computed locations as is indicated by the clustering of epicenters near the main shock. All these earthquakes occurred during the aftershock study and are the locations computed by the University of Utah from data recorded by the telemetry network supplemented by data from the local temporary array. The listed location qualities are generally excellent for these clustered events. Although the nine earthquakes may be near their true locations and, thus, not associated with the aftershock sequence, the above evidence suggests they are mislocated aftershocks. This suggests the level of seismicity immediately west of the 1977 earthquake cluster is lower than the earthquake plot alone would indicate.

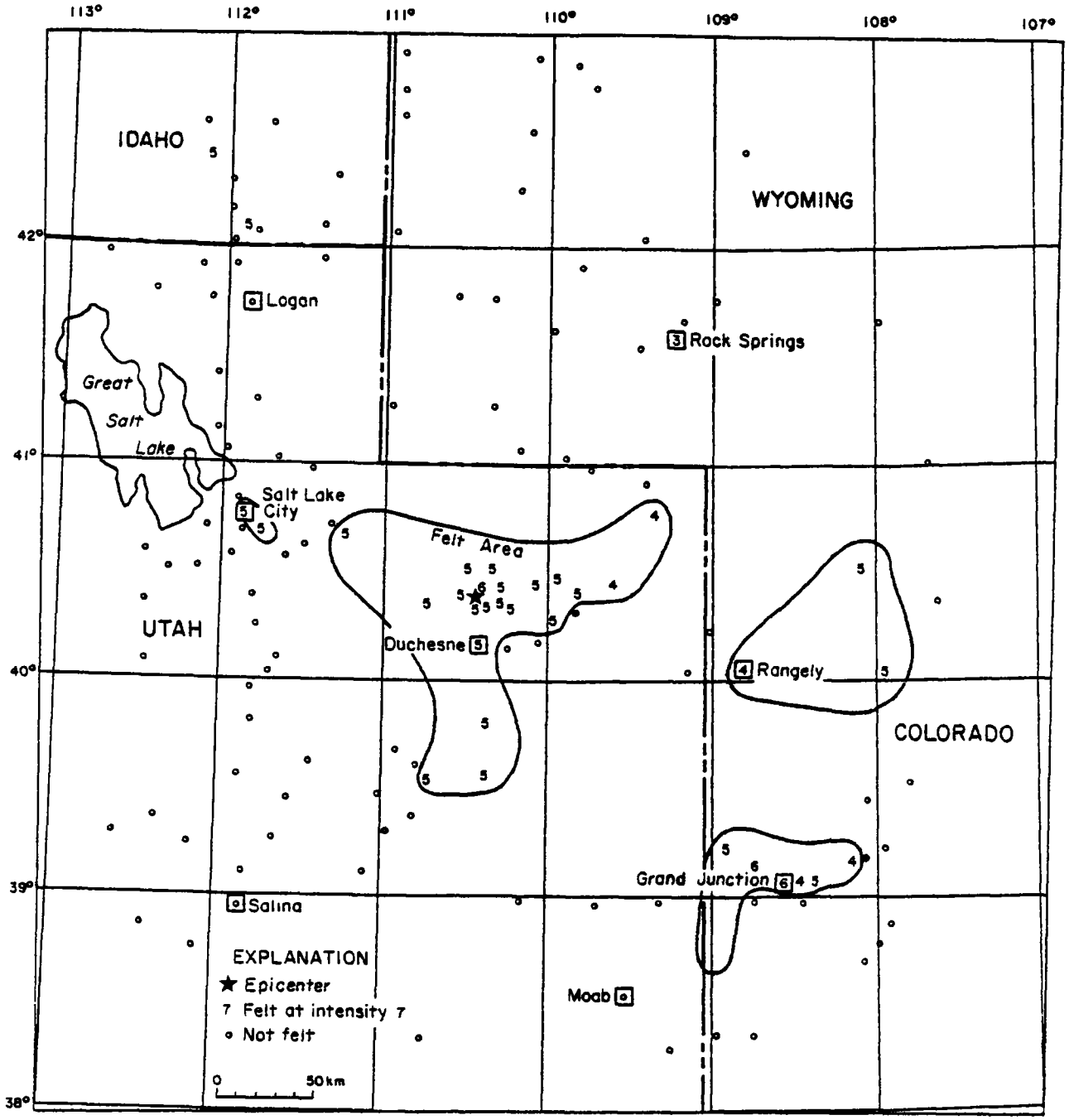

Figure 3.4. Intensity map for the September 30, 1977 magnitude 4.5 M_L earthquake near Moon Lake, Utah. (From USGS, 1977).

The recently published results of the aftershock study indicate the causative structure is a north- to north-northeast trending normal fault dipping about 45° E. (Carver and others, 1981). These conclusions are entirely seismologic in nature and are based on composite fault plane solutions from first motion patterns and on depth distribution plots of about 173 of the larger aftershocks recorded during the study. No association between the inferred faulting and local geology was suggested.

A report of this earthquake in "Survey Notes" (November 1977), published by the Utah Geological and Mineral Survey, indicated the September 30, 1977 earthquake occurred along the "Towanta Lineament," a zone of "fracturing and faulting, separate from the Uinta Mountains, (that) strike N. 70° E. along the south flank of the mountains and extend out into the basin to the south. These apparently reflect an ancient, deep-seated rupture of the earth's crust that can be traced from near the northeast corner of Utah nearly to the Nevada line. This fracturing and faulting is older than the Uintas and is apparently still active to some extent." The association of the September 30, 1977 earthquake with the N. 70° E. trending "Towanta Lineament" is inconsistent with USGS-determined fault orientation based on aftershock data (Martin and others, 1983).

3.2.4 Price Area

The final area of dense epicenters is north of Price. This is an area of intense coal mining and although the actual cause of these earthquakes has not been resolved, it is generally believed that the earthquakes are an induced phenomenon related to the extraction of coal (Smith and Arabasz, 1979).

3.2.5 Strawberry Valley Area

Other significant events include two earthquakes of magnitude 4.0 and 3.7 that occurred in 1963, about 19 and 23 km southwest of Soldier Creek Dam. This is near the southern limit of the mapped portion of the Strawberry fault. At least eight other events ranging in magnitude from 1.0 to 2.1 might be associated with the Strawberry fault. They appear as scattered events west and on the downthrown side of this west-dipping normal fault. These earthquakes occurred after installation of the telemetered array; thus, their locations are more accurate than the two 1963 events but still not sufficient to show a direct correlation with the Strawberry fault.

The earthquake to have been detected and located closest to Soldier Creek Dam was the magnitude 1.2 event shown between the surface traces of the Strawberry and Stinking Springs faults 6 km west-northwest of the dam. This earthquake occurred in 1971; thus, the location accuracy does not preclude a possible association with either of these faults.

3.3 Focal Depths

Of the three hypocentral parameters calculated during the earthquake location process, the focal depth is usually the least accurately determined. Only when the epicenter of an earthquake is within a focal depth of a seismic station recording the event can there be confidence in the computed depth to

the hypocenter. In Utah, including the area east of the Wasatch fault, almost all well-constrained focal depths are less than 20 km, and 90 percent are shallower than 10 km (Smith and Arabasz, 1979). Mean focal depths for earthquakes occurring along the Wasatch Front are between 5.3 and 6.2 km. The great majority of the earthquakes included in this data set, however, are in the magnitude range 0 to 3. Larger magnitude events can usually be expected to occur a few kilometers deeper.

3.4 Focal Mechanisms

Focal mechanism solutions have been computed by various investigators for both composite and single earthquakes at selected locations along the ISB in Utah (fig. 3.5). Most solutions indicate the stress regime is dominated by east-west extension with stress release occurring along generally north-trending high-angle normal faults. The least compressive stress axes (tensional axes) are horizontal and vary from west-southwest east-northeast to west-northwest east-southeast but, in general, reflect Basin-Range style east-west extensional tectonism. This rotation of stress axes may be due to stress release on older faults or zones of weakness that were formed under a somewhat different tectonic setting.

This simple regional pattern of east-west extension is complicated northeast of Provo near Heber City, where in two areas, composite solutions indicate this region is undergoing local compression similar to that observed in the interior of the Colorado Plateau (near Price). The east-west trending Uinta Mountains intersect the north-south trending Wasatch Mountains in this area and this apparent reverse faulting may be just the manifestation of regional east-west extension upon a complex local structural transition. East-west extensional tectonism is not restricted to the Wasatch Front. Recent studies have documented this style of faulting as far east as Moon Lake about 100 km east of the Wasatch fault at the northern boundary of the Colorado Plateau (Carver and others, 1981; Martin and others, 1983). Whether this represents a localized effect at the boundary of a major physiographic province or the possible easterly extension of Basin-Range tectonics is unclear.

3.5 Earthquake Recurrence

The recurrence intervals of earthquakes likely to occur in the mountains and back valleys east of the Wasatch fault, including the region near Soldier Creek Dam, can be estimated from an earthquake magnitude versus frequence of occurrence relationship of the usual form $\log_{10}N = a + bM$. In this equation, N is the cumulative number of earthquakes of magnitude M or larger occurring in a specified area per year, and a and b are constants empirically determined from the available historic record. Ideally, a large data set consisting of many earthquakes of varying magnitudes occurring over a long period of time is used to derive the appropriate relationship. The historic record in the Strawberry Valley region is short and incomplete and, therefore, data from a larger area must be used to arrive at a statistically acceptable solution for the constants a and b.

A recurrence relation has been developed for the Wasatch Front by Smith and Arabasz (1979) using the 129-year historic record of earthquake occurrence from 1850 through 1978. The 92 810-km^2 area is outlined in

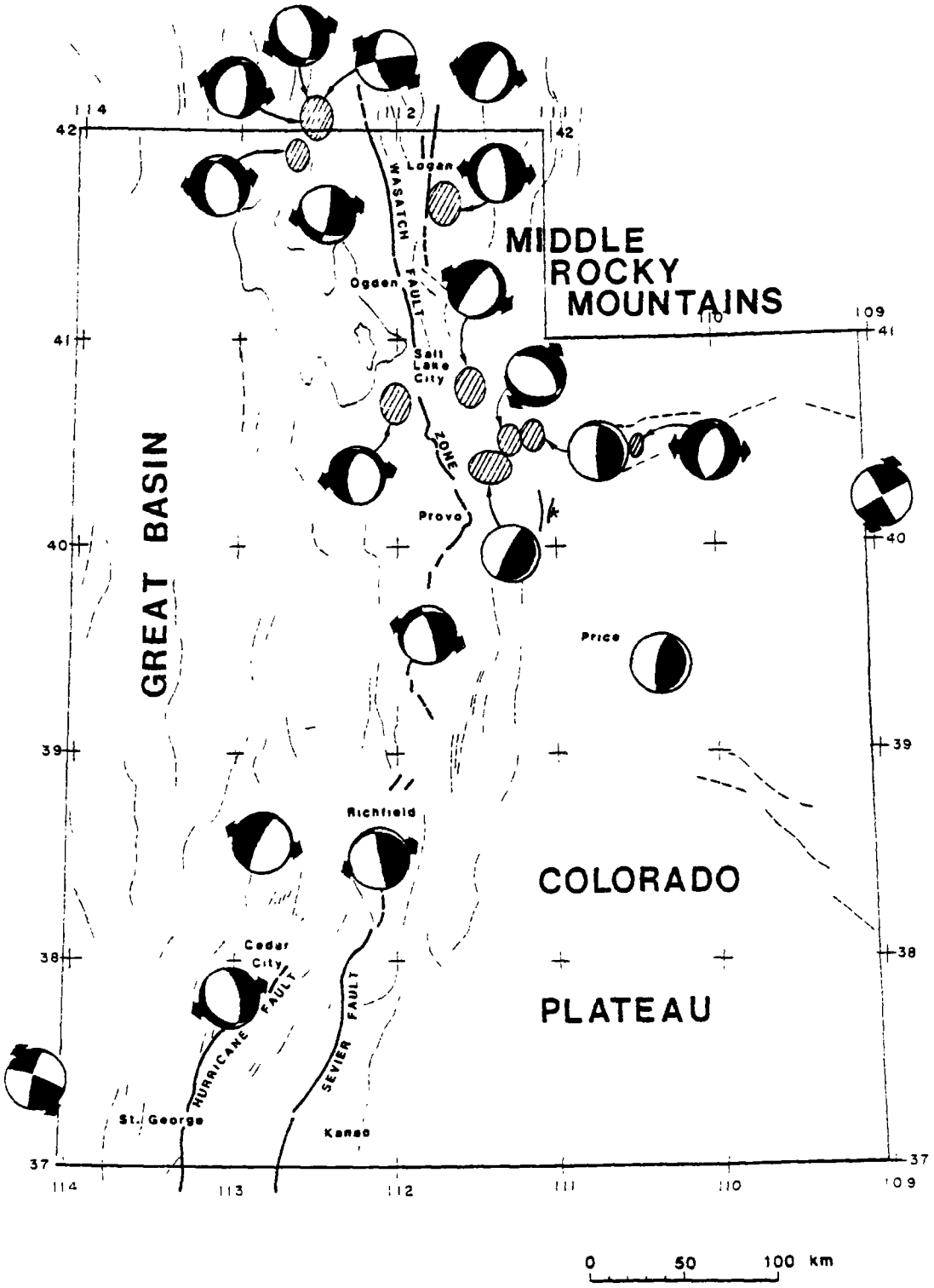

Figure 3.5. Schematic summary of fault plane solutions (lower-hemisphere projections) for the Utah region. Compressional quadrants are shaded. Trends of T-axes are shown by heavy arrows. Hachured zones show sample areas for composite solutions. "*" indicates Soldier Creek Dam. (Modified from Arabasz and others, 1979).

figure 3.2 and includes the entire study area. The well-known relationship of Gutenberg and Richter (1956), $M_L = 1 + 2/3I$ as justified applicable in Utah by the USGS (1976) was used to convert Modified Mercalli intensities to magnitudes for noninstrumental earthquakes. The data set was corrected for incompleteness using the method of Stepp (1972). The resultant formula scaled to 1000 km^2 is $\log_{10}N = 1.01 - 0.72M$ (fig. 3.6).

The $\underline{b}$ value equal to 0.72 is the slope of the logrithmic curve and is at the low end of the empirical range of values. Thus, the occurrence of earthquakes during the 129-year period is characterized by a low number of small magnitude versus large magnitude events and is indicative of relatively high ambient stress within the Wasatch Front area. The $\underline{a}$ value, equal to 1.01, is a measure of the earthquake flux within the 92 810 km^2 Wasatch Front area. It is affected by the numerous small subareas that have not experienced earthquakes during the 129-year period and that are included in the calculation as a consequence of the method of analysis. Therefore, the $\underline{a}$ value does not represent the expected activity on any given fault, but rather represents an average rate of the activity within any 1000-km^2 area within the sampled region.

The determination of fault-related earthquake recurrence requires knowledge of fault-specific earthquake activity. The available seismicity data in the ISB, and, in particular, east of the Wasatch fault, are not sufficiently dense and well-located to define the activity on specific faults. Therefore, in the study area, the average rate for the entire Wasatch Front is assumed to be applicable. Some recurrence interval information is available for large magnitude events from geologic studies on the Strawberry fault, the most recently active fault near Soldier Creek Dam (sec. 5.3.1).

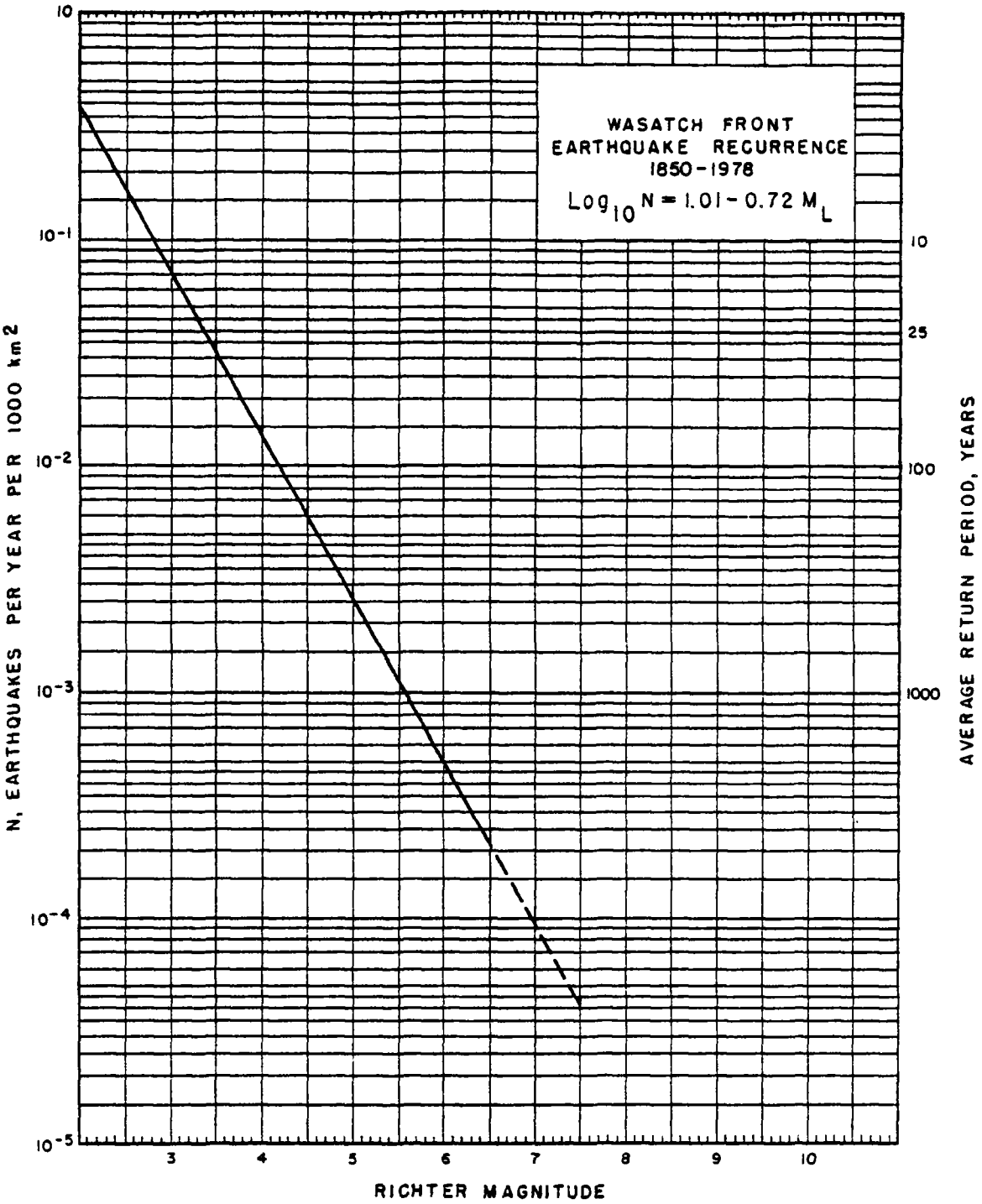

Figure 3.6. Earthquake magnitude versus frequency of occurrence relationship for the Wasatch Front area.

4. GEOLOGY OF THE STRAWBERRY VALLEY AREA

4.1 Strawberry and Soldier Creek Valleys

The 28-km-long Strawberry fault bounds Strawberry Valley on the east while Strawberry Ridge, 12 km to the west, forms the western edge of the valley. Eight kilometers to the east of the Strawberry fault the escarpment of the Stinking Springs fault (fig. 4.1) similarly bounds the east edge of the much smaller Soldier Creek Valley (pl. 2). Before Strawberry Reservoir was constructed, Strawberry and Co-op Creeks merged at the north end of Strawberry Valley, and the Strawberry River flowed south through the valley turning east and cutting across the 175-m-high Strawberry fault scarp where the present Strawberry Reservoir Dam is located. Indian Creek, at the south end of the valley, also cuts across the Strawberry fault scarp (fig. 4.2) and joins the Strawberry River about 2 km east of the fault. The river continues eastward 6 km where it is joined from the north by Soldier Creek and cuts across the Stinking Springs fault scarp. Soldier Creek Dam is located just east of the scarp in the narrow river valley. This area is covered by the Co-op Creek, Jimmies Point, and Strawberry Reservoir, NW., NE., SW., and SE. quadrangles.

4.2 Stratigraphy

The Tertiary bedrock which covers much of the Strawberry Valley area has been subdivided into three formations: the Green River Formation, overlying Uinta Formation, and the Duehesne River Formation (Bissell, 1952; compilation of Stokes and Madsen, 1961).

Lithologies consist of fine-grained and very fine-grained gray to red sandstones, siltstone, and conglomerate with the amount of conglomerate increasing upward in the section (Van Arsdale, 1979a, pp. 9-19). Ryder and others (1976) have described the depositional environments of the oldest Tertiary units in the area in detail and Anderson and Picard (1972) have described the Duschesne River Formation in its type area to the east. Because of pronounced lateral facies changes and the lack of biostratigraphic information, especially from the Uinta and Duchesne River Formations, Van Arsdale (1979a, p. 9) chose to disregard the previously used lithostratigraphic terms (Bissell, 1952; 1959; Osmond, 1965; Astin, 1977) and mapped the bedrock in the area into three informal lithostratigraphic units (units 1, 2, and 3) (Van Arsdale, 1979a, p. 19). The units were distinguished using slope form, continuity of colluvium and vegetative cover, amount of float blocks, continuity of dip slopes, amount of lensatic sandstone, and color.

> "The basal unit (unit 1) is interpreted as an alluvial plain deposit while the conformably overlying other two units (2 and 3) represent an encroaching alluvial fan complex. The basal unit correlates with the Green River Formation of Middle Eocene age, while the other two units may correlate with the Uinta Formation of Upper Eocene age or the Duchesne River Formation of Eocene-Oligocene age" (Van Arsdale, 1979a, abstract).

However, Bruce Bryant (USGS, Denver; oral communication, 1981) has noted that formational boundaries defined in the central Uinta Basin cannot be reliably followed into the Soldier Creek area because of facies changes.

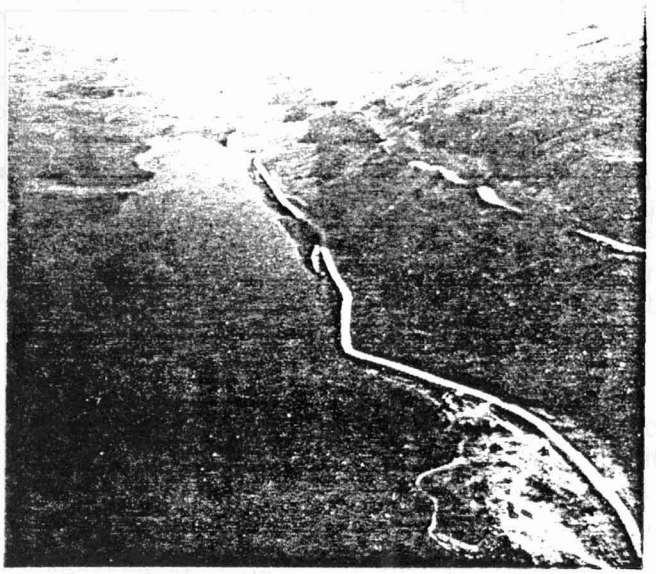

Figure 4.1. The topographically most prominent portion of the Stinking Springs fault scarp looking north from just north of Soldier Creek Dam. A much smaller inferred fault forming Soldier Creek Valley may bound the partially filled reservoir along its west edge.

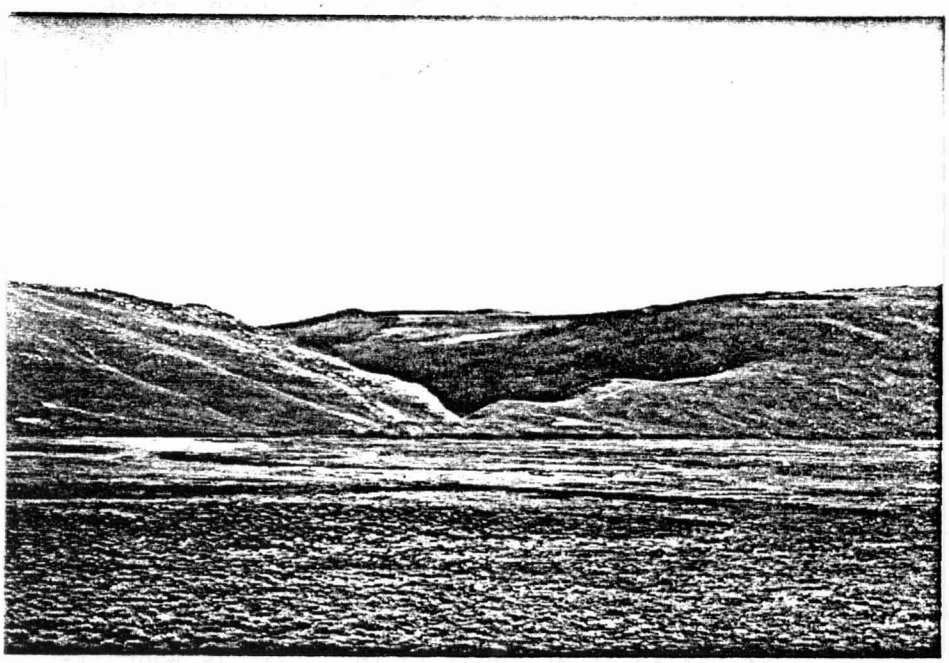

Figure 4.2. The alluvial plain and the scarp of the Strawberry fault (Green River Fm.) looking eastward where Indian Creek flows across it south of Strawberry Reservoir (pl. 2). The stepped morphology of the bedrock spur at the mouth of the canyon is suggestive of successively shorter periods of relative quiescence on the fault when Indian Creek was able to widen the mouth of the canyon alternating with periods of more rapid uplift.

4.3 Structure

"In the Co-op Creek quadrangle [(north of Strawberry Reservoir; pl. 2)], sedimentary rocks ranging from Pennsylvanian to Tertiary age are exposed * * *. Allochthonous geosynclinal rocks have been thrust eastward over authochthonous shelf rocks along the Strawberry Valley thrust in latest Cretaceous to Paleocene time (Bissell, 1952, 1959; Astin, 1977). The Strawberry Valley thrust [(west of L on pl.2)] is considered to be a continuation of the Charleston and Nebo thrusts (Bissell, 1952; 1959). Structures associated with the thrusting include imbricate thrust slices, folds, and normal faults. The imbricate thrust slices are believed to project southward under the Tertiary conglomerates within the Co-op Creek quadrangle (Astin, 1977). Younger normal faults and folds also exist in the Co-op Creek quadrangle.

"West of Strawberry Reservoir the Tertiary sedimentary rocks generally strike N.50°W and dip 15°NE, and east of the reservoir beds strike N.20°W and dip 8°E * * *. Local disturbances of the general structure are related to faulting. Most faults within the study area trend northerly and have normal displacements * * *."

4.3.1 Stinking Springs Fault

"Stinking Springs fault mapped in this study [(C and D on pl. 2)] is a northeast trending fault which bounds the eastern side of the alluviated plain of Soldier Creek [fig. 4.1] * * *. Stratigraphic offset of the fault measured in the field is approximately [30 m] 100 feet near Highway 40. Deformation within the fault zone is best seen in the divide near Highway 40 where beds of unit 2 dip 30° to the west in a zone approximately [30 m] 100 feet wide.

"A seismic profile across the fault near Highway 40 reveals only a 'kink' in the Flagstaff formation at about [3 000 m] 10,000 feet depth with an offset of no more than [30 m] 100 feet (Bill Hansen, Amoco Production Company, personal communication). Seismic energy breaks up at depth in traversing from east to west across the fault and this breakup is believed to reflect the presence of a small foreland fold belt in front of the Strawberry thrust sheet (Dan Davis, Gulf Oil Company, personal communication). Stinking Springs fault thus appears to mark the eastern limit of Strawberry thrust sheet deformation * * *."

4.3.2 Strawberry Fault

"Strawberry normal fault bounds the eastern side of Strawberry Valley and has a down-to-the-west stratigraphic and topographic offset of approximately [180 m] 600 feet where Indian Creek crosses the fault scarp (fig. 4.2) * * *. At this same location, seismic data reveal that the underlying Flagstaff Formation, which is at a depth of approximately [3 100 m] 10,200 feet on the eastern side of the fault, is offset [760 m] 2,500 feet

down-to-the-west (Bill Hansen, personal communication). Fault displacement, as indicated by scarp height, decreases south from the reservoir area. In the center of the northern half of section 18, township 5 south, range 11 west * * * [(north of E on pl. 2)], scarp height has decreased to essentially zero, yet seismic data reveal that there is a [150-m] 500-foot displacement on the Flagstaff Formation (Bill Hansen, personal communication). Strawberry fault is expressed as a single scarp from its southern end northward to the area of Trout Creek [(H on pl. 2)]. In the Co-op Creek quadrangle [(I on pl. 2)], Strawberry fault is expressed as multiple scarps in unit 3 and within alluvial fan material [(fig. 4.3 and 4.4)]. Faulting occurs over a zone approximately [5 km] 3 miles wide.

"Deformation is principally confined to the fault zone and downthrown block. Westward-dipping sandstones crop out along the base of Strawberry fault scarp at Indian and Trout Creeks * * * [(fig. 4.5)]. Near Trout Creek, deformation within the fault zone consists of an asymmetrical graben. Sandstone beds within the graben dip approximately 25° west. This structural style also occurs along Stinking Springs fault near Highway 40 and within the Indian Creek fault zone * * *."

4.3.3 Structural Origin of Strawberry Valley

"The major normal fault in Strawberry Valley is Strawberry fault * * *. The two westward trending faults south of the reservoir [(pl. 2)] * * * probably contribute little to the origin and overall geometry of the valley. Within the valley, the smaller Indian Creek fault in the southwest corner of the study area exhibits the same type of displacement as that on Strawberry fault. Absence of any continuous north trending down-to-the-east fault on the west side of the valley suggests a hinge type of motion resulting in a tilted block (half-graben) with Strawberry fault being the solitary bounding normal fault * * * [(pl. 2)].

"Based on the absence of down to the east faulting, the growth history of Strawberry fault, and similarities with the Idaho-Wyoming thrust belts, it is here suggested that Strawberry Valley is a half-graben bounded on the east by Strawberry normal fault. Strawberry fault is interpreted to be a westerly-dipping, listric normal fault that merges at depth with a ramp in the southern continuation of the Strawberry thrust zone * * *. Strawberry normal fault appears to reflect a more arcuate and southerly trace of the leading edge of the Charleston-Strawberry-Nebo thrust * * *, rather than a southwesterly trace as previously believed (Bissell, 1959; Astin, 1977).

"The Strawberry thrust zone lies at a depth between (2590 and 3350 m) 8,500 and 11,000 feet under Daniels Canyon in the western portion of the Co-op Creek quadrangle (Davis, 1979). At Indian Creek the Flagstaff Formation has been down-faulted [760 m]

Figure 4.3. The Strawberry alluvial fans, Strawberry fault, and Co-op Creek north of Strawberry Reservoir (Fig. 4.4) looking eastward. The two fault scarps cutting the fan surface and the main trace of the Strawberry fault in unit 3 of Van Arsdale, 1979a (in shadow just above fans) are clearly visible. The long terrace along Co-op Creek is entirely stream-cut.

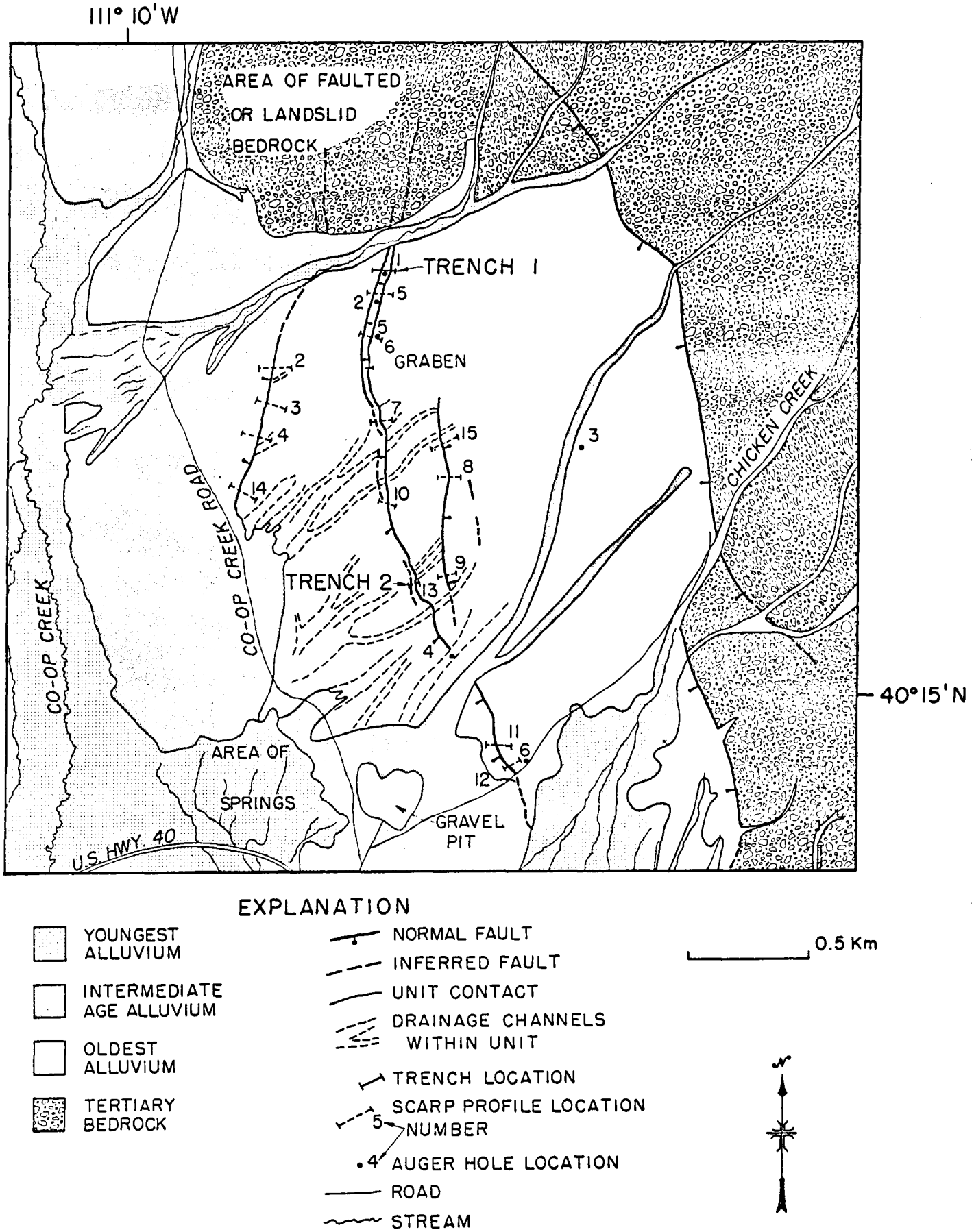

Figure 4.4. Sketch map of the Strawberry alluvial fans along Co-op Creek north of Strawberry Reservoir. The location of the Co-op Creek trenches across the largest fault scarp on the fans, the profiles measured across all 3 fault scarps, auger holes, drainage channels on the fans, and the main trace of the Strawberry fault at the head of the fans are shown.

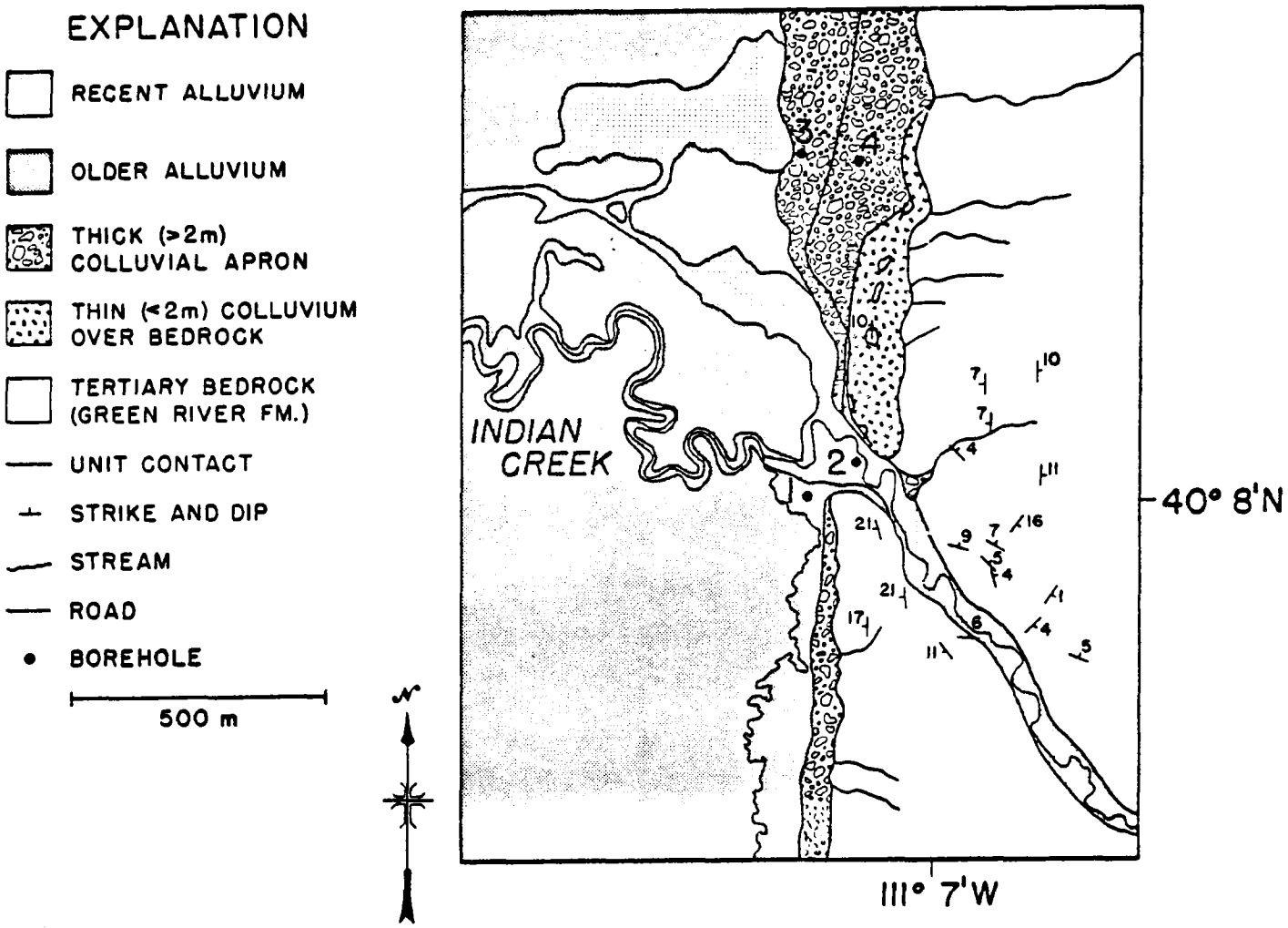

Figure 4.5. Sketch map of the area where Indian Creek flows across the Strawberry fault scarp showing the loaction of push-tube cores 1 and 2 (Fig. 5.5) and auger holes 3 and 4 (appendix B). The trace of the fault at the surface is close to the west edge of the thin colluvium unit. Near auger hole 4 the fault trace may bend or make an en echelon jump about 100m to the east. Westward dipping strike and dip symbols show drag within 400m of the fault in the Tertiary bedrock (regional dips about 10^{o} E-NE). Some more E-W oriented symbols along the canyon cut by Indian Creek may be due to adjustments of large slump blocks.

2,500 feet from an initial depth of approximately [3 100 m] 10,200 feet; therefore, the thrust zone at this locale probably lies at a depth exceeding [3 900 m] 12,700 feet. The Strawberry thrust zone thus plunges southward from its surface exposure in the eastern portion of the Co-op Creek quadrangle. Paleozoic and Mesozoic allocthonous rocks discend southward under Tertiary conglomerates in the southern portion of the Co-op Creek quadrangle, which also suggests a local southerly plunge to the Strawberry thrust zone."

4.4 Quaternary Geology

Accurate mapping and dating of Quaternary deposits are critical to seismic hazard assessment because displacement of Quaternary deposits where they overlie faults is usually the chief evidence for fault activity in the recent geologic past. Unfortunately, few extensive Quaternary deposits are preserved in the Strawberry Valley area, partially due to reservoir flooding of Strawberry and Soldier Creek valleys. Flood plains occur along Indian Creek south of Strawberry Reservoir, along the Strawberry River and Co-op Creek north of the reservoir, and in Soldier Creek Valley (Van Arsdale, 1979a, p. 22). The large alluvial fans north of Strawberry Reservoir are discussed in section 5.3. The only other deposits of any size are the high fluvial terraces along the central portion of Currant Creek (sec. 5.2.2) and landslides just south of Currant Creek Dam (Bissell, 1952, p. 618) and near Clarks Camp and Squaw Creek west and southwest of Strawberry Reservoir (pl. 2) (Van Arsdale, 1979a, p. 23). Minor areas of alluvium and colluvium occur throughout the area, and Bissell (1952) and Astin (1977) identified glacial deposits at higher elevations in the northern part of the area.

4.4.1 Chronology

No studies of the chronology of the Quaternary deposits in the area have been made, no doubt because the alluvial and colluvial deposits are difficult to relate to the climatic changes during the Quaternary which are the primary basis for correlation of Quaternary deposits. Astin (1977) suggested that major periods of alluvial fan sedimentation occurred during glaciations due to higher precipitation. However, precipitation was probably highest during the initial stages of deglaciation. The closest detailed work on Quaternary deposits in the region is that of Atwood (1909), Osborn (1973), Madsen and Curry (1979), Scott and others (1980), Sullivan and others (1983), Martin and others (1983), Shroba (1982), and Nelson and Krinsky (1982). These and other Quaternary studies in northeastern Utah and their regional correlation are discussed more extensively in Martin and others (1983) and Sullivan and others (1983).

Studies of Quaternary chronology in the Rocky Mountain region are only useful in a general way in providing soil profile development data for comparison with soils developed on the Co-op Creek alluvial fans (north of Strawberry Reservoir) and the terraces along Currant Creek (secs. 5.2 and 5.3).

Briefly, most Quaternary chronology studies in the Rocky Mountain region have subdivided deposits of the most recent major glaciations into those deposited during "Bull Lake" glaciation and "Pinedale" glaciation (Richmond, 1965; Madole, 1976; Pierce, 1979). In terms of soil development, soils on "Bull Lake" deposits commonly have weakly to strongly developed argillic B horizons with redder hues than underlying horizons, while soils on "Pinedale" deposits have only cambic to weak argillic B horizons (Birkeland and Shroba, 1974; Mahanney, 1978; Madole and Shroba, 1979; Pierce, 1979). Latest "Pinedale" and Holocene deposits commonly display soils without B horizons or with weak cambic horizons. Because the criteria used to subdivide these deposits into these relative-age groups (morphologic, surface and subsurface stone weathering, and soil development data) are relative within the local sequence, deposits from difference sequences in the region assigned to the same relative age group may be of widely differing ages (Pierce, 1979; Porter and others, 1982). We use these terms with quotation marks (for example, Nelson and others, 1979) to emphasize our use of them as informal regional quasi-geologic-climate units with time-transgressive boundaries based on major weathering and morphologic breaks in the local late Quaternary sequence.

However, numerical ages have been obtained for "Bull Lake" deposits in several areas (Pierce and others, 1976; Szabo, 1980; Colman and Pierce, 1981) and a number of 14C analyses set upper limits on the ages of the various phases of "Pinedale" glaciation (Porter and others, 1982). Many "Bull Lake" deposits are probably about the same age as those at West Yellowstone dated at about 140 Ka (Pierce and others; 1976); some others may correlate with the glacial event identified by Colman and Pierce (1981) dated at about 60 to 70 Ka. Although some may be as old as this latter event, most deposits assigned to a major "Pinedale" glaciation are probably in the range of 15 to 40 Ka (Pierce, 1979; Porter and others, 1982). Most latest "Pinedale" deposits are older than 11.5 Ka (Porter and others, 1982).

Closer to the Strawberry Valley, Shroba (1980, 1982) has calibrated age-dependent B- and Cca-horizon properties on deposits along the Wasatch Front using the age-dated stratigraphic framework of Scott and others (1980) and McCoy (1981). Late Holocene deposits lack B horizons, middle Holocene deposits have cambic B horizons, and early Holocene deposits have weak argillic B horizons, and Provo and Bonneville age deposits have only slightly better developed argillic horizons. Argillic horizons on deposits more than 100 Ka are thicker, more clayey, and generally redder than those on younger soils.

Despite the many problems in using relative soil development data for chronocorrelation (Birkeland, 1974; Pierce, 1979), careful comparison of quantitative relative-age data (such as soil profile parameters) from deposits of unknown age with similar data from these areas where numerical ages are available allows first approximation age limits to be set for the deposits of unknown age.

4.4.2 Geomorphology

The general Tertiary and Quaternary geomorphic development of the region is discussed by Sullivan and others (1983). Although little chronologic information is available, Van Arsdale's (1979a, p. 34-47; quoted below)

discussion of the geomorphology of the Strawberry Valley area (to which we have little to add) shows how Quaternary faulting continuing into the Holocene has influenced the drainage development of the area.

4.4.2.1 Fluvial

"Streams draining eastward from Strawberry Ridge [(pl. 2)] * * * into Strawberry Valley flow within strike valleys while many first order streams throughout the area flow down dip slopes, as mapped on aerial photographs. In general, however, second order and larger streams are consequent throughout the area (Threet, 1959). Strawberry Valley is structurally a single valley but includes Strawberry River and Indian Creek drainage basins. The drainage net of Strawberry River north of Strawberry Reservoir and those of Indian and Chipman Creeks south of the reservoir parallel the herringbone drainage pattern that lies to the east in the Uinta Basin.

"Most alluvial fans exhibit incised drainage and small, rather localized small areas of deposition. Sediment is largely bypassing the alluvial fans and entering the axial drainages of Strawberry River and Co-op Creek. Maximum alluvial thickness in the Co-op Creek quadrangle is estimated to be [27 to 37 m] 90 to 120 feet (Astin, 1977) whereas, south of Indian Creek, the valley floor is principally bedrock at the surface. Strawberry River has been aggrading recently as shown by alluvial drowning of bedrock inliers * * *. Alluviation has created a sharp angle between the inlier and the alluvium rather than the normal, gentle concave slope. The sharp angle also occurs along the sides of Strawberry Valley and up the tributary valleys. The present geomorphic processes appear to be alluviation of the valleys of axial streams, and erosion by tributary streams draining the sides of Strawberry Valley."

4.4.2.2 Structural Influence on Strawberry River and Indian Creek Valleys

"Indian Creek flows across an alluviated plain in Strawberry Valley and within a narrow bedrock canyon east of Strawberry fault [(pl. 2)] * * *. The bedrock canyon widens downstream into an alluviated plain which merges with the alluvial plain of Soldier Creek (now submerged beneath Soldier Creek Reservoir) * * *. Immediately east of Stinking Springs fault, Strawberry River again flows in a narrow bedrock canyon. This valley morphology and alluviation suggests that the area from Strawberry fault to Stinking Springs fault has been tilted down to the east * * *. Eastward tilting would promote downcutting in the upstream reach and lateral corrosion and alluviation in the lower reach. Soldier Creek drains approximately half of this easterly tilted block and flows southward along the base of Stinking Springs fault. Thus, the structural history and geomorphology of the alluviated valley of Soldier Creek is grossly similar to that of Strawberry Valley but of much smaller scale."

4.4.2.3 Pediments

"The area bounded by Strawberry Valley on the west, Soldier Creek on the east, Highway 40 on the north, and Strawberry River on the south shows relatively low topography and low relief [(pl. 2)] * * *. Two partially dissected pediment remnants capped by soil, and cobbles and boulders of quartzite, lie within this area [(southwest of C on pl. 2)] * * *. The pediments slope eastward at two to three degrees in their southern portions, and the underlying rocks of unit 2 dip northeast at approximately 9 degrees, resulting in a subtle truncation of structure * * *. Both pediments lie at approximately the same elevation. Pediment T [(T on pl. 2)] descends from [2440 m] 8000 feet in its northwest corner to [2330 m] 7640 feet in its southeast corner and pediment U [(U on pl. 2)] descends from [2400 m] 7880 feet in its northwest corner to [2300 m] 7560 feet in its southeast corner. Pediment T has eastward-flowing drainage which enters Badger Hollow Creek and pediment U has eastward-flowing drainage which enters Soldier Creek * * *. The pediments are cut in the lower and middle parts of unit 2 which contains few cobbles and no boulders. The cobbles and boulders which cover the pediments are believed to come from conglomeratic lenses stratigraphically higher in unit 2, which crop out in the headwaters of Badger Hollow Creek and Soldier Creek.

"The cross sections of Soldier Creek Valley and Badger Hollow are markedly asymmetric. Both valleys have a steep eastern side and a gentle-sloping pediment on the western side [fig. 4.1]. The asymmetry suggests that the creeks shifted eastward during incision. The pediments appear to have formed by lateral planation and incision by the two creeks. It is believed that as the creeks shifted eastward, cobbles and boulders derived from higher in the section, were deposited as a lag gravel.

"Soldier Creek and Badger Hollow Creek have approximately parallel courses for most of their upstream reach; however, in its lower reach, Badger Hollow makes a 90 degree turn to the southwest and enters Strawberry River * * *. Badger Hollow Creek appears to have undercut the northwest corner of pediment U, thereby producing the [37-m] 120-foot high Windy Ridge escarpment * * *. Windy Ridge, however, continues to the south beyond the point where Badger Hollow Creek turns southwest.

"Barbed tributaries of Badger Hollow Creek and Road Hollow Creek exist in the area where Badger Hollow Creek turns southwest * * *. The barbed tributaries suggest that the original drainage in this area was to the east as presently exists on pediment T. The barbed tributaries and the anomalous southwest bend in Badger Hollow Creek suggest that headward erosion along the lower reach of the present course of Badger Hollow Creek captured the headwaters of a previous, southeast flowing, higher-level course. The southern continuation of Windy Ridge may thus have formed by undercutting along a previous, south-east flowing, higher-level course of Badger Hollow Creek.

"A small graben has offset the pediment U surface by approximately [6 m] 20 feet [(pl. 2)] * * *. The southeast corner of pediment U also appears to have been truncated by movement on the Stinking Springs fault zone * * *. Thus movement on the graben, and at least the latest movement of Stinking Springs fault, appears to postdate the formation of pediment U.

"No faulted alluvial fans were found along Stinking Springs fault; however, the faulting of pediment U and the observation by Threet (1959) that Stinking Springs fault scarp still impounds the drainage on the upstream block certainly suggests recent movement along Stinking Springs fault."

4.5 Damsite Geology

4.5.1 Geomorphology

Soldier Creek Dam is located in the narrow gorge cut by the Strawberry River in the upper section of the Green River Formation (unit 3 of Van Arsdale, 1979a) on the upthrown side of the Stinking Springs fault about 180 m east of the fault scarp (fig. 1.1). No landslides or other significant geomorphic hazards have been identified at the damsite. The site geology has been well described by Thompson (1965, pp. 4-6):

"The right abutment is fairly steep having a slope of about 2-1/2:1 and is located on a long narrow north-trending ridge. This ridge is located between the gorge cut by the Strawberry River and the shallow valley eroded along the Stinking Springs fault. The ridge is about [50 m] 165 feet wide at crest elevation and is only about [335 m] 1100 feet wide from the stream channel to the fault trace. The ridge widens rapidly, however, downstream from the damsite. The left abutment is a fairly steep slope (about 2:1) which slopes up to a high, fairly flat-topped plateau, known as Currant Creek Mountain. The stream channel is about [46 m] 150 feet wide at the axis."

4.5.2 Stratigraphy

"The damsite is located entirely within members of the Green River formation. However, this is within the upper most members of the formation and is within rocks of the transition zone between the Green River and the overlying Uinta formation [units 1 and 2 of Van Arsdale, 1979a]. The Green River is typically lacustrine deposits. It consists predominantly of fairly even and continuous beds of siltstone and shale with some limestone and calcareous sandstone beds. At the damsite, the beds show definite fluvial action. Channels have been cut into the typical Green River beds and have been backfilled with clean sandstone. The lower portions of the channels are coarse-grained and include small lenses of conglomerates.

"The transition from the Green River to the Uinta is very gradual and a definite contact from one to the other is non-existent. The gradual change on the rocks at the damsite has

not affected them structurally, just lithologically, the sandstone beds are very lenticular, changing in short distances into siltstone and shale. The lenticular nature of the sandstone beds suggest deposition on meander curves of slow, heavily loaded streams. Correlation of bedding at the damsite, although not of any importance to the suitability of the site, is very difficult.

"The abutment rock is predominantly well cemented calcareous siltstone and interbedded calcareous sandstone with minor beds of shale and limestone. All of this rock has been eroded and backfilled by irregular sandstone channels. The shaley beds are softer and weather more easily than the other rocks. The sandstone within the old channels is the most resistant and stands as ledges on both abutment slopes. All of the rocks are of good quality; even the shales are fairly well cemented and of good quality. Distinct bedding occurs at [1.3 cm to 5 cm] 0.5 to 2 inch intervals in the shale and at [15 to 60 cm] 6 inch to 2 feet intervals in the siltstone. The sandstones are mostly massive and beddings are generally indistinct.

"There is very little overburden on the left side. A few feet of slopewash has accumulated at the base of the slope; otherwise only a few loose sandstone slabs and locally a few inches of lean clay derived from the weathering of the shale and siltstone cover the slope.

"The right abutment also has a few feet of slopewash at the base of the slope. Above that, the rock is exposed or is within a few inches of the surface all the way to crest elevation. On the downstream side of the axis, however, a considerable thickness of overburden has accumulated. The material consists of silty to clayey sand containing considerable angular sandstone talus, ranging in size from gravel to large blocks. Meandering of the stream when flowing at higher elevations has apparently cut into the rock and left fairly flat benches on which slopewash materials have accumulated. * * *"

4.5.3 Structure

"The Uinta formation constitutes the surface rock throughout most of the reservoir and surrounding area. Faulting, however, has exposed the upper beds of the Green River formation along the south and east side of the existing reservoir and also along the Strawberry River downstream from Stinking Springs. The bedrock formations are nearly horizontal with only a slight regional dip toward the east of about 3°. Drag along the faults has bent and badly broken the beds within the downthrown block for a few hundred feet upstream from the fault scarps, but appears to have had little effect on the overall structure of the area.

"The Stinking Springs fault scarp [(fig. 4.1)] is located about [120 m] 400 feet west from the right abutment at crest elevation. Amount of displacement is not easily discernible but is more than a few hundred feet vertically. The upthrown block at the site has exposed [90 to 120 m] 300 to 400 feet of upper Green River beds while the downthrown block is entirely of Uinta formation. Horizontal displacement appears to have been little if not insignificant.

"The fault is a zone about [1500 m] 5000 feet wide at Stinking Springs but the displacement is greater along the scarp at the east edge of the zone. The downdropped block is believed to be a small graben with the rocks broken and folded for only a few hundred feet upstream from the scarp. The beds of the upthrown block (the foundation rock of the dam) have been only slightly tilted to the west by the drag; otherwise, they have not been structurally affected and have remained unbroken and sound. The beds of the Uinta on the downthrown block are soft to moderately hard and incompetent. Being weak they have suffered the effects of the movement while the Green River beds are hard and competent and have remained essentially unchanged.

"The faulting does not present any structural problems at the damsite. The only significant structural defect of the foundation rock is the jointing. Regional joints spaced from [15 to about 76 cm] 6 to 30 inch apart are very prominent and are found throughout all of the exposed Green River formation. Two primary joint systems, both vertical, were recognized at the site, one trending N. 25-30° E., the other N. 50-55° W. Other joints are present which trend about north-south but are believed to be surface relief joints. All of the joints, as shown by the drill holes, are open near the surface but tighten with depth. Drilling has shown the joints, although open, are not badly weathered and some are filled with calcite. * * *"

5. SEISMOTECTONIC INVESTIGATIONS

5.1 Lineament Mapping

5.1.1 Methods

Seismotectonic investigations for Soldier Creek Dam began with an evaluation of previously mapped (Bissell, 1952; Stokes and Madsen, 1961; Baker, 1976; Astin, 1977; Van Arsdale, 1979a) and potential faults within 100 km of the dam which could generate earthquakes which would pose a hazard to the dam. This initial evaluation included a study of landsat imagery by Peterson and others.(1982) and a brief review of 1:60,000 and 1:80,000 scale black and white air photographs of most of this area. The imagery studies, existing mapping, and literature (Cluff and others, 1975; Anderson, 1979; Anderson and Miller, 1979; Swan and others, 1980), and concurrent USBR studies (Sullivan and others, 1983; Martin and others, 1983) show that the Wasatch fault, 45 km west of Soldier Creek Dam, is the most continuous and by far the most active tectonic structure in the area. All other structures at a greater distance from the dam were judged to pose much less hazard to the dam. Faults on the Wasatch Plateau (discussed by Sullivan and others, 1983) which extend to within 40 km of Soldier Creek Dam may pose some hazard to the dam, but ground motions from these structures would pose less of a hazard than those from the Wasatch fault. The hazard from the Wasatch Plateau faults will be addressed in future seismotectonic studies for Joes Valley and Scofield Dams. For these reasons, more detailed fault investigations were limited to those structures within 40 km of the dam.

With a more detailed review of 1:60,000 black and white air photographs in this area and 1:15,000 color photographs of selected areas nearer the dam, we identified most previously mapped faults and some additional lineaments suspected of being faults. Limited previous work in the area (Van Arsdale, 1979a) and our more detailed imagery review indicated that the Strawberry fault and the Stinking Springs fault, 8 and 0.2 km from the dam, respectively, were clearly the most active faults (definition of Wallace, 1981) in the vicinity of the dam. Thus, we limited our field reconnaissance of previously mapped faults and our identified lineaments (suspected faults) to those within 15 to 20 km of the dam (pl. 2).

During our field reconnaissance we attempted to confirm the presence of previously mapped faults in Tertiary or younger units as well as determine which of our mapped lineaments were faults. We divided these features into five categories (pl. 2):

a. Previously mapped faults for which we found good field evidence, such as an exposure of stratigraphic offset or prominent topographic expression of a fault scarp

b. Previously mapped faults where the field evidence was limited or ambiguous (less prominent or less continuous topographic expression and/or no exposures)

c. Previously inferred faults where field evidence was ambiguous (no exposures or topographic expression)

d. Additional faults identified in this study by stratigraphic offset or prominent topographic expression

e. Additional topographic lineaments which are strongly suggestive of faulting, but where field evidence is ambiguous

The faults and fault systems identified in the lineament study which were examined in the field reconnaissance are discussed below.

5.1.2 Faults in the Soldier Creek Area

5.1.2.1 Lower Currant Creek fault system (A on pl. 2)

These faults are 3 to 6 km in length, trend N. 5° E. and form a small horst. Discontinuous lineament segments extending southward on landsat imagery imply these faults might be longer than mapped (Peterson and others, 1982). The eastern two faults shown by Stokes and Madsen (1961), cut the Tertiary Uinta Formation. Stream alluvium is the only Quaternary unit which the faults cross, and no surficial offset was observed. Outcrops showing displaced bedrock units were found for each of the mapped faults in Currant Creek Canyon. Most appear to be expressed as topographic steps in ridge crests in the area.

5.1.2.2 Middle Currant Creek fault system (B on pl. 2)

These faults, shown by Stokes and Madsen (1961), are 8 to 13 km in length and trend N. 15° E., but edge-enhanced landsat imagery suggests these faults could extend much farther south (Peterson and others, 1982). No evidence of the two eastern inferred faults was found. The three other faults form a horst to the west (upstream side) and a graben to the east. Apparent vertical displacement on the center fault is about 15 m and about 10 m on the northernmost. Displacement on the southernmost fault could not be determined due to vegetation on exposures of the fault; however, topographic relief on ridge crests suggests a similar displacement. The faults offset the Tertiary Uinta and Duchesne River Formations (mapping of Stokes and Madsen, 1961). The only Quaternary units overlying the faults are stream alluvium and alluvial fans, both showing no surface offset (see sec. 5.2.2).

5.1.2.3 Northern Stinking Springs fault system (C on pl. 2)

This fault system trends N. 18° E. to N. 20° E. through the Tertiary Uinta and Duchesne River Formations. Four faults comprise this system forming two grabens and a horst. The Stinking Springs fault is mapped over a distance of 23 km, but its impressive physiographic scarp, extends for only 11 km with a maximum of 265 m of topographic offset (fig. 4.1). The main fault has 30 m of stratigraphic offset near U.S. Highway No. 40 (Van Arsdale, 1979a), but the height of the scarp to the south indicates considerably more offset of the segment forming the east shore of the present Solider Creek Reservoir. The remaining faults are 3 to 8 km long with about 60 m of topographic offset each. No bedrock exposures displaying offset bedding were found for these

faults. The east three faults are shown by Stokes and Madsen (1961), and the westmost was first mapped by Van Arsdale (1979a) (see sec. 5.2.2) Latest Quaternary alluvial fans and stream alluvium display no offset along the faults.

5.1.2.4 Southern Stinking Springs fault system (D on pl. 2)

This fault system, which trends N. 20° W. through the Uinta and Green River Formations, includes three faults shown by Stokes and Madsen (1961). A field investigation showed no offset beds in accessible areas although scarps suggestive of faulting extend for most of the mapped length of the faults. The two smaller faults are 8 and 17 km long, the longer of these extending south of plate 2. These faults displace Quaternary stream deposits were inaccessible for inspection; however, no topographic offset was observed on top of Willow Creek Ridge.

5.1.2.5 Fault system south of Strawberry fault (E on pl. 2)

These three faults, which trend N. 10° W. through the Uinta and Green River Formations, vary in length from 3 to 4-1/2 km. Exposures of the fault zone are partially to completely overgrown, impairing displacement measurements. The two eastern faults form a graben, but there are no exposures of the westernmost fault. Slope breaks along ridge crests suggest the easternmost fault may be a splay of the Strawberry fault (H on pl. 2). Tertiary fish scales were abundant in the Green River outcrops. Quaternary stream alluvium was not displaced in the fault zones.

5.1.2.6 Graben northwest of Willow Creek (F on pl. 2)

This graben trends due north about 1 km through the Uinta Formation. There is no bedrock exposure showing the fault, but the graben has about 60 m of topographic offset.

5.1.2.7 Willow Creek fault (G on pl. 2)

This fault inferred by Stokes and Madsen (1961) along Willow Creek is about 10 km long. Access to the canyon is difficult due to the steep topography and thick brush. No faulted bedrock is exposed, but the nearly horizontal Uinta Formation on the northwest side of the creek has been dropped to the same level as the older, also near horizontal, Green River Formation on the southeast side (Stokes and Madsen, 1961), indicating movement similar to the parallel Strawberry fault about 6 km to the northwest. This and the N. 35° E. trend of this fault suggest it could be a splay of the Stinking Springs fault. No inspection of the Quaternary stream alluvium in the creek valley was performed due to the inaccessibility of the canyon.

5.1.2.8 Strawberry normal fault system (H and I on pl. 2)

The main Strawberry fault (H on pl. 2) has previously been described by Van Arsdale (1979a) (sec. 4.3.2). The fault is mapped over a distance of 34 km, but its prominent topographic scarp extends from I on plate 2 to H, south of Strawberry Reservoir (28 km). Near the southern end of the fault (north of E on pl. 2) linear drainages and steps in ridge crests suggest a possible

southward splay off the fault or older northward extensions of the faults at E. Small inferred faults subparalled to the main fault southwest of The Narrows were mapped by Stokes and Madsen (1961) and inferred by Van Arsdale (1979a) on seismic evidence.

North of Strawberry Reservoir at Cow Hollow, a normal fault paralleling the main Strawberry fault was mapped in the Water Hollow tunnel (Thompson, 1971). It trends north, is of unknown length, dips 75 to 80° W., and lies 0.6 km east of the main fault. In a roadcut 2.5 km to the west on old U.S. Highway No. 40, a northeast-trending fault is exposed with Tertiary (?) gravels offset at least 3 m.

The main trace of the Strawberry fault makes an echelon jump to the west, north of Strawberry Reservoir, and then swings to the west where its striking topographic scarp dies out (I on pl. 2). Our mapping of the fault in this area (pl. 2) and the small parallel faults on the alluvial fan on the downthrown sides of the fault (fig. 4.4) (discussed in detail in sec. 5.3.2) is based on topographic expression of the fault scarp and differs only slightly from the earlier mapping of Astin (1977) and Van Arsdale (1979a).

5.1.2.9 Fault below Currant Creek landslide (J on pl. 2)

This fault is located about 0.8 km below the Currant Creek damsite. Investigation of this area was prompted by a lineament on the landslide formed by a lobe of the landslide creeping over an older surface of the landslide as evidenced by a buried soil. Closer inspection found a bedrock fault zone unrelated to the lineament trending due north with a near-vertical dip and a displacement in several fractures ranging from several centimeters to 2 m with faults both down to the east and down to the west. The fault displaces the Tertiary Currant Creek conglomerate, but the lack of bedding made displacement measurements difficult. The length of the fault zone could not be determined because there was no surface expression; no Quaternary deposits appeared displaced by the fault.

5.1.2.10 Fault west of Currant Creek Reservoir (K on pl. 2)

This fault was first mapped by Bissell (1952). Tertiary Uinta Formation is dropped down to the level of several Jurassic beds, but total displacement is unknown and there is no topographic expression of the fault. A search of the area turned up no offset Quaternary deposits; these may be covered by the thick forest. The fault is normal down to the west and convex eastward, suggesting a possible relationship with the Strawberry thrust sheet like that of the Strawberry fault (sec. 4.3.2).

5.1.2.11 Strawberry thrust faults (L on pl. 2)

This is the only area where the thrusts underlying Strawberry Valley are exposed. Mapping by Bissell (1952), Astin (1977), and Van Arsdale (1979a) shows the thrusts and associated small normal faults do not cut Tertiary units (except for the Strawberry fault). For this reason, we did not investigate these faults further.

5.1.2.12 Faults disclosed by the Water Hollow tunnel (M on pl. 2)

Five faults worth consideration were encountered in the tunnel (Thompson, 1971). Of these, only the eastmost and the westmost (Strawberry fault, sec. 5.1.2.8) showed any surface expression. The eastmost, 240 to 300 m in from the inlet portal, consists of several faults, each with a normal displacement from 0.3 to 30 m down to the east. This fault is traceable to an outcrop on Currant Creek just below Layout Canyon. Here the fault shows much jointing but only slight offset. The Quaternary stream deposits crossing the fault were not displaced. A 300-m-wide fault zone was encountered 2070 m in from the inlet. This, as well as the remaining faults in the tunnel, had no surface expression.

5.1.2.13 Grabens southwest of Strawberry Reservoir (N on pl. 2)

The eastmost graben was mapped by Van Arsdale (1979a). It is about 3 km long trending due north and narrowing northward. A probable extension of the graben is mapped south of Indian Creek. No outcrops displaying the fault were found, and some Quaternary stream deposits in Horse Creek appeared displaced; however, inspection showed the scarps to be caused by a resistant lens of limestone which had been eroded out of the shale surrounding it. No displacement of Quaternary deposits was found. The Streeper Creek graben cutting through the Tertiary Uinta Formation trends slightly east of north and lies about 3 km southwest of the previously mentioned graben. It is about 1 to 2 km long and shows a topographic offset of 60 m on the north edge. A faulted bedrock exposure in a roadcut indicates that the eastbounding fault extends south to Indian Creek Road making it about 3 km long. Hummocky topography makes the edge of the graben difficult to locate; however, no lineaments in the alluvium and colluvium were found.

5.1.2.14 Indian Springs faults (P on pl. 2)

These three faults are located at the headwaters of Indian Creek. They trend N. 10° W. and are 1 to 2 km long. The faults form a graben on the west and a horst on the east. Bedrock is Tertiary Uinta Formation primarily thin-bedded, friable shale. A field investigation of these air photograph lineaments turned up no exposures of faults; however, the abrupt change in slope, the steepness of the valley sides (considering the erodible nature of the bedrock) suggests fairly recent faulting. No fault scarps were discovered in the Quaternary alluvium in the bottom of the graben. Faults west of P on plate 2 mapped by Stokes and Madsen (1961) and Baker (1976) in the Rays Valley area will be investigated in future site-specific studies for the proposed Fifth Water Dam.

5.1.2.15 Currant Creek Mountain faults (R on pl. 2)

These faults are shown by Stokes and Madsen (1961). Field inspection disclosed normal faulting on the easternmost fault which was down to the west.

The westernmost fault is also normal with about 10 m of down to the east displacement measured just west of the junction of Timber Canyon with the Strawberry River. Apparent southward extensions of both faults are visible on enhanced landsat imagery (Peterson and others, 1982). Both faults

trend due north and displace the Tertiary Uinta Formation. Latest Quaternary stream alluvium deposited by the Strawberry River was not displaced across the faults.

5.1.2.16 Timber Canyon graben (S on pl. 2)

This graben was first mapped by us on 1:60,000 black and white air photographs. Field inspection showed abrupt vegetal and topographic changes along the edges of the graben. It trends N. 10° E. and extends for about 3 km. Quaternary stream alluvium along the east edge of the center of the graben is not offset. The area is extensively forested and bedrock exposures could not be found.

5.1.2.17 Additional faults

These are probable faults mapped by us on 1:60,000 black and white air photographs. In all cases, the striking linearity of the drainages suggests structural control, but no outcrops showing offset bedding could be found. The Timber Canyon and Avintaquin Canyon lineaments, in the laterally continuous Green River Formations, were not measured for offset since equivalent beds on either side could not accurately be determined and because there was no evidence of recent movement in the canyons.

5.1.3 Lineament assessment study

The lineament study indicates that the north-south trending Strawberry and Stinking Springs faults have by far the most pronounced and continuous topographic expression of any faults in the area and are therefore very likely the most recently active. We found no direct evidence that other faults offset Quaternary deposits. Further investigations in the region centered on the area around the Stinking Springs and Strawberry faults.

5.2 Stinking Springs Fault

The Stinking Springs fault is the closest probably active tectonic structure to Soldier Creek Dam (pl. 2; fig. 1.1). However, the only Quaternary deposits crossing the fault which might be used to assess the recent geologic activity of the fault (Van Arsdale, 1979a, p. 22) now lie under Soldier Creek Reservoir.

5.2.1 Colluvial wedge adjacent to the fault

A reconnaissance of the deeply dissected colluvial wedge extending westward from the Stinking Springs fault scarp just south of U.S. Highway No. 40 (fig. 5.1) (mentioned by Van Arsdale, 1979a, p. 23) did not provide any conclusive evidence of movement or stability on the fault. The colluvium is almost entirely fine-grained, and easily recognized marker beds in the deep gully extending down the center of the wedge do not extend far enough to determine if any beds of colluvium have been displaced. Soil profile development on the colluvium is minimal, and amino acid ratios (free aIle/Ile ratios) on snail shells (table 5.1) collected from as deep as 6.5 m in the gully suggest all the exposed colluvium is no older than Holocene.

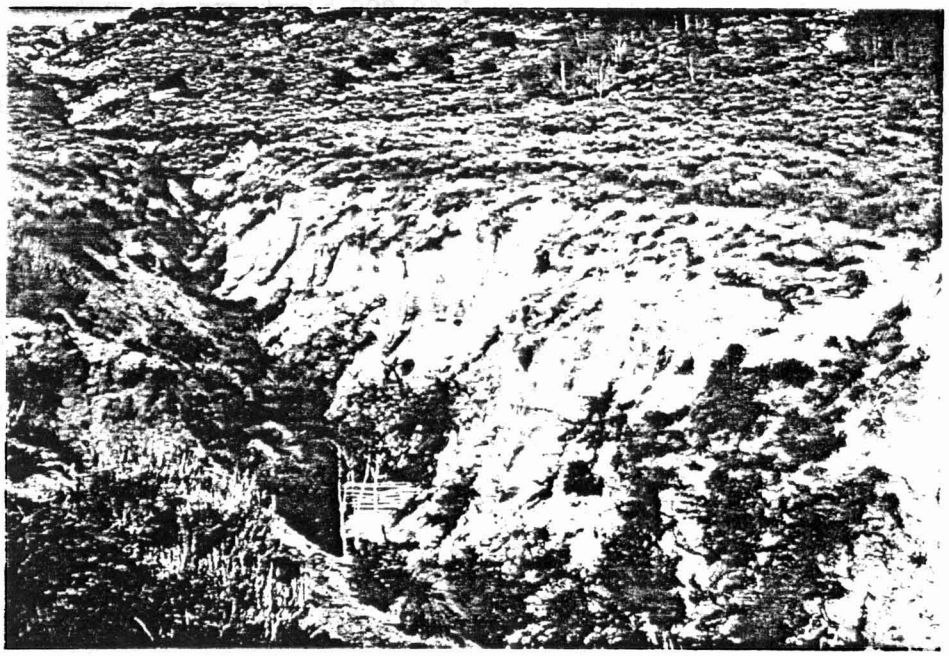

Figure 5.1. Part of the upper section of the gully eroded into the wedge of fine-grained colluvium near the base of the Stinking Springs fault scarp 0.4 km south of U.S. Highway 40. The dark layers in the colluvium are former A horizons of soils developed on the colluvium during periods of relative stability, but no beds of coarse-grained material which could be related to movement on the fault could be traced for more than a few tens of meters. Thus, the entire wedge may have been deposited by gradual slopewash and alluviation unrelated to faulting. Free amino acid fraction aIle/Ile ratios (Table 5.1) suggest the entire section of exposed colluvium is of Holocene age.

Table 5.1. - D-alloisoleucine/L-isoleucine ratios in free and total (free + peptide-bound) amino acid fractions and calculated ages for fossil gastropods from the Strawberry Valley area, Utah

INSTAAR Lab. No.	Depth below surface (m)	Species	Sample weight (mg)	Alle/Ile ratio 1/ free	Alle/Ile ratio 1/ total	14C age (yr BP x 10^3)	Estimated mean diagenetic temperature (°C) 2/ Minimum	Estimated mean diagenetic temperature (°C) 2/ Maximum	Calculated age (yr BP x 10^3) 3/ Minimum	Calculated age (yr BP x 10^3) 3/ Maximum
Indian Creek, Wasatch County, Utah (SW1/4 NW1/4, sec. 15, T. 4 S., R. 11 W.) (fig. 4.5)										
Core 1										
DAN-125A	1.9	Vallonia cyclophorella	2.5		0.039	8.2		6.5	-	-
DAN-125H	1.9	Vallonia cyclophorella	2.6		0.030	8.2	-	4.4	-	-
DAN-125J	1.9	Pisidium	6.0		0.060	8.2	-	9.5	-	-
DAN-125B	1.9	cf. Lymnaea	8.2		0.038	8.2	-	6.3	-	-
DAN-125D	1.9	cf. Lymnaea	4.5		0.030	8.2	-	4.4	-	-
DAN-125E	1.9	cf. Lymnaea	8.1		0.150	(reworked)	-	-	-	-
DAN-125C	1.9	Pupilla muscorum	3.3		0.030	8.2	-	4.4	-	-
DAN-126A	6.7	Vallonia cyclophorella	3.0		0.089	(probably reworked)	-	-	-	-
DAN-126E	6.7	Vallonia cyclophorella	4.2		0.061	>37	-2	1.5	-	73
DAN-126F	6.7	Vallonia cyclophorella	2.2		0.080	(probably reworked)	-	-	-	-
DAN-126B	6.7	Pupilla muscorum	4.8		0.090	(probably reworked)	-	-	-	-
DAN-126C	6.7	Pupilla muscorum	5.1		0.082	(probably reworked)	-	-	-	-
DAN-126D	6.7	Pupilla muscorum	7.6		0.070	>37	-2	2.4	-	86
DAN-128A	7.0	cf. Lymnaea	6.5		0.127	(reworked)	-	-	-	-
DAN-128B	7.0	Pupilla muscorum	0.8		0.067	-	-2	2.4	35	82
DAN-127	9.1	cf. Lymnaea	1.0		0.135	(reworked)	-	-	-	-
DAN-133A	10.5	Pisidium	2.0		0.103	-	2	5.4	33	62
DAN-133B	10.5	Pisidium	2.0		0.116	-	2	5.4	37	71
DAN-133C	10.5	Vallonia cyclophorella	2.2		0.083	-	-2	1.5	54	105
Core 2										
DAN-130A	1.5	cf. Lymnaea	8.1		0.015	3.0	1.5	-	-	-
DAN-130B	1.5	cf. Lymnaea	5.2		0.015	3.0	1.5	-	-	-
DAN-130C	1.5	cf. Lymnaea	20.3		0.017	3.0	3.6	-	-	-
DAN-129	1.6	cf. Lymnaea	5.1		0.037	(reworked)	-	-	-	-
Stinking Springs fault colluvial fan arroyo, Wasatch County (NE1/4 SW1/4, sec. 33, T. 3 S., R. 10 W.)										
DAN-113	6.0	Pupilla	0.6	0.06		Low free ratios in all these samples indicate they are probably all of Holocene age.				
DAN-114	3.5	Pupilla	0.8	0.02						
DAN-115	1.6	Pupilla	2.0	0.02						
DAN-117	5.0	Pupilla	0.7	0.04						
DAN-118	2.8	Pupilla	1.3	0.06						

1/ Alle/Ile ratio (peak heights) measured using methods of Miller and Hare (1980).
2/ Mean effective diagenetic temperature (Wehmiller and others, 1977) estimated from the regional data of McCoy (1981) and Porter and others (1982), and the effective diagenetic temperature calculated using listed 14C dates for calibration samples assuming Arrhenius parameters determined for Lymnaea by W. D. McCoy (1981), using 14C dated samples, heating experiments, and values of constants in Arrhenius equation (No. 9 in Williams and Smith, 1977).
3/ Age calculated using equation 18 in Williams and Smith (1977) with K' = 0.77 and modern ratio of 0.011.

5.2.2 Currant Creek terraces

The mapped trace of the Stinking Springs fault bends to the northeast north of U.S. Highway No. 40 (pl. 2). Lineaments and mapped faults (Stokes and Madsen, 1961) parallel with the northern segment of the fault trend into the area where two high fluvial terraces are preserved along the southwest side of Currant Creek valley (fig. 5.2). The terraces do not appear displaced, suggesting major displacements on these faults predate the deposition of the terraces. A soil profile on the lower terrace (table 5.2; app. A, profile SC-4) is not strongly developed, suggesting an approximately "Pinedale" age for the soil (sec. 4.4.1). However, the height of both terraces above the present Currant Creek (37 and 73 m) suggests both terraces are much older, probably of at least "Bull Lake" age (sec. 4.4.1). The surface of the lower terrace has probably been eroded (making the soil indicative of only a minimum age).

5.2.3 Faulted pediment west of the fault

The soil profile developed on the faulted pediment (U on pl. 2; sec. 4.4.2.3) was investigated to determine if the profile would provide any clues to the age of the pediment. Augering to 5-m depth on the upthrown side of the graben on pediment U just south of U.S. Highway No. 40 and examination of a few small exposures on the edge of the pediment showed that the pediment surface is being eroded relatively rapidly and that the soil on the pediment is much younger than the original pediment surface and probably the graben as well.

5.2.4 Assessment summary

Although the geomorphology along the central portion of the Stinking Springs fault indicates it has experienced repeated Quaternary displacement (fig. 4.1), we have been unable to make a more detailed assessment of its movement history. For this reason, we have assumed, as suggested by its structural and physiographic similarity with the Strawberry fault, that its movement history has been similar to that of the Strawberry fault where deposits are available for a more detailed assessment.

5.3 Strawberry Normal Fault

Two areas of Quaternary deposits adjacent to the prominent topographic scarp (28 km long) of the Strawberry fault were selected for detailed study to obtain data on the recent movement history of the fault. Two trenches were excavated across the fault scarps in a large alluvial fan complex previously studied by Van Arsdale (1979a) in the Co-op Creek quadrangle north of Strawberry Reservoir (pl. 2; fig. 4.3). Push-tubing coring in the second area, the alluvial plain along Indian Creek south of the reservoir (pl. 2; fig. 4.2), also provided some information on the slip rate of the fault.

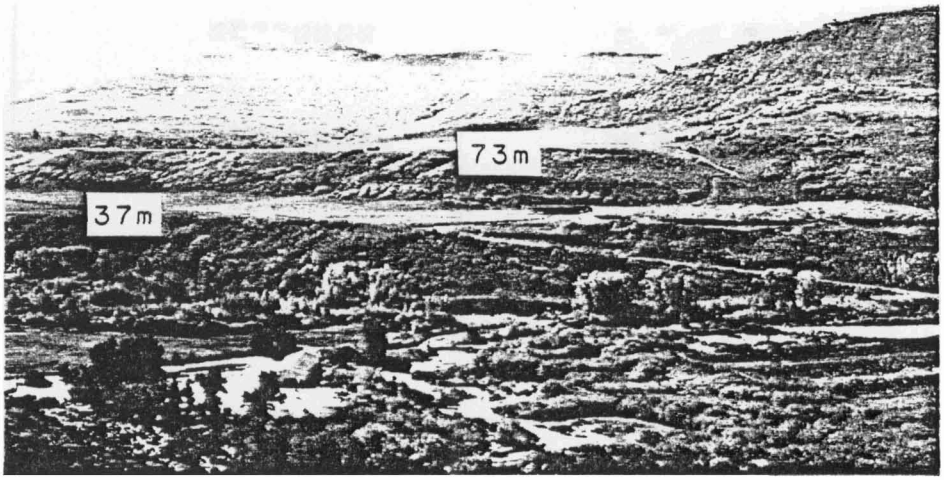

Figure 5.2. Fluvial terrace remnants at 37m and 73m above Current Creek just south of its confluence with Water Hollow. The northern end of the Stinking Springs fault system is mapped through the ridge in the background and trending through the terraces, but the terraces do not appear to be displaced.

Table 5.2. - Data summary for soil profiles from Strawberry Reservoir area

Profile	Horizon 1/	Average depth (cm)	Parent material	Munsell dry color	Estimated percent by volume			Percent by weight 2/			0.5μ/2μ 3/ (clay)	Percent 4/ carbonate	Percent 5/ organic matter
					Gravel (0.2 - 8 cm)	Cobbles (8 - 25 cm)	Boulders (>25 cm)	Sand (2 - 0.5 mm)	Silt (50 - 2 μm)	Clay (<2 μm)			
Co-op Creek Trench 1													
SC-1	A1	0-10	Colluvium	10YR 3/3	10	25	5	45	36	19	0.60	0	10.1
	A2	10-38	Colluvium	10YR 3/3	10	25	5	49	33	18	0.57	0	3.4
	2E	38-60	Alluvial fan	5YR 7/5	10	25	5	57	28	15	0.57	0	0.3
	2Bt	60-114	Alluvial fan	2.5YR 5/6	10	20	2	52	25	23	0.77	0	0.2
	2C	114-149	Alluvial fan	2.5YR 5/6	25	10	0	55	26	19	0.85	0	0.3
	2Ckj	149-210	Alluvial fan	2.5YR 5/7	25	10	0	54	28	18	0.88	12	0.2
	3Ckj	210-273	Alluvial fan	5YR 6/7	10	5	30	80	14	6	0.89	11	0.1
	4Ckj	273-334+	Alluvial fan	5YR 6/7	30	15	0	64	22	14	0.86	8	tr
SC-2	A1	0-26	Colluvium	7.5YR 4/3	5	0	0						
	A2	26-58	Colluvium	7.5YR 4/3	5	0	0						
	A3	58-80	Colluvium	7.5YR 4/3	5	0	0						
	E	80-110	Colluvium	7.5YR 5/4	1	0	0						
	2Bw	110-155	Colluvium	7.5YR 6/4	1	0	0						
	2C	155-230	Colluvium	7.5YR 6/4	1	0	0						
	3C	230-300+	Alluvium	7.5YR 6/4	15	20	5						
Co-op Creek Trench 2													
SC-3	A1	0-11	Colluvium	7.5YR 5/4	10	0	0	38	40	22	0.59	0	7.3
	A2	11-76	Colluvium	7.5YR 5/4	10	0	0	40	38	23	0.62	0	2.6
	A3	76-105	Colluvium	7.5YR 5/4	10	0	0	40	38	22	0.33	0	2.3
	Bw	105-149	Colluvium	5YR 6/7	15	5	0	36	42	22	0.31	0	0.5
	2CB	149-183	Colluvium	5YR 7/3	20	10	0	61	30	9		0	0.2
	2C1	183-204	Colluvium	5YR 7/5	20	20	0	64	28	9		0	0.1
	2C2	204-279	Colluvium	5YR 7/5	20	20	0	60	28	12		0	0.1
	3C	279-360+	Alluvial fan	2.5YR 5/6	5	10	0	49	29	22		0	0.2
Currant Creek Terrace													
SC-4	A1	0-8	Outwash	7.5YR 5/3	40	15	2						
	A2	8-23	Outwash	7.5YR 4/4	40	15	2						
	Bw	23-80	Outwash	5YR 5/7	40	15	2						
	Cwj1	80-122	Outwash	7.5YR 5/6	40	15	2						
	Cwj2	122-140+	Outwash	7.5YR 6/6	40	15	2						

1/ Nomenclature follows Soil Survey Staff (1981) with addition of "j" (Canada Soil Survey Committee, 1978) for horizons with minimal development.
2/ Particle size distribution of <2 mm fraction using sieve-pipette methods (e.g., Carver, 1971) and Sedigraph for some silt-clay fractions with prior removal of carbonates and organic matter using methods of Jackson (1956).
3/ Fine to total clay ratio from Sedigraph analysis.
4/ Percent carbonate by method of Dreimanis (1962).
5/ Percent organic matter by Walkley-Black (1934) method.

5.3.1 Co-op Creek alluvial fan complex

5.3.1.1 Geomorphology

a. Drainage channel morphology. - Van Arsdale (1979a, p. 38) used the morphology of drainage channels on the Co-op Creek alluvial fans (fig. 4.4) to argue that the faulting indicated by the fault scarps on the fans was relatively recent and concurrent with southerly tilting of the fan complex. He (1979a, p. 38) noted that:

> "The alluvial fan drainage * * * may be divided into gullies with symmetrical cross sections and gullies with asymmetrical cross sections. The largest streams head in the mountains east of the fans, have symmetric cross sections, and are unaffected where they cross the two prominent fault scarps * * *. Large gullies that head on the fans have asymmetrical cross sections and also are unaffected where they cross the scarps. Small gullies heading on the fans have asymmetric cross sections and are vertically offset at the two scarps. The greater erosional capacity of the larger gullies has apparently reduced the vertical offset and produced smooth profiles across the scarps while the smaller streams have not. Small alluvial fans lie at the base of the scarps where fan drainage has been vertically offset * * *.
>
> "The asymmetry of the gullies heading on the fans is constant with steep southern banks and long, gentle northern banks * * *. This asymmetry is believed due to tilting of the fan complex down to the south. * * *. The fault scarps * * * increase in height from 0 displacement in the south to heights near [8 m] 25 feet in the north, thereby also suggesting a down-to-the-south tilt * * *."

b. Fault scarp morphology. - Van Arsdale (1979a, p. 42) also estimated the age of the faulting on the alluvial fans using the scarp morphology methods of Wallace (1977) and Bucknam and Anderson (1979). He measured 23 scarp profiles across the longest fan scarp (fig. 4.4) and reached the following conclusions:

> " * * * Like the areas studied by Bucknam and Anderson, Strawberry Valley is semiarid, and the principal vegetation cover on the fans is sagebrush (Artemisia tridentata). The regression equation for the Strawberry fault scarp is $\theta = -3 + 27.54 \log H$, and the regression coefficient is significant at the .01 level [(VA on fig. 5.3)] * * *. Since it is not known whether fault scarp angles are normally distributed, the nonparametric Spearman Rank Correlation Coefficient test was performed. A correlation between scarp angle and scarp height was found to be significant at the .05 level.
>
> "Measurements of the Strawberry scarp profiles principally lie between regression lines for data from fault scarps in the Drum Mountains and near Panguitch, thus suggesting

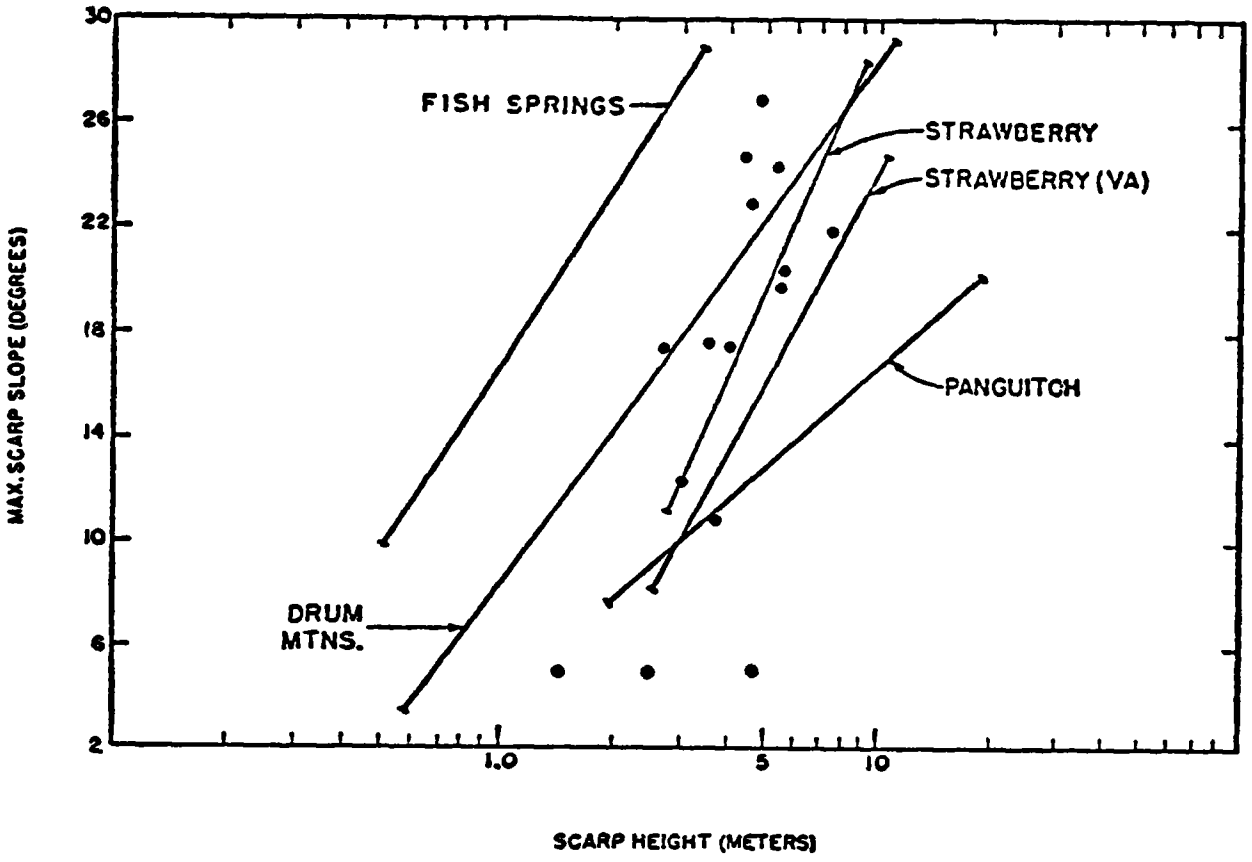

Figure 5.3. Regression lines for maximum slope angle versus log of scarp height for fault scarps in unconsolidated sediment from Fish Springs (<<12 ka), the Drum Mountains (about 12 ka), and Panguitch (possibly 100 ka)(from Bucknam and Anderson, 1979), an earlier study of the Strawberry alluvial fans (VA) by Van Arsdale (1979a), and this study of the Strawberry alluvial fans. Dots are data from this study only.

> that the most recent movement along Strawberry fault was between 12,000 and 100,000 years ago [(fig. 5.3)] * * *. However, although the scarp profile data supports the regression line is steeper than the Drum Mountains and Panguitch data, thus making the application of these regression lines to the Strawberry Valley data questionable * * *."

We also measured 14 scarp profiles on upper, lower, and a small eastward facing scarp on the alluvial fans using the methods of Bucknam and Anderson (1979). A regression line for our data (Strawberry on fig. 5.3) is very similar to Van Arsdale's (1979a) [Strawberry (VA) on fig. 5 3]. We also applied the methods of Nash (1980) in estimating the age of the scarps from profile data, but the scatter in our data (dots on fig. 5.3) does not allow a more accurate age estimate than Van Arsdale's (1979a). Stratigraphic data from trenching across the scarps (discussed below) show the scarps are the product of multiple faulting events, probably extending over the younger portion of the timespan suggested by Van Arsdale (1979a).

5.3.1.2 Scarp trenching

a. Co-op Creek trench 1. - A 91-m-long, 1.5- to 2-m-wide trench (CC-1) was excavated across the longer, 7-m scarp on the alluvial fans and the linear graben parallel to it (figs. 4.3, 4.4). The shored portion of the trench averaged 2.5 to 4 m in depth, but between stations 25 and 27 and between stations 40 and 42 the trench was excavated to 7.6 and 5.7 m respectively (pl. 3). These zones were backfilled to the depths indicated on plate 3 before shoring because initial examination of these zones from the top of the trench did not indicate any significant change in lithology with depth. Hydraulic vertical shoring every 2-m with 20-cm wide horizontal wooden lagging every 1 m and 10-cm mesh wire fencing over each wall of the trench prevented logging the entire south wall (dots on pl. 3 show inferred contacts covered by lagging).

Lithology, degree of stratification, sharpness of contacts, and unit geometry and its relationship to the present ground surface were used in our interpretation of the genesis of stratigraphic units. Because both alluvial and colluvial units are derived from the faulted alluvial fan sediments and transported minimal distances, many units of different genesis look very similar. Proximal fault-scarp-derived colluvium is particularly difficult to distinguish from the stream-reworked colluvium and alluvial fan sediment into which it grades laterally. Furthermore, intense rainfalls on the alluvial fan may have resulted in the deposition of units off the fan fault scarps which we have interpreted as fault-related colluviums. Our interpretation of the stratigraphic sequences in both trenches is conservative (from a hazard viewpoint); where available evidence suggests possible fault displacement we have assumed it. Fortunately, uncertainty in the genesis of particular stratigraphic units does not affect our conclusions on the hazard posed by the Strawberry fault.

(1) Stratigraphic units. -

(a) Alluvial fan sediments. - The trench exposed well to nonstratified braided stream and debris flow deposits on the upthrown block and western third of the trench (units 1 through 7, pl. 3; table 5.3). Very similar materials were encountered in five 50-cm (18-in) diameter auger holes elsewhere on the alluvial fans (fig. 4.4). The well-stratified stream deposit, unit 6, is not found on the upthrown block, suggesting a facies change typical of alluvial fan sediments (Bull, 1977) or an unconformity at the base of unit 7. Thus, the age of unit 6 relative to units 1 through 5 is not known. The thickness, lithology (table 5.3), stratigraphic position, and soil profile developed on unit 7 (unit 7B is an argillic horizon and units 7E and 16 eluvial horizons) (table 5.2; app. A, profile SC-1) indicate the same unit is present along both the eastern and western thirds of the trench.

The contacts between the alluvial fan units dip gently westward paralleling the surface of the fan. The alluvial fan units are the oldest units in the trench, and there may be unrecognized unconformities between some of the units.

Based on projections of the fan surface above and below the graben, the net vertical tectonic displacement of the alluvial fan units (Swan and others, 1980) across the fault zone was only about 1.2 m. However, over most of the graben (stations 32-63, pl. 3) the alluvial fan units have been displaced below the bottom of the trench (apparently >6 m at station 45; see note 4, pl. 3). In fault zone 3 units 1, 2, and 3 have been offset about 1 m (table 5.4) by a fault dipping 63° striking perpendicular to the trench about 1 m west of an apparent step in a conglomeratic facies of the Tertiary bedrock. The shear zone is thin (1 to 5 cm wide) and difficult to discern in places because of the lithologic similarity and heterogeneity of the alluvial fan units. This fault was not recognized prior to logging the trench, but must extend through the excavated but unshored portion of the trench between stations 29 and 32 (n1, pl. 3).

(b) Stream-reworked colluvium and alluvial fan sediments. - In the graben portion of the trench, between stations 33 and 63, somewhat better sorted, poorly to moderately stratified units (8 and 10; table 5.3) near the bottom of the trench are interpreted as fan sediments and fault and stream-scarp-derived colluvium reworked by intermittent streams flowing parallel with the scarp through the graben. The reworked colluvial deposits were probably produced by faulting events predating those represented by the colluvial units in the trench. The better sorting of unit 10b than in 10a suggests a shift of the stream axis to the west. The genesis of units in this part of the trench is not clear, but the gradational facies changes between 10b and unit 7, and between units 8 and 6, suggest lateral westward erosion of units 6 and 7 obliterating what was probably a fault scarp forming the western edge of the graben (fault zone 2). The highly unconsolidated character of the units between stations 50 and 63 may indicate mechanical adjustment (and resulting

Table 5.3 - Lithologic description of stratigraphic units in Co-op Creek Trench 1

Stratigraphic Unit	Subunit	Description	Munsell color 1/	Matrix texture 2/	Estimated percent by volume: Pebbles	Cobbles	Boulders	Angularity (percent) 3/: A	SA	R	WR	Carbonate 4/: Reaction	Stage	Lower boundary 2/: Distinctness	Topography	Remarks
Alluvial fan deposits																
1		Fine gravelly alluvium	2.5YR6/7													
	1a 5/		2.5YR5/6	Sandy loam	25	0	0	12	38	42	8	0	0	-	-	Prominent internal stratification with minor lenses of fine sand
	1b				20	0	0	10	40	42	8	0	0	Clear	Smooth	
	1c	Bouldery		Loamy sand	40	3	50	9	35	38	18	0	0	Clear	Smooth	Some fine gravel lenses; rare very thin seams of carbonate
2		Gravelly debris flow	2.5YR5/7	Loamy sand	-	-	-	-	-	-	-	0	0	Abrupt	Smooth	Some fines may be due to infiltration
	2a															
	2b	Bouldery			40	3	50	10	38	42	20	0	0	Clear	Smooth	Some fine gravel lenses; rare very thin seams of carbonate
	2c				35	2	0	12	42	30	16	0	0	Gradual	Smooth	
3		Cobbly alluvium	2.5YR6/7	Sandy loam												
	3a		2.5YR6/6		60	20	0	24	41	32	3	0	0	Abrupt	Smooth	
	3b				60	2	0	-	-	-	-	0	0	Gradual	Smooth	
	3c		2.5YR5/7	Loamy sand	20	30	0	0	48	44	8	0	0	Gradual	Smooth	
4		Coarse gravelly alluvium	2.5YR6/7	Loamy sand	70	3	0	8	53	32	7	M=4; C=4	1-	Clear	Smooth	Well stratified and clast-supported
5		CO_3 - rich bouldery debris flow	2.5YR6/7	Loamy sand	25	10	30	8	39	47	6	M=4; C=3	1	Clear	Smooth	Nonclast-supported; fine gravel lenses on top of unit; carbonate on clast bottoms
6		Well-stratified gravelly alluvium	5YR6/4	Loamy sand	-	-	-	-	-	-	-	M=4; C=4	1	-	-	Well stratified with beds of medium gravel and cobbles
7		Cobbly debris flow	2.5YR5/6	Sandy loam	25	5	2	11	44	39	6	M=2	1-	Clear	Wavy	
	7B	Bt soil horizon	2.5YR5/8	Sandy clay loam	20	5	2	10	44	38	8	0	0	Gradual	Wavy	No internal stratification, but gravel lenses and 10- to 20-cm thick fine sand lenses at base of unit; rare carbonate mottles
	7E	Elluvial soil horizon	5YR7/5	Sandy loam	20	3	0	3	42	37	18	0	0	Abrupt	Wavy	Angular blocky structure; argillans (see soil profile description No. 1; App. A)
Stream-reworked colluvium and fan deposits																
8		Well-stratified sandy alluvium	2.5YR6/8 to 5YR7/4	Sandy loam	40	3	0	0	48	32	20	M=4	1+	-	-	Well-stratified; carbonate mostly in upper part of unit on clast bottoms; clay mottles (2.5YR5/8); its stratigraphic position suggests the eastern 6m of this unit may be scarp-derived colluvium
Stream-reworked alluvium																
10		Sandy alluvium		Loamy sand												
	10a		5YR7/4		10	20	2	4	36	44	16	0	0	Clear	Smooth	Poorly stratified with some gravel lenses
	10b	Loose structure	5YR7/4		10	10	0	8	36	36	20	0	0	Abrupt	Smooth	Generally nonstratified but poorly stratified zones with gravel lenses
	10E	Elluvial soil horizon	7.5YR7/4		10	10	0	-	-	-	-	0	0	Diffuse	Irregular	
Scarp-derived colluvium																
9		Gravelly colluvium	5YR6/6	Loamy sand	10	5	0	-	-	-	-	0	0	Abrupt	Smooth	Very gradational lateral facies change with unit 10a; clay mottles
11		Sandy colluvium														
	11a		5YR6/8 to 7.5YR7/4	Loamy sand	5	0	0	-	-	-	-	0	0	Abrupt	Smooth	Weak prismatic structrue; clay mottles
	11b	Cobbly			5	15	0	-	-	-	-	0	0	Gradual	Smooth	
12		Fine-grained colluvium	7.5YR6/4	Silt loam	5	0	0	4	64	32	0	0	0			
	12B	B soil horizon	7.5YR6/4	Sandy clay loam	3	0	0					0	0	Abrupt	Wavy	
13		Sandy colluvium		Sandy loam												
	13a	Cobbly	2.5YR5/6		10	40	0	4	44	32	20	0	0	Abrupt	Wavy	Cobbly bed with cobbles parallel to dip at base of unit
	13b		5YR6/7		10	3	0	4	48	44	4	0	0	Abrupt	Smooth	
14		Sandy colluvium	5YR7/5	Sandy loam	25	5	0	4	48	39	9	0	0	Clear	Smooth	
15		Loose sandy colluvium	10YR5/3	Loamy sand	15	30	0	-	-	-	-	0	0	Clear	Irregular	
Near-surface colluvium																
16		Thin slope wash and elluvial horizons on older units	5YR7/4 to 7.5YR7/3	Sandy loam	20	5	0	8	40	44	8	0	0	Clear	Wavy	Lithology of unit varies depending on underlying units
17		Modern A soil horizon	7.5YR4/3 to 10YR3/3	Loam	7	0	0	0	56	40	4	0	0	Clear	Wavy	Lithology of unit varies depending on underlying units

1/ Dry color of Oyama and Takehara (1967).
2/ Methods of Soil Survey Staff (1975).
3/ Scale: A = angular, SA = subangular, R = rounded, WR = well rounded.
4/ Scales of Soil Survey Staff (1975) and Bachman and Machette (1977): M = matrix, C = clasts.
5/ Lowercase letters denote subunits distinguished by minor lithologic differences and pronounced bed contacts.

Table 5.3
Unit descriptions
in Co-op Creek Trench 1

Table 5.4 - Correlation of stratigraphic units, soils, and fault events in the Co-op Creek trenches and estimated displacements

Co-op Creek Trench 1								Co-op Creek Trench 2							
Stratigraphic units	Units partially formed by soil processes	Fault Event	Fault Zone	Stratigraphic displacement (m) Estimated from colluvial wedge thickness 1/	Total stratigraphic	Preferred estimate	Proportion of measured cumulative 2/ net vertical tectonic displacement (m)	Stratigraphic units	Units partially formed by soil processes	Fault Event	Fault Zone	Stratigraphic displacement (m) Estimated from colluvial wedge thickness 1/	Total stratigraphic	Preferred estimate	Proportion of measured cumulative 2/ net vertical tectonic displacement (m)
1-5								1							
6															
7	7B	a	1	>1.4	>0.7	?	?	2	2B						
8		b	1	>1.8->4.8	<1.9	1.8	0.4			a 5/	1	>2.8	3.2	3.0	5/ 1.8
9	7E							3a	2E						
10		c?	1	>1.8->3.8	<2.2-4.5	3.2	0.8								
	10E		2	-	1.3±0.5	1.3	-0.3	3b and 3c							
11a															
11b	11bE														
12				E 3/ W 4/	E W	E W						E 3/ W 4/		E W	
		d	3 and 1	<1.4 <1.4	1.1 >0.5	1.1 0.9	0.2	3d		b	2 and 1	<2.9	1.1 2.2	1.1 1.2	0.6
13a and 13b															
14 and 12B	12B			E W	E W	E W		4 and 5 6/	4B						
	16	e?	3 and 1	<0.2 <0.02	0.02 <0.2	0.2 0.2	0.1			c?	2	?	<0.4	<0.03	0.2
15								5 7/							
16								6							
17															

Time

1/ An equilibrium scarp in easily erodible sediments would suggest a displacement ≥2 times the maximum colluvial wedge thickness.
2/ As discussed by Swan and others (1980), net vertical tectonic displacements across the 7-m-high scarp as measured from topographic profiles are 1.2± 0.2 m for trench 1 and 2.6± 0.2 m for trench 2.
3/ East side of small graben between fault zones (pls. 3 and 4).
4/ West side of small graben between fault zones (pls. 3 and 4).
5/ Based on the event sequence in trench 1 this may be two separate events, if so, it would reduce displacement estimates.
6/ Unit 5 was probably deposited following both fault events b and c
7/ In trench 2 a unit similar to unit 16 in trench 1 is too thin and discontinuous to log and is therefore included with units 2E, 4B, and 5.

increased eluviation rates) without significant displacement on a graben-bounding fault (zone 2) antithetic to the main fault (fault zone 1) in this portion of the trench, which is not detectable in the loose, nonstratified units exposed in this part of the trench. Similar materials were noted by Martin and others (1983) adjacent to a fault zone in outwash in the Uinta Basin. We interpret unit 10E as an eluvial horizon - the equivalent of unit 7E, but both vertical and lateral contacts are very gradational. Later faulting between stations 48 and 51 produced opposing scarps and probably offset unit 10a, 0.8 to 1.8 m down to the east relative to 10b (table 5.4).

(c) Colluvial sediments. - Overlying the stream-reworked deposits in the middle of the trench are finer-grained colluvial units (12, 16, 17) which grade into coarser units (9, 11) toward the main scarp. Again contacts are gradational, but unit 10a (stream deposit) appears to grade into unit 9 (proximal scarp-derived colluvium) and unit 12 (finer distal colluvium) grades primarily into unit 11 (proximal colluvium).

The older colluviums (units 9 and 11, and possibly the eastern 6 m of unit 8) appear to have been faulted and backtilted into fault zone 1 as shown by the eastward dip of unit 9 contacts at station 33. An indistinct contact and more cobbles in the upper half of the unit (table 5.3) suggests unit 11 may be the product of two colluvial events (units 11a and 11b) in fault zone 1. Unit 12B is a B horizon developed on unit 12. The scarp contacts between units 10 and 12 at stations 48 and 51 are interpreted as fault or possibly erosional scarp-free faces with no displacement between units 10 and 12.

Units 13a and 13b are very proximal colluvial wedges derived from later faulting of about 1 m displacement in zone 3 (fig. 5.4) and faulting in zone 1 with a reversed sense of displacement from previous faulting, respectively. Unit 14 is finer later colluvium. Unit 15 may have been produced by a similar later event of smaller displacement.

Except where it is thickest (at station 31), the loose white colluvium (unit 16) containing little clay that extends the length of the trench is probably the product of both eluviation of clay into lower horizons (see table 5.2, E horizon) and slopewash across the fan surface, producing a thin surface colluvium.

Unit 17 is the modern A horizon of the surface soil. Where it is thickest in the middle of the trench, its fine-grained character suggests a partial eolian origin. Although there are several small 10- to 20-cm-high steps in the lower boundary of unit 17 in fault zone 1, similar steps are also present along this boundary in several other areas of the trench which do not coincide with fault zones. For this reason, we do not interpret these steps as tectonic features.

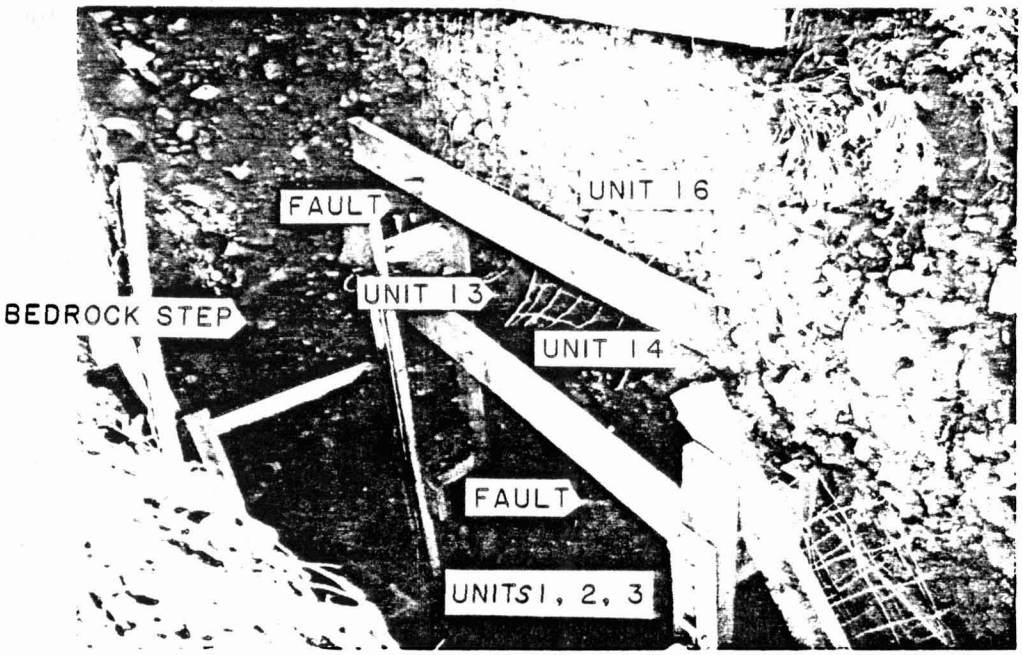

Figure 5.4. Fault zone 3 between station 27 and 31 in Co-op Creek trench 1 showing the bedrock step to the left, the indistinct fault offsetting alluvial units 1, 2, and 3 (arrow), and overlying colluvial units 13, 14, and 16.

(2) Estimated ages of units. - The soil developed on unit 7 (a Paleboroll) has an argillic Bt horizon (unit 7B) (4 percent more clay than C horizon) of variable thickness, but averaging 60 cm thick (table 5.2; pl. 3). Clay coats clasts to a greater degree in this horizon than in others (although all coarse units probably contain some infiltrated clay, for example, Walker and others, 1978), and a few (less than 5 percent) clasts (mostly conglomeratic facies of unit 3 of Van Arsdale, 1979a, quartzite, and sandstone) are highly weathered. Above the argillic horizon are eluvial pink and tan units (7E, 16) of similar lithology, but with very little clay. Along most of the trench these units are interpreted as E and BA horizons from which clay has been eluviated into the Bt although in some areas they are clearly colluvial. The thickness of these units, particularly unit 7E in the western third of the trench, is quite variable, perhaps through concentrated eluviation through coarser zones in unit 7 or to ground disturbance by burrowing or tree-uprooting. Stage I carbonate, almost certainly related to the present soil profile, has accumulated well below the B horizon in unit 5.

This soil profile (SC-1) is the best available evidence with which to assess the age of the fan surface, but this is difficult because of the lack of independently dated profiles on similar materials in the region with which to compare these soils. Comparison of this profile with those described from glacial deposits in the Rocky Mountain region (sec. 4.4.1) suggests a "Bull Lake" (ca. 60 to 150 Ka) to older "Pinedale" (ca. 30 to 70 Ka) age. However, the criteria of Shroba (1980, 1982) from soils along the Wasatch Front indicate an early Holocene to Bonneville age (ca. 7 to 20 Ka). Temperatures on the Strawberry fans are lower than along the Wasatch Front (1200 m higher elevation), but annual precipitation is much higher (17 inches vs. 24 inches). Higher precipitation should allow more rapid clay translocation, but the dust influx rate must be much higher along the Wasatch Front than on the fans. Considering these factors, relatively weak argillic horizon development (considering the amount of clay in the parent material) suggests this soil is much younger than "Bull Lake" deposits elsewhere in the region but is older than Bonneville soils along the Wasatch Front. Thus, active deposition on the fan surface near the trench site probably last took place during pre-Bonneville or "Pinedale" time (ca. 15 to 70 Ka). Higher than present precipitation may have been required to activate the now inactive fan surface (Astin, 1977) although significant displacements on the main Strawberry fault (fig. 4.4) could produce the same effect (Bull, 1977). The glacial period temperature estimates for the region of McCoy (1981) and Porter and others (1982) suggest higher precipitation rates were not likely until the climatic warming that led to "Pinedale" deglaciation. Thus, a best estimate for the age of the fan surface is roughly 15 to 30 Ka.

Similar alluvial fan sediments with apparent argillic horizons were encountered in auger holes 3, 4, 5, and 6 (app. B) elsewhere on the fan surface (fig. 4.4) indicating much of the fan surface is the same age as the areas near the trench sites.

The lack of well-developed soil profiles on any of the colluvial units suggests there have been no long periods of scarp stability since they were deposited and thus, that the fan surface is relatively young. The soil on finer colluviums in the middle of the trench is weakly developed (table 5.2; app. A, profile SC-2). The slightly higher clay content and redder color of unit 12B relative to unit 12 is due mostly to the gradual upward change in parent material (more homogeneous, finer colluvium in unit 12B). Thus, unit 12B is at best a cambic B horizon and possibly only a C horizon.

Age assessment of the colluvial units is also difficult because of no dated comparison profiles in a similar setting. However, the lack of an argillic horizon in material of this fine texture and comparisons with profiles described from fine-grained Lake Bonneville sediments (Shroba, 1980) makes it difficult to argue that profile SC-2 on the younger colluvium is significantly older than mid-Holocene.

(3) Sequence of events. - Based on the lithologies (table 5.3), stratigraphic relationships (pl. 3), and estimated ages of units in Co-op Creek trench 1, we infer the following sequence of events:

(a) Units 1 through 5 were deposited successively on the alluvial fan by small braided streams and debris flows over the top of and parallel with the bedrock step at stations 22 to 29 perhaps 15 to 30 Ka (the lack of very large boulders in these units suggests the step is in a bedrock high protruding into the fan sediments rather than simply a large boulder).

(b) Unit 6 was deposited by braided streams locally reworking older alluvium on the fan surface.

(c) Unit 7 was deposited as a debris flow over the entire area exposed by the trench about 15 to 30 Ka. Thin surficial colluvium deposited by local slopewash processes began forming, and soil development on unit 7 began.

(d) One or more faulting events offset units 1 through 7 down to the west near station 32 (fault zone 1) with probable antithetic faulting down to the east somewhere between stations 48 and 63 (fault zone 2), forming a graben parallel with the present main scarp (faulting event a, table 5.4). This graben was required to divert the stream which deposited unit 8. Displacement during this event(s) cannot be determined.

(e) Intermittent diversion of part of the streamflow in the tributary to Co-op Creek just north of the trench (fig. 4.4) took place through the graben, reworking colluvium deposited in the graben and alluvial fan sediments and depositing them locally as unit 8 (unit 8 may consist mostly of scarp-derived colluvium east of station 39).

(f) Renewed down-to-the-west faulting at station 32 (fault zone 1) produced a thick colluvial wedge (units 9 and 11). Two lines of evidence suggest this wedge was produced by at least two displacement

events (b and c?, table 5.4). (1) Unit 9 upper and lower contacts are indistinct, but definitely dip eastward suggesting backtilting of initial fault-scarp-derived colluvium. (2) Following a fault event, the tributary of Co-op Creek was diverted intermittently along the graben reworking the distal part of the wedge (unit 9) to form unit 10a. Westward lateral erosion of unit 7 by the stream allowed the main channel to migrate westward where unit 10b was deposited. Unit 10 is apparently offset down to the east about 0.8 to 1.8 m at station 50 with a smaller antithetic offset at station 49 (fault zone 2). It is very likely that this displacement in fault zone 2 was contemporaneous with faulting in fault zone 1, but unit 10a postdates the deposition of unit 9. The higher percentage of cobbles in unit 11b also suggests a later colluvial event. If unit contacts have been incorrectly interpreted and this colluvial wedge is the product of one fault event, the wedge thickness suggests a minimum stratigraphic displacement of 4.8 m. Two or more events suggest smaller displacements (table 5.4).

The tributary to Co-op Creek cut to below the level of the graben during this period and was no longer diverted parallel to the scarp (fig. 4.4). More distal colluvium composed of finer material derived from the scarp was deposited with an increasing eolian component in the upper part of unit 12, filling the small graben at 49. Soil development continued on units 7 and 10 with thickening of units 7B, 7E, 10E, and 16 (particularly over areas with a gentler slope) and the beginning of soil development on unit 12 during the Holocene.

(g) Down-to-the-west faulting of about 1.1-m displacement at station 29 (fault zone 3) and down-to-the-east faulting (either vertical or reverse faulting) of 0.9 m-displacement at 32 (event d; fault zone 1). The graben block between 28 and 32 was tilted westward and there appears to have been some drag or slumping (10 to 20 cm) in addition to previous backtilting of units 11 and 9. Proximal scarp-derived colluvium was deposited (13a from main scarp; 13b from colluvium scarp) into the graben between fault zones 1 and 3 immediately after faulting. This was followed by more gradual deposition of unit 14 in the small graben with material derived from both graben scarps along with surface colluvium and E horizon material from above the main scarp. There may have been some offset of unit 16 between stations 50 and 56 during this event, but this unit lacks stratification, its contacts are very gradational, and no shear zones have been located. Deposition of the upper part of unit 12 and soil development on units 7, 10, and 12 (12B) continued with the thickening of units 7E, 10E, and 16. A soil began to develop on unit 14 with some slopewash deposition and eluviation producing the lower part of unit 16 at station 31.

(h) Later faulting or possibly compaction (event e?) took place with small displacements on the graben faults in fault zone 3 (10 to 20 cm) and fault zone 1 (20 to 90 cm) producing a small step in the unit 14 upper contact at station 28 and a wedge of loose brown colluvium (unit 15) at station 32. Identifiable shear zones were not recognized in these materials. Unit 16 thickened over the

graben due to infilling by slopewash material from the scarp and rapid eluviation took place in the sandy colluvium of unit 14. Soil development continued with deposition of material making up the present A horizon (unit 17) over the whole trench by slopewash and eolian deposition (thicker in depressions and thinner on slopes) with a more rapid deposition rate in the main graben depression.

b. Co-op Creek trench 2. - A second shorter (27 m) trench (CC-2) was excavated across the 7-m scarp 0.8 km south of the site of CC-1 (fig. 4.4). The trench was about the same depth as CC-1 (2.5 to 3.5 m), but was somewhat narrower due to the more stable trench walls in the finer-grained units in this trench (pl. 4).

(1) Stratigraphic units. -

(a) Alluvial fan sediments. - Alluvial fan sediments exposed in CC-2 were similar to those in CC-1 (table 5.5) except that all were somewhat finer-grained and the lower half of the upthrown block consisted of clayey silt with very few clasts (unit 1). Auger hole 4 (fig. 4.4) shows sediment similar to unit 1a extends to a depth of 7 m on the downthrown side of the scarp at this location. Unit 2 is similar to unit 7 in CC-1, but has less clasts (table 5.5). All units were probably deposited by mud and debris flows moving across the surface of the fan. The soil on unit 2 is almost identical to that on unit 7 in CC-1; unit 2B is the equivalent of unit 7B and units 2E, and part of unit 5 is similar to units 7E and 16.

Units 2a and 1b form a carbonate-rich horizon (stage I) which truncates the bedding in the alluvial fan sediments demonstrating its relationship to the present topography in the upper half of the trench. A fault (event b) striking 147° and dipping 42 to 72° clearly displaces unit 1a 1.1 m down to the west in fault zone 2. However, unit 2, which overlies 1 on the upthrown block, is missing on the downthrown side of the fault.

Unit 2 (B?) in the downthrown part of the trench is clayey like unit 1, but cobbly like unit 2. It is most likely the downthrown equivalent of the upper part of unit 2 (either a lateral facies change or 2B, the argillic horizon), although it could be part of unit 1. Apparently unit 2B was eroded from above unit 1a between stations 13 and 16 before displacement in fault zone 2.

(b) Colluvial sediments. - CC-2 contains colluvial units very similar to those in CC-1, but unit contacts in the older colluviums are even more gradational and difficult to trace. Lithologic changes within unit 3 suggest it was produced by a series of colluvial events. Fault event a (table 5.4) produced down-to-the-west displacement in fault zone 1. Unit 3a is the result of erosion off the scarp in unit 2 (now entirely eroded) at station 16-17. The progressively gentler dip of the faint contacts between units 2, 3a, and 3b and slightly coarser texture of unit 3b suggests it was also derived from a former scarp at station 16 during a subsequent displacement or possibly fluvial event. The eastward dip of these unit contacts

Table 5 5 - Lithologic description of stratigraphic units in Co-op Creek Trench 2

Stratigraphic Unit	Subunit	Description	Munsell color 1/	Matrix texture 2/	Estimated percent by volume			Angularity (percent) 3/				Carbonate 4/		Lower boundary 2/		Remarks
					Pebbles	Cobbles	Boulders	A	SA	R	WR	Reaction	Stage	Distinctness	Topography	
Alluvial fan deposits																
1		Mud flow	2.5YR4/8 to 5YR7/6	Silty clay												
	1a 5/				2	0	0	-	-	-	-	0	0	-	-	Faintly stratified with seams and lenses (0.5 to 3 cm thick); rare carbonate nodules
	1b	CO_3-rich			1	0	0	-	-	-	-	M=3	I+	Abrupt	Smooth	Common carbonate filaments
2		Debris flow	2.5YR5/6	Silty clay loam												Poorly to nonstratified; gravel lenses (2 to 10 cm thick)
	2a	CO_3-rich	2.5YR5/7		15	5	0	4	38	38	20	M=3;C=4	I	Abrupt	Smooth	Carbonate clast coatings and filaments in lower half; cobble lenses near E end
	2b		2.5YR5/8		10	3	0	4	44	36	12	0	0	Clear	Smooth	
	2B	Argillic B soil horizon	2.5YR5/6		20	0	0	16	24	30	30	0	0	Clear	Wavy	Prismatic structure; some clay may be infiltrated
	2E	Eluvial soil horizon	5YR6/5	Sandy loam	20	5	0	4	48	28	20	0	0	Clear	Smooth	
Scarp-derived colluvium																
3		Sandy colluvium		Sand	15	10	0	8	38	38	20					Nonstratified with fragments of reddish clay and faint gravel lenses
	3a		5YR5/8									0	0	Clear	Smooth	More red clay fragments than upper units
	3b		5YR7/4									M=0; C=3	0	Diffuse	Smooth	Carbonate seams along lower contact
	3c		7.5YR7/5									0	0	Diffuse	Smooth	
	3d		5YR6/6									0	0	Clear	Smooth	Lenses and pods of clay in sandier matrix; weakly stratified pebble beds very heterogeneous
4		Sandy distal colluvium	5YR7/3	Loamy sand	20	5	0	0	32	38	30	0	0	Gradual	Smooth	
	4B	B soil horizon	5YR7/4	Silty clay loam	15	15	0	0	42	34	24			Clear	Smooth	Angular blocky structure
5		Sandy proximal colluvium	5YR7/4	Loamy sand								0	0	Clear	Smooth	Nonstratified
Near-surface colluvium																
6		Modern A horizon	7.5YR5/4	Silt loam	10	0	0	-	-	-	-	0	0	Abrupt	Wavy	

1/ Dry color of Oyama and Takehara (1967).
2/ Methods of Soil Survey Staff (1975).
3/ Scale A = angular, SA = subangular, R = rounded, WR = well rounded.
4/ Scales of Soil Survey Staff (1975) and Bachman and Machette (1977): M = matrix, C = clasts.
5/ Lowercase letters denote subunits distinguished by minor lithologic differences and pronounced bed contacts.

suggest slight backtilting during faulting. The thickness of units 3a and 3b suggests displacements of >0.8 to >2 m for one or more fault events, but no shear zone in this part of the trench has been recognized. The more distinct colluviums in the same stratigraphic position in CC-1 suggest more than one fault event may be represented by units 3a-3c in CC-2. However, poor stratification, less clay, fewer highly weathered clasts, and brighter, more oxidized color in unit 3c may indicate slight reworking of proximal colluvial sediments by very intermittent flows from one of the small local drainages on the fan.

Later (event b) down-to-the-west faulting of about 1-m displacement in fault zone 2 and down-to-the-east antithetic faulting of similar displacement in fault zone 1 (reversed from previous displacements) produced a small graben between stations 13 and 16 (pl. 4). Rapid infilling of the graben resulted in unit 3d. Thus, unit 3d probably consists of remnants of unit 2, some very proximal blocks of units 3a and 3b, colluvium derived from units 3a, 3b, and 3c, and colluvium derived from the main scarp (units 1 and 2).

Unit 4, the upper part of which is a weak Bt horizon (4B), consists of more distal, fine-grained colluvium deposited gradually by slopewash and eolian processes.

Units 2E and 5 were deposited by slopewash and eluviation of fines into unit 2B, but unit 5's thickness and the step in its lower contact just east of fault zone 2 (fig. 5.5) suggest a possible small (<30 cm) displacement (event c?) at station 11 with subsequent infilling of the step by unit 5 material.

As in CC-1 the upper unit (6) is the modern A horizon which was partially removed near the west end of the trench during excavation (n6 on pl. 4).

(2) Estimated ages of units. -

(a) Soil relative dating. - The soil developed on the alluvial fan sediments on the upthrown block of trench CC-2 is very similar to that on the same sediments in CC-1, indicating a similar "Pinedale" age of about 15 to 30 Ka.

Thin argillans coating clasts and lining pores in unit 4B in profile SC-3 (app. A), a probable slight increase in clay, and a slightly higher chroma (table 5.2) indicate this unit is a cambic B horizon developed on unit 4 colluvium as it accumulated. This cambic B is more weakly developed toward unit 3d where the unit 4 colluvium becomes coarser, but otherwise is very similar to unit 12B in CC-1. The degree of soil development in this finer-grained colluvium suggests a mid- to early Holocene age for the colluvium (sec. 4.4.1); this is confirmed by the 14C dates discussed below.

(b) Radiocarbon dating. - Five small areas of organic-rich sediment between stations 16 and 18 in unit 3 (n1 through n4 on pl. 4) allow

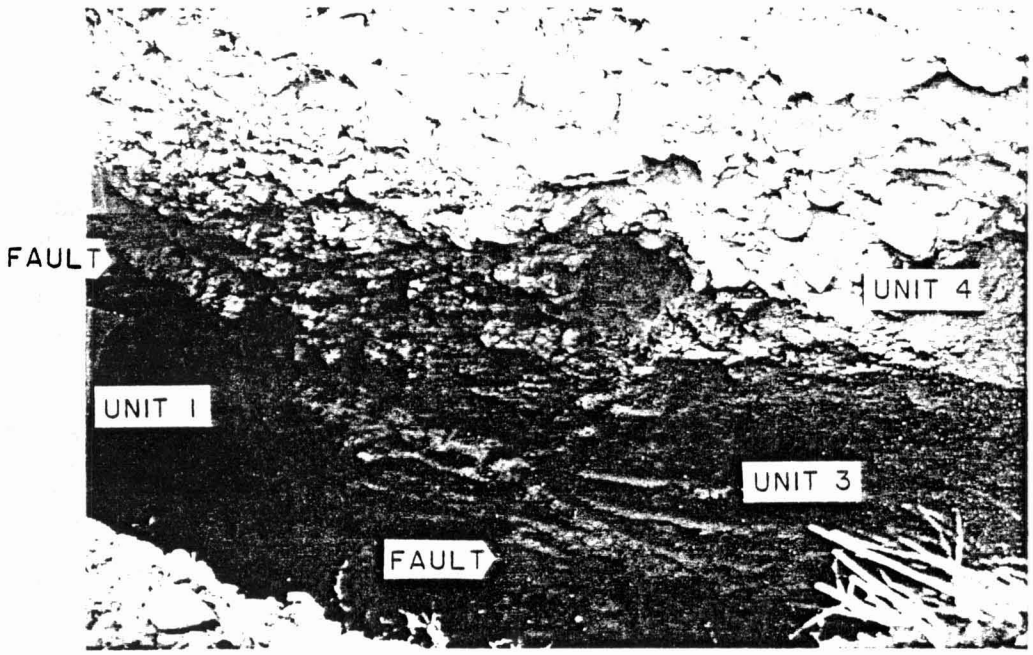

Figure 5.5. South wall of Co-op Creek trench 2 between stations 12 and 14 showing the color contrast across fault zone 2 (near left edge of photo; unit 1 on left, unit 3 on right)(pl. 4). Light-colored material in upper third of photo is unit 4.

its age to be assessed by 14C methods. At the contact between units 3 and 2 at station 18, 5 kg of black silty clay were collected from a flattened oval area much darker in color than either units 2 or 3 (n5 on pl. 4; fig. 5.6). The depth, size (5 by 15 cm), sharp contacts, oval shape, and location at the top of a more consolidated bed suggest this is the remains of a small mammal burrow (probably a Uinta ground squirrel burrow reoccupied by a striped skunk; David Armstrong, University of Colorado Museum, oral communication, 1981). The concentrated clay-silt/humus fraction (methods of Kihl, 1975) of 2.5 kg of sediment (0.03 g estimated carbon) from this burrow gave a 14C age of 2990 ± 650 (pl. 4; table 5.6). The burrow material provides only a minimum age for unit 3 and overlying units because it could have been dug by an animal from the present ground surface relatively recently (Armstrong, oral communication, 1981).

However, the organic-rich sediment in the burrow was probably derived primarily from A horizon material washed into the burrow after it was abandoned. The 14C age on this material would be an apparent mean residence age (Scharpenseel and Schiffmann, 1977); an age probably somewhat older than the burrow (discussed in more detail below).

The other zones of organic-rich sediment (n1 through n4, pl. 4) are alined more or less vertically through unit 3 at station 16. These zones are smaller (5 cm diameter), much more irregular in shape, and have more gradational contacts (with the nonorganic-rich colluvium) of unit 3 than the burrow did (fig. 5.7). Small (<1-cm-wide) blotches of organic-rich sediment are found between the zones marked on plate 4 (n1, n2, n3, n4), but were too small to sample easily. Although it is possible that the organic sediment at station 16 was originally deposited in small burrows, the colluvium must have been considerably disturbed after the burrows were abandoned. A more likely origin is that A horizon material was incorporated into ground cracks during fault displacement of the colluvium (event b, table 5.4) at station 16. Radiocarbon analysis of the silt-clay/humus fraction of 1.5 kg of sediment collected from the upper three zones at station 16 (n1, n2, n3) gave an age of 3135 ± 205 (pl. 4; table 5.6), about the same age as the date on the burrow.

There are many interpretive problems (Mathews, 1980) which complicate using these 14C ages to date the fault events recorded in CC-2. The dispersing, sieving, and drying procedures used to concentrate the organic fraction of the samples has probably introduced some modern carbon into the sample. Additional younger carbon has probably been added through downward percolation of humic acid and fine root penetration (Geyh and others, 1971), but use of only the finer fraction (<125 u) of the samples and treatment with HCl and NaOH should have significantly reduced the proportion of younger carbon in the samples (Scharpenseel, 1971; Mathews, 1980). Although mean residence 14C ages on soil material from the late Holocene are commonly doubled to allow for younger carbon contamination (R. J. Schelmon, oral communication, 1982), even if the samples contained as much as 30 percent modern carbon when analyzed (very unlikely) the actual age of the samples would not exceed 4.3 Ka (Olsson, 1968).

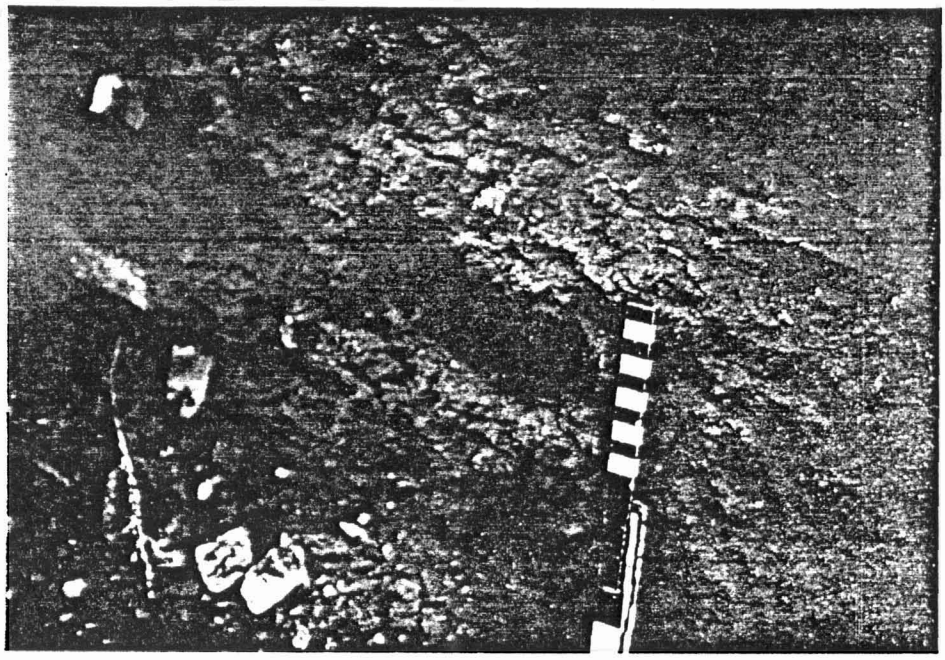

Figure 5.6. Burrow infilled with silty organic-rich sediment at the top of unit 2(B?) between stations 17 and 18 in Co-op Creek trench 2 (n5 on pl. 4) that was ^{14}C dated. Scale in centimeters and decimeters.

Table 5.6. - Radiocarbon dates for samples from the Strawberry Reservoir area

Depth (m)	^{14}C Laboratory No.	Dated Material	Sample Weight (g)		Estimated carbon (g)	^{14}C date (yr. BP)	^{13}C (0/00)
			Untreated	Clay-silt/humus concentrate			
Co-op Creek Trench 2							
2.5	GX-8208	Silty sand	1500	272	0.065	3,135 ± 205	-29.6
3.5	GX-8209	Sandy silt	2950	591	0.030	2,990 ± 650	-29.0
700 m north of Indian Creek							
7.3	Beta-2520	Clayey silt	767	183	0.9	11,290 ± 220	
Indian Creek Core 1							
1.7-2.2	GX-8211	Clayey silt	343	267	>1.0	8,230 ± 190	-27.0
6.6-6.9	GX-8213	Sandy clay	506	199	>1.0	>37,000	-26.7
8.9-9.2	GX-8214	Silty clay	255	167	>1.0	25,840 ± 1,300	-28.6
10.6-10.7	GX-8210	Silt and peat	345	-	>1.0	>37,000	-27.8
Indian Creek Core 2							
1.3-1.7	GX-8212	Silty sand	461	134	>1.0	2,955 ± 145	-26.7

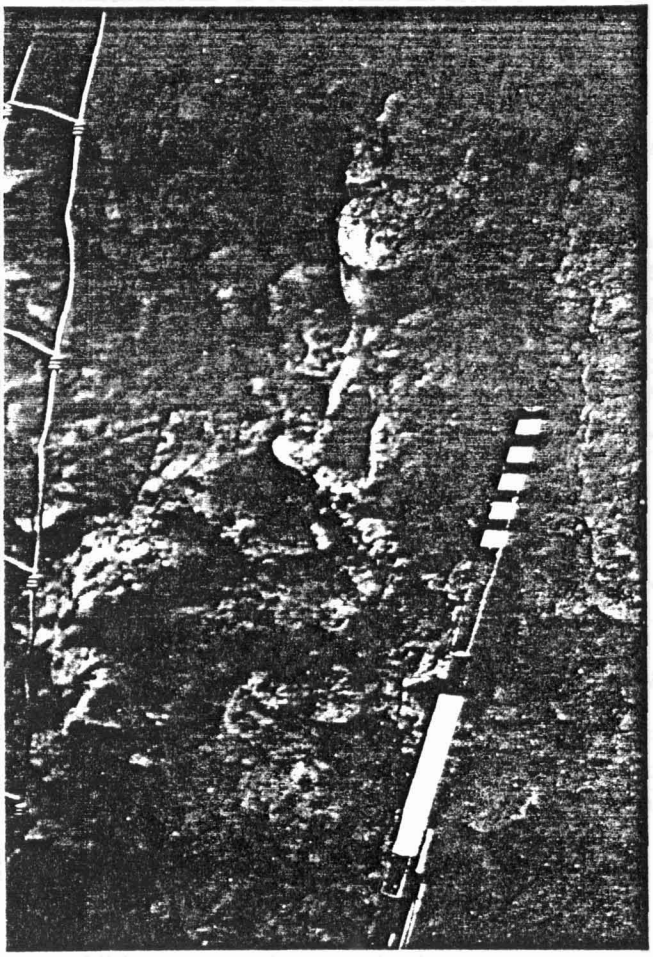

Figure 5.7. Infillings of organic-rich sandy sediment (dark areas) at station 16 in Co-op Creek trench 2 (n1 and n2 on pl. 4) that were ^{14}C dated. Scale in centimeters and decimeters.

The 14C ages, however, probably provide a maximum estimate of the time when the A horizon material was incorporated into the burrow and the fault zone because the ages are apparent mean residence ages of the soil organic material which (barring significant very recent younger carbon contamination) must be older than the time when the A horizon material was buried.

The burrow could have been dug more recently, but the undisturbed cambic B horizon above the upper organic zones at station 16 suggest no movement has taken place in fault zone 1 in the last few thousand years (the estimated minimum time needed to develop the cambic horizon). Thus, whether the organic sediment was incorporated in unit 3d during fault event b (table 5.4) or small infilled burrows were deformed during event b, 3 Ka is a reasonable rough estimate for the age of this event. Certainly the event took place between 2 and 4 Ka ago. Postulated event c? is younger than event b by an unknown amount.

(3) Sequence of Events. - Based on the lithologies (table 5.5), stratigraphic relationships (pl. 4), and estimated ages of units in Co-op Creek Trench 2, we infer the following sequence of events:

(a) Units 1 and 2 were deposited on the alluvial fan by mudflows and debris flows followed by soil development on unit 2 about 15 to 30 Ka.

(b) A fault (event a, table 5.4) that is not exposed in the trench offset units 1 and 2 down to the west, either approximately 1 and 2 m in two events, or about 3 m in one event. Colluvium (unit 3a) eroded from unit 2 on the upthrown block was deposited off of a scarp at station 16 which no longer exists. The second probable event on the same fault with total displacement of about 2 m may have produced colluvial wedges 3b and 3c with minor backtilting of the wedges. All of unit 2 near the edge of the scarp was apparently eroded during this period.

Intermittent high flows from a small drainage near the trench site probably reworked the upper 40 cm of unit 3 to form unit 3c. Soil development on unit 2 continued with argillic B horizon development (2B).

(c) Later faulting at station 12 (event b, table 5.4) offset unit 1 about 1 m down to the west and between 16 and 17 dropped unit 1 east of 16 down to the east a similar amount relative to the colluviums previously derived from it and unit 2 to form a graben as in CC-1 about 2 to 4 Ka. Organic material was incorporated into fault zone 1 at this time, and an animal dug the burrow at station 18. Unit 3d was deposited by dumping of material eroded from the main scarp and the scarp in units 3a, 3b, and 3c into the narrow graben between 12 and 17.

(d) Soil development on unit 2 continued thickening units 2E and 2B with carbonate (stage I) accumulation at depth. Unit 4 began forming by slope wash and eolian processes.

(e) This was followed by a possible small offset (event c?) of <40 cm in unit 5 at station 11 with thickening of unit 5 due to filling of the resulting step. If this offset is due to displacement on fault zone 2 rather than to nontectonic compaction near the fault zone, the fault in unit 5 apparently dips at less than 45° W. because units 1 and 2 at station 11 are not displaced. Soil development continued on units 2 and 4 gradually forming a cambic B horizon on unit 4 (4B). Slight scouring by storm drainage along the scarp may have produced the depression at stations 19-20. Deposition of fine-grained material by slopewash and eolian processes to gradually form unit 6 has continued to the present.

c. Correlation of faulting events and displacements. - Correlation of stratigraphic units and faulting events between the two trenches indicates each site (fig. 4.4) has had a similar fault movement history (table 5.4) as would be expected for sites 0.8 km apart on the same 7-m scarp. Units in CC-1 could represent as many as six fault events or as few as three (four is our preferred number). Three and possibly four events may be represented in CC-2. Because units in the downthrown block correlative with upthrown units were not reached in CC-1, several early fault events may be unrecognized. However, the downthrown block was reached in CC-2 suggesting significantly more unrecognized events did not occur in CC-1.

Stratigraphic relationships in both trenches suggest stratigraphic displacements of 1 to 3 m for most events with smaller displacements for probable younger events. Limits were set on stratigraphic displacements by dividing total offset for a stratigraphic interval by the number of events suggested by colluvial units (for example, Swan and others, 1980). Displacements have also been estimated by doubling the maximum colluvial wedge thickness. Given sufficient time for scarp degradation this should provide a reasonable minimum estimate of stratigraphic displacement (for example, Nash, 1981). If there were only short intervals of time (relative to scarp erosion rates) between displacement events, colluvial wedge thickness displacement estimates are too low.

Swan and others (1980) determined that the net tectonic vertical displacement across the fault zone was about half the measured stratigraphic offset on the Wasatch fault. Our estimates of net vertical tectonic displacement across the upper fan scarp fault zone, measured from scarp topographic profiles, are a much smaller proportion of stratigraphic displacement (table 5.4) because of significant graben formation and backtilting. We have calculated the proportion of total net vertical tectonic displacement accounted for during each event (negative values are due to antithetic faulting), but these values are clearly not meaningful when compared with the empirical plots of displacement data of Slemmons (1977) (discussed in section 6.4.1). Furthermore, the 7-m scarp is only subsidiary to the main trace of the Strawberry fault. Fault slip almost certainly took place on the 5-m-high scarp west of the trenched scarp, the 2-m-high east-facing scarp east of the trenched scarp, and/or along the main trace of the fault at the fan-bedrock contact during at least some of events recorded in the trenches (fig. 4.4). Morphologic data do not suggest the 5- or 2-m scarps differ significantly in age from the 7-m scarp. Net vertical tectonic displacement per event and long-term slip

rates across the entire fault zone cannot be accurately estimated because of unknown displacements on the main fault trace and the other scarps. However, doubling the maximum single event and total displacements from the trenches probably provides conservative estimates of these parameters. They yield a maximum net vertical tectonic displacement per event of 3.6 m and a slip rate of 0.14 to 0.4 mm/yr.

5.3.2 Alluvial Plain Coring

5.3.2.1 Site geology

Eleven km south of the trench sites, Indian Creek flows from the west across a 9-km^2 alluvial plain on the downthrown side of the Strawberry fault into a 175-m-deep stream cut valley on the upthrown block. The benches cut in the bedrock spur, forming the south side of the stream valley (fig. 4.2), suggest alternating periods of relative stability and uplift along the fault. The juxtaposition of a broad alluvial plain covered with Holocene alluvium and the 200-m-high bedrock scarp on the Strawberry fault (which steepens near the base; fig. 4.2) are suggestive of relatively recent movement on the fault.

Detailed mapping of the Tertiary beds near the site (fig. 4.5) and shallow seismic refraction profiling (units 1 and 2 of Van Arsdale, 1979a) show the main trace of the fault runs along the west edge of the bedrock spur 120 m west of the main scarp. Refraction work shows the fault scarp dips about 58° at depth, similar to that measured on the fault by Thompson (1971) north of Strawberry Reservoir. Refraction data also suggest bedrock is within 4 m of the surface in the stream valley and greater than 60 m deep 80 m west of the bedrock scarp (fig. 5.8). These relationships suggest recurrent movement on the Strawberry fault displaced relatively recent alluvial sediments below the bedrock lip in the stream valley. Large displacements probably produced temporary ponding behind the scarp (for example, King and Vita-Finzi, 1981).

Eight-cm (3-in) diameter Shelby push-tube samples of finer-grained alluvial sediments were taken inside a hollow-stem auger to a depth of 11 m (36 feet) 80 m west of the scarp and 2.6 m (8.6 feet) east of the trace of the scarp at the edge of the stream valley to determine the age of the alluvial fill on the alluvial plain and in the stream valley. Age and depth data can be used to calculate minimum displacement rates across the fault. Continuous samples were taken at 60-cm (2-ft) intervals except where gravelly beds prevented penetration of the corer. Core 1 consists of all samples from the 11-m auger hole and core 2 those from the 2.6-m hole.

Both cores contain brown to gray-green silty clays to silty sands (app. C.) typical of alluvial plain sediments deposited by a meandering stream as well as coarse sandy gravels which were deposited during periods of higher discharge. Fairly thick beds of organic clay in core 1 do suggest periods of ponding, but these could be the result of the filling of oxbow lakes as well as more extensive ponding during faulting events. Alternating coarse and fine beds, accumulations of organic-rich sediments and even peats, and orange mottling in coarser zones lower in core 1 all indicate widely varying sedimentation rates typical of a cut and fill alluvial environment.

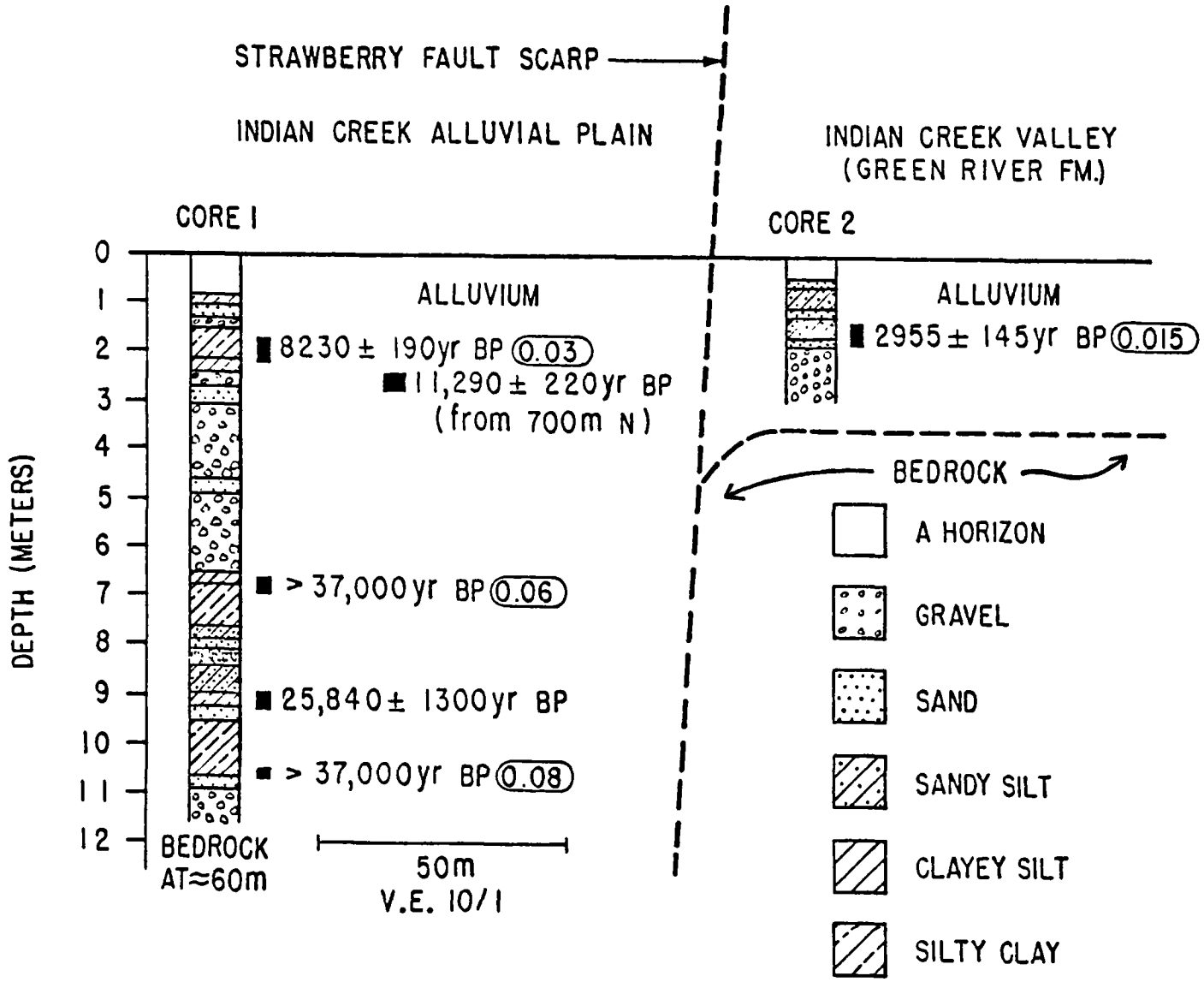

Figure 5.8. Skematic crossection showing the relationship of Indian Creek push-tube cores 1 and 2 to the bedrock scarp of the Strawberry fault. Refraction profiling was used to estimate depth to bedrock and the angle on the fault scarp below the surface. The lithology of the cores, ^{14}C dates on organic-rich sediments, and aIle/Ile ratios on gastropods (circled) are also shown. Core samples were not recovered from the thicker gravel sections.

During initial investigation of the site, an auger hole (borehole 3, fig. 4.5, app. B) was drilled about 700 m north of the site of core 1. Similar alluvial plain stream and lake sediments were encountered between 4 and 8 m depth below the distal edge of the fine-grained colluvial apron extending out from the main fault scarp. A second auger hole (bore hole 4, lt scarp. A second auger hole (bore hole 4, fig. 4.5) high up on the apron encountered only fine-grained colluvium to 9 m.

5.3.2.2 Radiocarbon dating

One sample from core 2 and four from core 1 were analyzed for 14C activity to determine the age of the sediment in each core. A bulk sediment sample with a 2-cm peat bed was analyzed from near the base of core 1, but the other samples required concentration of organics in the silt-clay fraction (see section 5.3.1.2) to obtain enough carbon for dating (table 5.6).

The 14C age from core 2 was from loamy sediment of the modern A horizon. This and its shallow depth indicate the 14C age is an apparent mean residence age (section 5.3.1.2). Because this sample probably contained organic material reworked from older sediments, its 14C age is probably a maximum age for this level (1.9 m) in core 2. However, the upper age from core 1 may be a minimum age. The clayey organic sediment analyzed suggests quiet water deposition and the contact with overlying coarser sediments suggests burial without long exposure at the surface. Both dated samples probably retained a small proportion of younger carbon even after HCl and NaOH treatment of the fine fraction, but the percentage of contamination was probably small. Especially in core 2, the error in the 14C ages may have been offset by an error (<20 percent) in the opposite direction due to the hard water effect on the carbon isotopes incorporated in the aquatic organic material in the dated samples (for example, Broecker and Walton, 1958) and by older reworked organic material.

Considering these age estimates, the 2.5-m level in core 1 is probably about 8 to 10 Ka. A sample of organic-rich silty clay at the base of the 7.3-m (24-ft) thick sequence of peats and gray-green silty clay from near the east edge of the alluvial plain was 14C dated at 11,290 yr BP (table 5.6). The site of the auger hole is at least 5.5 m (18 feet) higher than the site of core 1 and thus, an 11 Ka age in the auger hole at 7.3 m (24 feet) is not inconsistent with a date of 8,230 yr BP from 2.1 m (7 feet) in core 1 (fig. 5.8).

The three lower 14C ages from core 1 are interpreted as minimum ages. Two ages were reported as infinite (>37 Ka) by the dating laboratory, but the middle age was finite (table 5.6; fig. 5.8). This sample was almost certainly contaminated by a small amount of modern carbon giving a finite age to a sample >40 Ka (H. G. Krueger, Geochron Labs, oral communication, 1981). If the true age was as young as 40 Ka, less than 3 percent modern carbon would be needed to give a 14C age of 25 Ka (Olsson, 1968). These infinite ages below the sand and gravel section of core 1 between 3 and 6.5 m (which could not be cored) indicate a major unconformity is present here. Age and depth data from core 2 and the upper part of core 1 cannot be used to calculate displacement rate data because about 8 to 10 Ka sediments on the down-

thrown side of the fault occur at about the same level as <3 Ka sediments on the upthrown side. Considering the cut-and-fill environment of the alluvial plain there is nothing unusual in this apparent age-depth inversion. In addition, the rate of downcutting of Indian Creek east of the fault, although probably rapid (Hamblin and others, 1981), is not known. Thus, the minimum ages from the lower core can not even be used to calculate maximum displacement rates, but finite age estimates for the lower core would allow more meaningful estimates of displacement rates.

5.3.2.3 Amino acid age estimates

Amino acid ratios derived from the analysis of the organic matrix within carbonate fossils have proven very useful in the relative dating and correlation of a variety of Quaternary stratigraphic units worldwide (Schroeder and Bada, 1976; Williams and Smith, 1977). Many earlier studies attempted to calculate numerical-age dates using amino acid racemization data, but because of the large uncertainties in racemization kinetics and the difficulty in estimating the exact temperature history of fossils, the reliability of many of these dates is questionable (Miller and Hare, 1980; McCoy, 1981). However, if independently dated calibration samples are available from the same region as samples of unknown age, the approximate age of the unknown samples can be estimated by using amino acid ratios to interpolate from the calibration samples (for example, Bada and Protsch, 1973).

Both land and freshwater gastropods were found in three of the four samples from core 1 during sample preparation for 14C analysis and in an additional seived sample from the base of the core. Only recently have attempts been made to use amino acid ratios measured on terrestrial gastropods in relative dating of Quaternary deposits (Miller and others, 1979; 1982). At Indian Creek, we can use the D-alloisoleucine/L-isoleucine ratio in the total hydrolyzate amino acid fraction (the primary ratio used in relative dating) of the gastropods 14C dated at 8,230 yr BP to calibrate the rate of isoleucine epimerization in the older gastropod samples at this site (methods of Bada and Protsch, 1973, and Miller and Hare, 1980). Ratios on shells from the 14C-dated sample from core 2 (table 5.1) are less reliable for calibration because the 14C date probably a maximum age.

The rate of amino acid epimerization is exponentially dependent on temperature. High temperatures have a much greater effect on the reaction rate than equally low temperatures experienced for the same amount of time. Because of the lower temperatures during the "Pinedale" glaciation the average effective diagenetic temperature (Wehmiller, 1977) experienced by the >37 Ka gastropods would be considerably lower than the effective temperature experienced by the 8.2 Ka snails during the warmer Holocene period. Recent research (Porter and others, 1982; McCoy, 1981) indicates full glacial temperatures may have been 10 to 15 °C lower than present temperatures in the Rocky Mountain region. Unpublished analyses (A. R. Nelson, 1982) of some of the same species of gastropods as those at Indian Creek show that apparent effective diagenetic temperatures over the last 600 Ka at Baggs, Wyoming, and near Carbondale, Colorado, were about 6 to 10 °C lower than the present mean annual temperature at these localities. Because the epimerization rate in carbonate fossils has been shown to be much more rapid in younger fossils (Wehmiller and Belknap, 1978) it is unlikely that effective temperatures for

these samples were this much lower than present mean annual temperatures at Indian Creek.

Taking these factors into consideration, we have estimated the effective diagenetic temperature experienced by the older samples at Indian Creek (table 5.1). Using these temperatures and the temperatures calculated using the calibration samples from the 8.2 Ka level we have calculated a range of ages for the lower gastropod samples in the core. Small increases or decreases in the temperature estimates will produce large age differences. An additional problem is that about one-third of analyzed samples are apparently reworked from older sediments. Despite these uncertainties analyses of Vallonia and Pisidium suggest the 6.7 level in core 1 is at least 40 Ka and the 10.5-m level at least 50 Ka, most likely 60 to 80 Ka. Our temperature estimates indicate the base of the core is very unlikely to be older than 120 Ka.

While there is uncertainty in these age estimates, they do not contradict what little is known about late Pleistocene climate in the region. The thick gravel section in the middle of core 1 may represent higher discharge in Indian Creek during "Pinedale" (ca. 15 to 40 Ka) deglaciation. The lower fine-grained interval probably represents part of the time between this "Pinedale" event and the earliest Pinedale (60 to 70 Ka) or Bull Lake (ca. 140 Ka) events of Coleman and Pierce (1981). If so, the gravels in the base of the core could have been deposited during earliest Pinedale or Bull Lake deglaciation.

5.3.2.4 Estimated minimum slip rates

Using the above age estimates for various levels in the cores, a range of maximum slip rates across the fault can be calculated. At least 8 m of sediment has been displaced below the depth of bedrock in the channel in the upthrown block. This is a minimum thickness estimate because we do not know the rate of erosion of the bedrock channel. Using our age estimates, the sediment interval between our estimated ages was deposited in a total of 40 to 110 Ka giving a maximum slip rate of 0.07 to 0.2 mm/yr. Because the age of the basal alluvium in the channel is less certain and we do not have estimates of channel erosion rates, minimum slip rates cannot be calculated.

5.3.3 Fault Activity Summary

Investigations north of Strawberry Reservoir along the Strawberry fault suggest a repeated history of fault events of 1 to 3 m stratigraphic displacement on individual fault breaks and 0.4- to 3.6-m net vertical tectonic displacement across the whole fault zone over at least the last 15 to 30 Ka. At least one and possibly two surface displacement events occurred during the Holocene, the larger occurring about 3 Ka. This shows recurrence rates on earthquakes large enough to produce 0.4- to 3.6-m net tectonic displacements are in the range of 1.5 to 10 Ka, most probably about 5 Ka.

Fault slip rates calculated from estimated tectonic displacement (table 5.4) across the Strawberry fault zone are 0.14 to 0.4 mm/yr, higher than the longer term rates of 0.2 to 0.07 mm/yr calculated from Indian Creek core data (fig. 5.8). Thus, the Strawberry fault has slipped during the Holocene,

but its apparent late Quaternary slip rate is probably almost an order of magnitude less than that of the Wasatch fault.

The structural and scarp physiographic similarities of the Strawberry and Stinking Springs faults suggest similar slip rates on both faults. Relatively recent movement on both faults is also suggested by the impounded drainages on the upstream blocks of both faults (sec. 4.4.2.3).

6. MAXIMUM CREDIBLE EARTHQUAKES AND RECURRENCE INTERVALS

6.1 Regional Seismicity Considerations

The occurrence of earthquakes in the mountains and back valleys east of the Wasatch fault, as represented in the historic record (especially post-October 1974), can best be described as spatially diffuse but locally intense. With the possible exception of the East Cache fault (Doser and Smith, 1982), no conclusive association between seismicity and mapped faulting is possible with the presently available data. The historic record, therefore, is of little use in estimating the MCE appropriate for specific seismogenic structures. The available data, however, do provide an upper limit for the MCE of faults not expressed at the surface.

The only earthquake to have produced surface faulting in Utah during historic times was the 1934 magnitude 6.6 Hansel Valley event which was accompanied by 0.5 m of offset. Seven other earthquakes of magnitude greater than or equal to 6.0 but less than 6.6 have occurred in Utah without producing surface rupture. This suggests the magnitude threshold for surface displacement in Utah is in the range M = 6.0 to M = 6.5. Because the Stinking Springs fault is considered capable of generating a magnitude 6.5 earthquake (section 6.4.3) at the damsite, no further consideration of MCE's on structures without surface expression is needed.

6.2 Empirical Earthquake Magnitude-Fault Parameter Relationships

Because of the inadequacy of the historic record in most areas of the world, determination of MCE's requires estimates of the magnitude of paleoearthquakes during the late Quaternary (Wallace, 1981). In areas of late Cenozoic faulting, empirical studies of the relationship between earthquake magnitude and fault surface rupture length (Tocher, 1958; Bonilla and Buchanan, 1970; Mark and Bonilla, 1977; Slemmons, 1977), maximum fault displacement (Bonilla and Buchanan, 1970; Slemmons, 1977), various combinations of these parameters (Slemmons, 1977), fault rupture area (Wyss, 1979; Singh and others, 1980), and seismic moment (Kanamori and Anderson, 1975; Doser and Smith, 1982) provide the principal means of estimating paleoearthquake magnitude. The considerable scatter in plots of magnitude versus these parameters is due to a small statistical sample and the variable quality of field studies and magnitude determinations (Slemmons, 1977). However, earthquake focal mechanism studies (for example, Wyss and Brune, 1968; Chinnery, 1969) tend to support these empirical plots. Single standard deviations in the regressions of these data result in about $\pm$0.3 M (Slemmons, 1977; Wyss, 1979; Singh and others, 1980), but because of the difficulty in accurately measuring field parameters, magnitude estimates derived from these regressions can at best be reliable to 0.5 magnitude. Furthermore, these empirical plots yield "most likely" magnitude estimates, not maximum magnitudes.

6.2.1 Fault Rupture Length

Estimating the length of past surface ruptures on faults is difficult (Slemmons, 1977). Swan and others (1980) suggest that the 370-km-long Wasatch fault zone is composed of 6 to 10 fault segments each ranging in length from 30 to 60 km. Individual segments behave similarly, but somewhat independently of one another.

The two other faults of concern in the Soldier Creek area are the Strawberry fault (section 5.3) and the Stinking Springs fault (section 5.2). The mapped length of the Strawberry fault zone is 35 km (pl. 2) although subtle photolineaments near the southern end of the fault suggest splays off the main fault could extend its length to 39 km. Similarly, our photolineament mapping suggests the Stinking Springs fault zone is about 30 km long, but the compilation of Stokes and Madsen (1961) and landsat imagery (Peterson and others, 1982) indicates it may extend farther to the south for a total of 46 km. However, in neither case does the prominent topographic scarp of each fault extend as far as the mapped trace of the fault. We feel the length of the prominent topographic scarps of the fault zones gives a much better estimate of repeated past surface rupture lengths on the faults and, hence, a better estimate of future rupture lengths and earthquake source lengths (Bonilla, 1979; Wyss, 1979) than does the total mapped length. The length of the two prominent topographic scarps of the Strawberry and Stinking Springs fault zones are 28 and 11 km, respectively (table 6.1).

6.2.2 Fault Displacements

Swan and others (1980) and Hanson and others (1981) used the stratigraphic relationships in trenches across traces of the Wasatch fault to estimate net tectonic displacements of 0.8 to 3.7 m during fault events of the past 13 Ka (table 6.2). Estimated stratigraphic offsets of units in these trenches that include the effects of backtilting and graben formation are approximately double these values. In our trenches across the faults on the alluvial fans downthrown to the Strawberry fault, estimated stratigraphic displacements per event ranged from 0.2 to 3.2 m, but net vertical tectonic displacements were much less (0.1 to 1.8 m) due to backtilting and graben formation (tables 5.4 and 6.2).

No data are available on late Quaternary displacements on the Stinking Springs fault.

6.3 Fault Recurrence

6.3.1 Scarp Physiographic Expression

The topographic expression, wide areas of Holocene stream alluvium downthrown to the faults, and continuity of the scarps of the Strawberry and Stinking Springs faults indicate they have experienced repeated displacements during Quaternary time. The stepped topography of the bedrock spur on the south side of Indian Creek where it crosses the Strawberry fault (fig. 4.2) is suggestive of periods of uplift and quiescence on the fault similar to those identified by Hamblin (1976) (sec. 2.4.1) on the Wasatch fault. Although the length of the prominent Stinking Springs fault scarp is much less than that of the Strawberry fault, both are morphologically very similar. The drainage basin of Soldier Creek, which flows south along the Stinking Springs fault scarp, is too small to have provided the flows needed to significantly increase the height of the scarp during the Quaternary. This suggests total Quaternary displacement is similar for both faults, but if so, either the empirical fault length and displacement relations of Slemmons (1977) do not hold for the Stinking Springs fault (1- to 3-m surface displacement events on an 11-km fault), or the recurrence of small surface

Table 6.1. - Typical scarp parameters, recurrence intervals, and slip rates for faults of concern to Soldier Creek Dam

Fault	Fault scarp parameters				Average recurrence interval for surface faulting events (years) 1/	Slip rate 1/ (mm/yr)
	Height (m)	Gradient max.	Gradient mean	Topographic length (km) 1/		
Wasatch				370		
Kaysville segment	1372	0.56	0.28	30-60		2.8-1.2
	1098	0.60	0.46			
	1281	0.84	0.52			
	854	0.75	0.38			
Hobble Creek segment	1471	0.78	0.53	30-60	1,500-2,600 (2,000)	1.1-0.9
Little Cottonwood segment	1379	0.79	0.37	30-60	450-3,300 (2,200)	1.9-0.6
North Creek segment	1425	0.75	0.46	24	1,300-5,200 (1,700-2,600)	1.4-1.2
	1866	0.67	0.45			
	1403	0.66	0.34			
Strawberry				28	1,500-10,000 (5,000)	0.4-0.07
	732	0.67	0.26			
	625	0.43	0.15			
	183	0.38	0.30			
	145	0.38	0.25			
	214	0.30	0.23			
Stinking Springs				11		
	195	0.39	0.16			
	238	0.38	0.21			
	244	0.50	0.46			
	165	0.60	0.34			

1/ Wasatch fault data from Swan and others (1980) and Hanson and others (1981); preferred values in parentheses.
2/ The larger heights on the Strawberry fault include the additional height of fault scarps on splays east of the main trace of the northern part of the fault; over most of their topographically well-expressed lengths the heights of the Strawberry and Stinking Springs fault scarps are similar.

Table 6.2. - Estimates of paleoearthquake magnitude using fault length, displacement, area, and calculated moment data on faults of concern to Soldier Creek Dam

Fault	Fault rupture length (km)	Fault plane 1/ width (km)	Avg. vert. fault displacement (m) stratigraphic (D_s)	Avg. vert. fault displacement (m) NVTD (D_N) 2/	Moments (M_o) calculated using displacement data and estimated paleoearthquake magnitudes (M) 3/ $M_o(10^{26}$xdyne-cm)	Moments (M_o) calculated using displacement data and estimated paleoearthquake magnitudes (M) 3/ M	Estimated paleoearthquake magnitude using tables in Slemmons (1977) — Worldwide data: log D_s	log (2 x D_N) 4/	log L	log LD_s	log LD_s^2	log A 5/	North American data: log D_s	log (2 x DN) 4/	log L	log LD_s	log LD_s^2	Normal fault data: log D_s	log (2 x D_N) 4/	log L	log LD_s	log LD_s^2
Wasatch 6/																						
Kaysville segment	7/ 30-60	12	3.7-7.3	≤3.3-≤3.7	3.9-8.8	7.1-7.3	7.4-7.8	≤7.7-≤7.8	6.9-7.3	7.2-7.6	7.3-7.6	6.9-7.2	7.3-7.6	≤7.6-≤7.6	6.6-7.0	7.0-7.5	7.2-7.5	7.4-7.7	≤7.7-≤7.7	7.0-7.3	7.2-7.5	7.2-7.5
Hobble Creek segment	30-60	12	1.6-5.6	0.8-2.8	0.9-6.7	6.7-7.2	7.0-7.6	7.0-7.6	6.9-7.3	6.9-7.5	7.0-7.5	6.9-7.2	6.9-7.5	6.9-7.5	6.6-7.0	6.8-7.4	6.9-7.4	7.0-7.6	7.0-7.6	7.0-7.3	7.0-7.5	7.0-7.4
Little Cottonwood segment	30-60	12	4.3-5.5	1.3-2.0	1.5-4.8	6.7-7.1	7.5-7.7	7.2-7.5	6.9-7.3	7.2-7.5	7.3-7.6	6.9-7.2	7.4-7.6	7.2-7.3	6.6-7.0	7.1-7.4	7.2-7.5	7.5-7.7	7.3-7.5	7.0-7.3	7.3-7.5	7.3-7.5
North Creek segment	24	12	4.0-6.0	2.2-3.8	2.1-3.6	6.9-7.0	7.5-7.7	7.5-7.8	6.8	7.1-7.2	7.2-7.4	6.7-6.8	7.3-7.5	7.4-7.6	6.4	7.0-7.1	7.2-7.3	7.5-7.6	7.5-7.8	6.9	7.2-7.3	7.2-7.3
Strawberry	28	12							6.9			6.7-6.8			6.5					7.0		
Co-op Creek trench 1			0.2-3.2	0.1-0.8	0.1-0.9	6.9-6.5	5.9-7.3	5.9-7.0		6.3-7.1	6.2-7.2		6.0-7.2	6.0-6.9		6.1-7.0	6.1-7.1	6.1-7.4	6.1-7.0		6.5-7.2	6.5-7.2
Co-op Creek trench 2			<0.4-3.0	8/ 0.2-1.8	0.2-2.0	6.0-6.9	<6.3-7.3	6.3-7.4		<6.5-7.1	<6.2-7.4		<6.3-7.2	<6.3-7.3		<5.9-7.3	<5.3-7.1	<6.4-7.3	6.4-7.4		<6.8-7.0	<6.7-7.2
Stinking Springs	11	5 9/							6.4			5.9-6.1			5.9					6.5		

1/ Estimated by assuming 60° dip on Wasatch fault and maximum depth of faulting of 10 km (Doser and Smith, 1982) and from cross sections in Van Arsdale (1979a, pl. 1) with limitations of Wyss (1979) (5< width <20 km and width <2/3 length).
2/ Net vertical tectonic displacement per event across fault zone as discussed by Swan and others (1980).
3/ Using equation 16 and figure 8 in Doser and Smith (1982) and figure 4 in Kanamori and Anderson (1975).
4/ Double the net vertical tectonic displacement is the suggested value for use with tables of Slemmons (1977) by Swan and others (1980).
5/ Method of Wyss (1979), Singh and others (1980) (A = length x width of fault plane).
6/ Data from Swan and others (1980) and Hanson and others (1981).
7/ Dash indicates a range of values.
8/ Displacement is probably the result of two separate fault events (table 5.5).
9/ Cross sections in Van Arsdale (1979a, pl. 1) suggest the Stinking Springs fault becomes listric at a shallower depth than the Strawberry fault.

Table 6.2
Estimates of
paleoearthquake magnitude

displacement events on the Stinking Springs fault is higher than the estimated recurrence for larger events on the Strawberry fault. Thus, whether latest Quaternary recurrence rates of displacement events on both faults were similar is uncertain. Although the Stinking Springs fault appears anomalous, neither fault shows nearly the continuity and physiographic expression of the Wasatch fault (compare scarp heights and gradients, table 6.1) indicating that at least the long-term Quaternary recurrence of events large enough to produce surface ruptures was much less frequent on these faults than on the Wasatch fault.

6.3.2 Fault Slip Rates

Calculated slip rates (table 6.1) provide a further measure of the late Quaternary movement history of the subject faults. The Wasatch fault appears to have a slip rate 2 to 40 times that of the Strawberry fault. No late Quaternary data are available for the Stinking Springs fault, but geophysical data (Van Arsdale, 1979a) suggest total displacement on the Strawberry fault is 25 times that on the Stinking Springs fault. However, this seismic line was run across the faults near U.S. Highway No. 40 where the scarp of the Stinking Springs fault is only 10 to 20 m high. From the topography of the fault scarp it appears that displacement on the fault increases rapidly south of the highway to at least 250 m in the vicinity of Soldier Creek Dam. Thus, total maximum displacement on the Strawberry fault is probably at most 3 to 4 times that on the Stinking Springs fault. However, the similar morphology and heights of both fault scarps suggest similar Quaternary total displacements and slip rates. If this is the case, the Stinking Springs fault has apparently experienced more displacement during this period. Using the classification of Matsuda (1975; in Slemmons, 1977, p. 15), the Wasatch fault would have a high activity rate (1 to 10 mm/yr) while the Strawberry and presumably the Stinking Springs faults would have a moderate activity rate (0.1 to 1 mm/yr).

6.3.3 Estimated Recurrence Intervals

Swan and others (1980) and Hanson and others (1981) have calculated recurrence intervals of 450 to 5,200 years for surface faulting events on studied segments of the Wasatch fault (table 6.1). "If the recurrence intervals on these segments of the Wasatch fault zone are typical of the other segments of the zone, the recurrence interval of moderate to large magnitude earthquakes for the entire Wasatch fault zone may be 50 to 430 yr." (Swan and others, 1980).

Limited data from the Co-op Creek trenches (sec. 5.3) suggest recurrence intervals for surface faulting events are in the range of 1.5 to 10 Ka. Our best estimate is about 5 Ka. However, estimated slip rates for the Strawberry fault zone north of Strawberry Reservoir are twice the maximum longer term rates calculated from data south of the reservoir. This suggests our estimates of the age of the trench sediments north of the reservoir may be too young; if so, recurrence intervals would be longer. A second possibility is that displacements revealed by our exploratory trenching are representative of total displacement across the fault zone during single events. Unfortunately, the accuracy of our data does not allow resolution of these uncertainties.

Because our data do not permit meaningful direct estimates of recurrence intervals on the Stinking Springs fault, we assume that event recurrence has probably been similar to that on the Strawberry fault.

6.4 Recommended Maximum Credible Earthquakes

6.4.1 Wasatch Fault

The detailed studies summarized by Swan and others (1980; 1981) and Hanson and others (1981) have demonstrated that there have been recurrent earthquakes in the magnitude range M = 6.5 to 7.5 on the Wasatch fault during the Holocene (the last 10 Ka). Various MCE's have been proposed for the Wasatch fault including M = 7.75 in Thenhaus and Wentworth (1981) and M = 8 in Woodward-Clyde Consultants (1981). These estimates presumably reflect the practice of adding one-quarter to one-half a magnitude to documented events occurring on a fault to determine the MCE. While we agree with this practice in many instances, we feel it is not warranted in the case of the Wasatch fault, because a sufficient measure of conservatism has already been incorporated in estimates of the Holocene surface displacement that subsequently led to the conclusion that magnitude 6.5 to 7.5 earthquakes have repeatedly occurred on the fault.

Estimated magnitudes for paleoearthquakes on the Wasatch fault using the displacement data summarized in Hanson and others (1981) yield values of 6.9 to 7.8 using the empirical tables in Slemmons (1977) (table 6.2). Use of the three applicable data sets and the methods of Wyss (1979) and Singh and others (1980) yield very similar values as do magnitude-moment relationships (Doser and Smith, 1982) (table 6.2). Swan and others (1980) discuss displacement mostly in terms of net vertical tectonic displacement across the fault zone, but Slemmons (1977, p. 88) states that the displacement data used to develop the normal slip curve are the "* * * maximum resultant displacements, which include both fault slip and distortion." Graben development and backtilting along the Wasatch fault make stratigraphic displacements about double net vertical tectonic displacements (Swan and others, 1980); thus, either value gives similar magnitudes (table 6.2). However, the maximum displacement values listed by Hanson and others (1981) are maximum possible values based on trench stratigraphic relationships. Average values are lower (giving magnitudes of 7.0 to 7.5) and additional unrecognized displacement events would further reduce these displacements and the paleoearthquake magnitudes calculated from them. Furthermore, while the length of time represented by the preserved stratigraphic record along the Wasatch Front is less than 15 Ka, the estimated recurrence intervals for large magnitude events (table 6.1) indicate the preserved stratigraphic records span at least three seismic cycles. No record of events clearly larger than M = 7.5 during this period has been found. Therefore, we feel an M = 7.5 earthquake is the maximum credible event on the Wasatch fault.

6.4.2 Strawberry Fault

Displacement data are much more limited for the Strawberry fault. Using the methods outlined above, paleoearthquake magnitudes range from 5.9 to 7.4 (table 6.2). However, the largest displacements used are maximum values derived from the most ambiguous stratigraphic relationships in the

trenches, and, if our correlations are correct (table 5.4), the 3.2-m displacement in trench 2 is probably the product of two events. Average trench displacements yield event estimates of $M < 7.0$ using either displacement-magnitude or moment-magnitude methods and even adding a 0.5-M uncertainty to average values does not result in magnitudes significantly above $M = 7.0$.

Fault rupture length-magnitude and area-magnitude relationships also suggest $M = 7.0$ is an appropriate magnitude for the MCE (table 6.2), even if the entire topographic scarp length (28 km) of the Strawberry fault ruptures in a single event. Finally, the order of magnitude lower slip rate on the Strawberry fault than on the Wasatch fault argues for lower magnitude earthquakes or at least much longer recurrence intervals. For these reasons, $M = 7.0$ is a conservative MCE for the Strawberry fault.

6.4.3 Stinking Springs Fault

The anomalously high scarp on the Stinking Springs fault relative to the 11 km length of the topographically prominent portion of the fault has been discussed above (sections 6.3.1 and 6.3.2).

No displacement data are available for the Stinking Springs fault, but fault rupture length-magnitude relationships using an 11-km length suggest $M = 6.5$ is the maximum credible event. We have found no geomorphic evidence that longer segments of the fault have ruptured during the late Quaternary; in fact, the central highest topographic part of the fault scarp (fig. 4.1) is only 8 km long. Fault area-magnitude relationships suggest an even lower 6.1 magnitude event assuming the geometry of the fault is similar to that suggested by Van Arsdale (1979a, his pl. 1). However, the magnitude threshold for surface faulting in the Intermountain Seismic Belt appears to be $M = 6.0 - 6.5$ and the presence of the Stinking Springs fault scarp, therefore, suggests repeated events in the $M = 6.5$ range.

7. CONCLUSIONS

7.1 Design Earthquakes for Soldier Creek Dam

Table 7.1 lists the Richter magnitudes and hypocentral parameters of the design earthquakes for those seismic sources capable of generating earthquakes hazardous to Soldier Creek Dam. Focal depths for the Strawberry and Stinking Springs faults are estimated from Van Arsdale (1979a, his pl. 1). The rationale used to assign the following MCE's was discussed in section 6.0. The magnitudes of the 25- and 100-year earthquakes were estimated from the magnitude versus frequency of occurence curves shown in figure 7.1.

Table 7.1. - Design earthquakes for Soldier Creek Dam

Seismogenic structure	MCE (M_L)	100-year (M_L)	25-year (M_L)	Epicentral distance (km)	Focal depth (km)
Wasatch fault	7.5	5.8	5.0	45	7
Strawberry fault	7.0	5.2	4.3	8	6
Stinking Springs fault	6.5	5.2	4.3	0	4.5

The slope of the curves shown in figure 7.1, 0.72, is the b value derived from the historic seismicity record for the Wasatch Front area (sec. 3.5). The vertical axis intercepts, the a values, which are reflected in the relative position of each curve, were computed using recurrence estimates derived from the previously mentioned trench data for the Wasatch and Strawberry faults (sec. 5.3.1).

The recurrence curve for the Wasatch fault assumes an average return period of 1,500 years for a magnitude 7.5 earthquake on any individual segment. The curve for the Strawberry fault assumes a return period of 2,200 years for a magnitude 7.0 earthquake on that fault. Though the trench data suggest that 5 Ka is the most probable return period for surface faulting events on the Strawberry fault, derived estimates of the range of possible values includes return periods as short as 1.5 Ka. Considering that the Wasatch fault, with its much more pronounced geomorphic expression, is believed to experience major surface faulting events every 1.5 Ka, it is unlikely that the Strawberry fault has such a high recurrence rate. Because our data do not allow better definition of the expected earthquake activity on the Strawberry fault, a conservative estimate of 2,200 years for the magnitude 7.0 MCE was used to fix the level of the Strawberry fault recurrence curve. This results in reasonable estimates of 4.3 and 5.2 for the magnitude of the 25- and 100-year earthquakes. Because no data exist from which to estimate the recurrence of surface faulting events on the Stinking Springs fault, the curve for the Strawberry fault is used to estimate the return period of earthquakes up to magnitude 6.5 on the Stinking Springs fault.

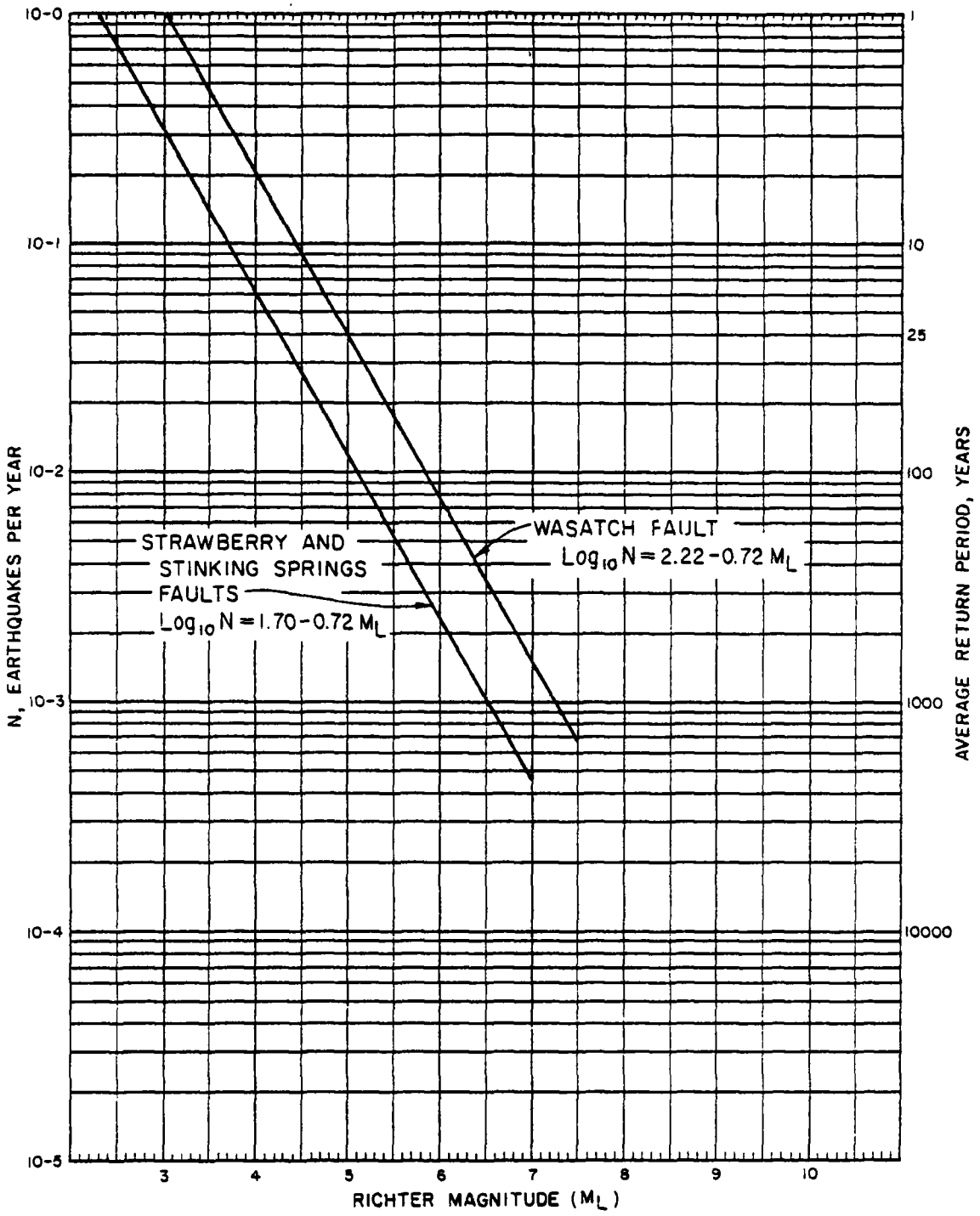

Figure 7.1. Earthquake magnitude versus frequency of occurrence relationships for the Wasatch fault and the Strawberry and Stinking Springs faults.

7.2 Surface Faulting

Our air photograph lineament study (sec. 5.1), general geologic mapping near the dam, and previous engineering geology investigations (Murdock, 1948; Thompson, 1965; Randolph, 1974) did not reveal any faults with significant displacements extending under or trending into Soldier Creek Dam. However, the dam foundation, particularly the right abutment, is extensively jointed (Thompson, 1965; Randolph, 1974), and it is probable that a large magnitude earthquake on the Stinking Springs fault would produce some shifting of the foundation rock along preexisting joints. Further analysis of this potential hazard is beyond the scope of this report. If an M = 6.5 earthquake occurred on the Stinking Springs fault, Slemmons (1977) data suggest about 1 m of down-to-the-west displacement along the trace of the fault 180 m west of the dam.

7.3 Reservoir-induced Seismicity

In order for induced seismicity to occur, the region must be under tectonic stress, but increased pore pressure is the dominant factor in stimulating earthquake activity (Kisslinger, 1976; Simpson and Negmatullaev, 1981). Focal mechanisms of small events are generally consistent with regional tectonics and are, therefore, difficult to discriminate. Reservoir-induced seismicity has been empirically related to reservoirs with the following general characteristics: (1) active faults in the reservoir, (2) water depth in excess of 92 m, and (3) water volume in excess of 10^{10} m^3 (Packard and others, 1977), although induced earthquakes may have occurred near relatively small reservoirs (Toppozada and Cramer, 1978). Although induced seismicity has been well documented for a number of reservoirs, it has not been observed for the great majority of cases.

The recent activity of the Strawberry fault shows the future enlarged Strawberry Reservoir is in a region experiencing significant tectonic stresses. The enlarged reservoir will be fairly large (10^9 m^3), but relatively shallow (81 m deep). Using the methods of Baecker and Keeney (1982) based on data from existing large reservoirs, the probability of the enlarged Strawberry Reservoir inducing seismicity is (very roughly) about 1 percent. during a severe earthquake" (Peck, 1981). Upstream of zone 1, alluvium and colluvium beneath zone 2 might slump to some extent, but a large portion would remain to buttress zone 1. Thus, liquefaction of foundation materials is not considered a potential threat to the security of the dam (Peck, 1981).

7.4 Landsliding and Landslide-induced Water Waves

No large areas of landslides apparently active during the Holocene adjacent to shoreline of the future enlarged Strawberry Reservoir were identified during imagery studies or aerial reconnaissance. The slide west of Clarks Camp (SW1/4, sec. 29, T. 7 S., R. 11 W.), noted by Van Arsdale (1979a, p. 23), is the only area of any size (0.15 km^2) that has apparently been subject to geologically recent mass movement. Limited slope instability and bank caving may occur as a result of saturation and subsequent wave erosion along some steeper portions of the future reservoir shore where the proportion of shale in the bedrock is high or where thicker, fine-grained colluvial deposits have accumulated.

The potential for rockfall along the east shore of the present Strawberry Reservoir and the canyons of Strawberry River and Indian Creek is low, and the volume of rock would be small. Also, the existing Strawberry Reservoir will be increased in height only 13 m, making activation of any large new slides unlikely. For these reasons, landsliding and landslide-induced water waves should not pose a significant hazard to Soldier Creek Dam.

7.5 Reservoir Seiche

> "The amplitude of the seiching motion induced in a body of water [by earthquake ground motions] is dependent upon the amplitude of the long-period surface waves generated by the earthquake and the similarity between the period of the surface waves and the natural periods of oscillation of the body of water." (Houston, 1979.)

Seiche due to ground motions will probably not be a significant hazard in the future enlarged Strawberry Reservoir, but a detailed analysis of this problem is beyond the scope of this report.

Displacement on either the Strawberry or Stinking Springs faults would probably produce a more significant seiche hazard. An MCE of 7.0 on the Strawberry fault could produce about 2 m of down-to-the-west displacement, and an MCE of 6.5 on the Stinking Springs fault could produce about 1 m of down-to-the-west displacement (table 6.2; Slemmons, 1977). Thus, a displacement on either fault would produce a relative increase in the height of the dam to the reservoir. Because our structural interpretation of both faults includes eastward tilting of the downthrown fault blocks, the degree of tilting and net vertical displacement would decrease to the west away from the dam.

7.6 Liquefaction

The only potentially liquefiable materials (Marcuson and others, 1980) identified at Soldier Creek Dam during preconstruction investigations were sandy and gravelly alluvium in the Strawberry River channel and silty-sand colluvial aprons along the edge of the river gorge (Thompson, 1965). These materials were removed in the core trench (Randolph, 1974), but alluvium and colluvium were not stripped from the foundation and abutments upstream and downstream of zone 1. However, "liquefaction of the granular materials downstream of zone 1 does not appear to be a reasonable possibility even

during a severe earthquake" (Peck, 1981). Upstream of zone 1, alluvium and colluvium beneath zone 2 might slump to some extent, but a large portion would remain to buttress zone 1. Thus, liquefaction of foundation materials is not considered a potential threat to the security of the dam (Peck, 1981).

REFERENCES

Allen, C. R., 1975, Geological criteria for evaluating seismicity: Geological Society of America Bulletin, vol. 86, pp. 1041-1057.

Andersen, D. W., and M. D. Picard, 1972, Stratigraphy of the Duchesne River Formation (Eocene-Oligocene), northern Uinta Basin, northeastern Utah: Utah Geological and Mineralogical Survey, Bulletin No. 97, 29 pp.

Anderson, L. W., and D. G. Miller, 1979, Quaternary fault map of Utah: Long Beach, California, Fugro, Inc.

Anderson, R E, 1979, Quaternary tectonics along the Intermountain Seismic Belt south of Provo, Utah: Brigham Young University Geology Studies, vol. 25, part 1, pp. 1-10.

Anderson, R. C., R. C. Bucknam, and R. E. Wallace, 1978, Seismotectonics of Utah and Nevada (abstract): U.S. Geological Survey Professional Paper No. 1100, pp. 259-261.

Anderson, T. C., 1977, Compound faceted spurs and recurrent movement on the Wasatch fault zone, North Central Utah: Brigham Young University Geology Studies, vol. 24, pp. 83-101.

Arabasz, W. J., 1979, Historical review of earthquake related studies and seismograph recording in Utah, in, Arabasz, W. J., R. B. Smith and W. D. Richins, eds., Earthquake studies in Utah 1850 to 1978 : University of Utah Seismograph Stations, Department of Geology and Geophysics, University of Utah, Salt Lake City, Utah, pp. 33-56.

Arabasz, W. J., and R. B. Smith, 1979, Introduction: What you've always wanted to know about earthquakes in Utah, in, Arabasz, W. J., R. B. Smith, and W. D. Richins, eds., Earthquake studies in Utah 1850 to 1978 : University of Utah Seismograph Stations, Department of Geology and Geophysics, University of Utah, Salt Lake City, Utah, pp. 1-14.

Arabasz, W. J., R. B. Smith, and W. D. Richins, 1979, Earthquake studies along the Wasatch Front, Utah: Network monitoring, seismicity, and seismic hazards, in, Arabasz, W. J., R. B. Smith and W. D. Richins, eds., Earthquake studies in Utah 1850 to 1978 : University of Utah Seismograph Stations, Department of Geology and Geophysics, University of Utah, Salt Lake City, Utah, pp. 253-285.

Armstrong, R. L., 1968, Sevier Orogenic Belt in Nevada and Utah: Geological Society America Bulletin, vol. 79, pp. 29-458.

Astin, G. K., 1977, Structure and stratigraphy of the Co-op Creek Quadrangle, Wasatch County, Utah: Brigham Young University Geology Studies, vol. 24, part 1, pp. 13-34.

Atwater, T., 1970, Implications of plate tectonics for the Cenozoic tectonic evolution of western North America: Geological Society America Bulletin, vol. 81, pp. 3513-3536.

Atwood, W. W., 1909, Glaciation of the Uinta and Wasatch Mountains: U.S. Geological Survey Professional Paper No. 61, 86 pp.

Bachman, G. O., and M. N. Machette, 1977, Calcic soils and calcretes in the southwestern United States: U.S. Geological Survey Open-File Report No. 77-795, 163 pp.

Bada, J. L., and R. Protsch, 1973, Racemization reaction of aspartic acid and its use in dating fossil bones: Proceedings National Academy Science, vol. 70, pp. 1331-1334.

Baecher, G. B., and R. L. Keeney, 1982, Statistical examination of reservoir-induced seismicity: Bulletin of the Seismological Society of America, vol. 72, pp. 553-569.

Baker, A. A., 1959, Faults in the Wasatch Range near Provo, Utah, in, Guidebook to the geology of the Wasatch and Uinta Mountains transition area: Intermountain Association of Petroleum Geologists, 10th Annual Field Conference, pp. 153-158.

Baker, A. A., 1976, Geologic Map of the west half of the Strawberry Quadrangle, Utah: U.S. Geological Survey Miscellaneous Investigations Series Map I-931.

Beutner, E. C., 1977, Causes and consequences of curvature in the Sevier Orogenic belt, Utah to Montana, in E. L. Heisey, D. E. Lawson, E. R. Norwood, P. H. Wach, and L. A. Hale, eds., Wyoming Geological Association Guidebook, Twenty-Ninth Annual Field Conference, pp. 353-366.

Birkeland, P. W., 1974, Pedology, Weathering, and Geomorphological Research: New York, Oxford University Press, 285 pp.

Birkeland, P. W., and R. R. Shroba, 1974, The status of the concept of Quaternary soil-forming intervals in the western United States, in, Mahaney, W. C., ed., Quaternary Environments, Proceedings of a Symposium, Geographic Monograph, No. 5, Toronto, York University, pp. 241-276.

Bissell, H. J., 1952, Stratigraphy and structure of northeast Strawberry Valley Quadrangle, Utah: American Association of Petroleum Geologists Bulletin, vol. 36, pp. 575-634.

Bissell, H. J., 1959, North Strawberry Valley sedimentation and tectonics, in, Guidebook to the Geology of the Wasatch and Uinta Mountains Transition Area: Intermountain Association Petroleum Geologists, vol. 10, pp. 159-165.

Bonilla, M. G., 1979, Historic surface faulting - map patterns, relation to subsurface faulting, and relation to preexisting faults, in Speed, R., R. Sharp, and J. F. Evernden, Proceedings of Conference VIII, analysis of actual fault zones in bedrock: U.S. Geological Survey Open-file Report No. 79-1239, pp. 36-65.

Bonilla, M. G., and J. M. Buchanan, 1970, Interim report on worldwide historic surface faulting: U.S. Geological Survey Open-file Report, 32 pp.

Bonilla, M. G., H. A. Villalobos, and R. E. Wallace, 1980, Exploratory trench across the Pleasant Valley fault, Nevada: U.S. Geological Survey Open-file Report No. 80-1245.

Bromfield, C. S., A. A. Baker, and M. D. Crittenden, Jr., 1970, Geologic map of the Heber Quadrangle, Wasatch and Summit Counties, Utah: U.S. Geological Survey Geologic Quadrangle Map GQ-864.

Bromfield, C. S. and M. D. Crittenden Jr., 1971, Geologic Map of the Park City East Quadrangle, Summit and Wasatch Counties, Utah: U.S. Geological Survey Map GQ-852.

Broecker, W. S. and A. Walton, 1959, The geochemistry of C14 in freshwater systems: Geochimica et Cosmochimica Acta, vol. 16, pp. 15-38.

Bucknam, R. C., and R. E. Anderson, 1979, Estimation of fault-scarp ages from a scarp-height-slope-angle relationship; Geology, vol. 7, pp. 11-14.

Bull, W. B., 1977, The alluvial-fan environment: Progress in Physical Geography, vol. 1, pp. 222-270.

Burchfield, B. C., and C. W. Hichcox, 1972, Structural development of central Utah: Utah Geological Association Publication No. 2, pp. 55-66.

Canada Soil Survey Committee, Subcommittee on Soil Classification, 1978, The Canadian System of Soil Classification: Canadian Department of Agriculture Publication 1646, Supply and Services Canada, Ottawa, 164 pp.

Carver, D., C. J. Langer, W. D. Richins, and R. Henrisey, 1978, Aftershocks of the September 30, 1977 Uinta Basin, Utah earthquakes (abstract): Earthquake Notes, vol. 49, No. 1, p. 41.

Carver, D., C. J. Langer, and W. D. Richins, 1981, Fine details of the aftershock process following the September 30, 1977 Uinta Basin, Utah, earthquakes (abstract): Earthquake Notes, vol. 52, No. 1, p. 62.

Carver, R. E., 1971, ed., Procedures in Sedimentary Petrology: New York, Wiley-Interscience, 653 pp.

Cluff, L. S., C. E. Glass, and G. E. Brogan, 1974, Investigation and evaluation of the Wasatch fault north of Brigham City and Cache Valley fault, Utah and Idaho: A guide to land use planning with recommendations for seismic safety [unpublished report]: Oakland, CA, Woodward-Lundgren and Associates, 147 p.

Cluff, L. S., L. F. Hintze, G. E. Brogan, and C. E. Glass, 1975, Recent activity of the Wasatch fault, northwestern, Utah, U.S.A.: Tectonophysics, vol. 29, pp. 161-168.

Cluff, L. S., A. S. Patwardhan, and K. J. Coppersmith, 1980, Estimating the probability of occurrence of surface faulting earthquakes on the Wasatch fault zone, Utah: Bulletin of the Seismological Society of America, vol. 70, No. 5, pp. 1463-1478.

Chinnery, M. A., 1969, Earthquake magnitude and source parameters: Seismological Society of America Bulletin, vol. 59, pp. 1969-1982.

Colman, S. M., and K. L. Pierce, 1981, Weathering and rinds on andesitic and basaltic stones as Quaternary age indicators, western United States: U.S. Geological Survey Professional Paper No. 1210, 56 pp.

Crittenden, M. D. Jr., 1961, Magnitude of thrust faulting in northern Utah: U.S. Geological Survey Professional Paper No. 424D, pp. D128-D131.

,1964, General geology of Salt Lake County: Utah Geological Mineralogical Survey Bulletin No. 60, pp. 11-48.

,1976, Stratigraphic and structural setting of the Cottonwood area, Utah, in J. G. Hill, ed., Symposium on the Geology of Cordilleran Hingeline: Rocky Mountain Association of Geologists, pp. 363-379.

Crosby, G. W., 1972, Dual origin of Basin and Range faults: Utah Geologic Association Publication 2, pp. 67-73.

Davis, D., 1979, Thrustbelt structural styles of the Charleston-Strawberry plate near Weber City, northeast Utah: Update on the Wyoming-Idaho-Utah thrustbelt: joint meeting of the Wyoming Geological Association, Wyoming Geological Survey, and the Department of Geology at the University of Wyoming (abstract), p. 5.

Doser, D. I., and R. B. Smith, 1982, Seismic moment rates in the Utah region: Bulletin of the Seismological Society of America, vol. 72, pp. 525-551.

Dreimanis, Aleksis, 1962, Quantitative gasometric determination of calcite and dolomite by using chittick apparatus: Journal Sedimentary Petrology, vol. 32, pp. 520-529.

Eardley, A. J., 1934, Structure and physiography of the southern Wasatch Mountains, Utah: Michigan Academy of Science Arts and Letters Papers, vol. 19, pp. 377-400.

Geyh, M. A., J. H. Benzler, and G. Roeschmann, 1971, Problems of dating Pleistocene and Holocene soils by radiometric methods, in, Yaalon, D. H., ed., Paleopedology: Origin, Nature, and Dating of Paleosols: International Society of Soil Science and Israel Universities Press, Jerusalem, pp. 63-75.

Gilbert, G. K., 1890, Lake Bonneville: U.S. Geological Survey Monograph No. 1, 438 pp.

Gilbert, G. K., 1928, studies of basin and Range structure: U.S. Geological Survey Professional Paper 153, 89 pp.

Gile, L. H., and R. B. Grossman, 1979, The Desert Project Soil Monograph: U.S. Department of Agriculture, Soil Conservation Service, 984 pp.

Grubbs, K. L., and R. van der Voo, 1976, Structural deformation of the Idaho-Wyoming overthrust belt (USA) as determined by Triassic paleomagnetism: Tectonophysics, vol. 33, pp. 321-336.

Guttenburg, B. and C. F. Richter, 1956, Earthquake magnitude, intensity, energy and acceleration (second paper): Seismological Society of American Bulletin, vol. 46, pp. 105-145.

Hamblin, W. K., 1965, Origin of "reverse drag" on the downthrown side of normal faults: Geological Society America Bulletin, vol. 76, pp. 1145-1164.

Hamblin, W. K., 1976, Patterns of displacement along the Wasatch fault: Geology, vol. 4, pp. 619-622.

Hamblin, W. K., P. E. Damon, and W. B. Bull, 1981, Estimates of vertical crustal strain rates along the western margins of the Colorado Plateau: Geology, vol. 9, pp. 293-298.

Hanson, K. L., F. H. Swan, and D. P. Schwartz, 1981, Study of earthquake recurrence intervals on the Wasatch Fault, Utah [Sixth semiannual technical report for U.S. Geological Survey Contract No. 14-08-0001-19115]: Woodward-Clyde Consultants, San Francisco, CA, 22 pp.

Hays, W. W., R. D. Miller, and K. W. King, 1980, Ground response in the Salt Lake City-Ogden-Provo, Utah, urban corridor, in, Proceedings of the 7th World Conference on Earthquake Engineering, Istanbul, Turkey, vol. 2, pp. 89-96.

Hintze, L. F., 1973, Geologic history of Utah: Brigham Young University Geology Studies, vol. 20, part 3, Studies for Students No. 8, 181 pp.

Hintze, L. F., 1980, Geologic map of Utah: Utah Geological and Mineral Survey [1:500,000 scale]

Houston, J. R., 1979, Tsunamis-, seiches-, and landslide-induced water waves: U.S. Army Engineer Waterways Experiment Station, State-of-the-art for assessing earthquake hazards in the United States Report No. 15, 88 pp.

Jackson, M. L., 1956, Soil Chemical Analysis, Advanced Course [unpublished]: University of Wisconsin, Department of Soil Science, 656 pp.

Jones, D. J., and R. E. Marsell, 1955, Pleistocene sediments of lower Jordon Valley, Utah: Guidebook to the Geology of Utah number ten, pp. 85-112.

Kanamori, H., and D. L. Anderson, 1975, Theoretical basis of some empirical relations in seismology: Bulletin of Seismological Society of America, vol. 65, pp. 1073-1095.

Kihl, R., 1975, Appendix: Physical preparation of organic matter samples for C14 dating, in, Andrews, J. T., Radiocarbon date list II from Cumberland Peninsula, Baffin Island, N.W.T., Canada: Arctic and Alpine Research, vol. 7, pp. 90-91.

King, G. C. P., and C. Vita-Finzi, 1981, Active folding in the Algerian earthquake of 10 October 1980: Nature, vol. 292, pp. 22-26.

Kisslinger, C., 1976, A review of theories of mechanisms of induced seismicity: Engineering Geology, vol. 10, pp. 85-98.

Kucera, R. E., 1954, Geology of the Joes Valley and North Dragon area, central Utah [M.S. thesis]: Columbus, Ohio State University, 210 pp.

Langer, C. J., G. R. Keller, and R. B. Smith, 1979, A study of aftershocks of the October 1, 1972 m_b = 4.7, Heber City, Utah earthquake, in, Arabasz, W. J., R. B. Smith, and W. D. Richins, eds., Earthquake studies in Utah 1850 to 1978: University of Utah Seismograph Stations, Department of Geology and Geophysics, Salt Lake City, Utah, University of Utah, pp. 383-394.

Longwell, C. R., 1936, Geology of the Boulder reservoir floor, Arizona-Nevada: Geological Society America Bulletin, vol. 47, pp. 1393-1476.

Madole, R. F., 1976, Glacial geology of the Front Range, Colorado; in, Mahaney, W. C., ed., Quaternary Stratigraphy of North America: Stroudsburg, Pennsylvania, Dowden, Hutchinson, and Ross, pp. 297-318.

Madole, R. F., and R. R. Shroba, 1979, Till sequence and soil development in the north St. Vrain drainage basin, east slope, Front Range, Colorado, in, Ethridge, F. G., ed., Geological Society of America, Rocky Mountain Section, Guidebook for Fieldtrips, 32nd Annual Meeting: Fort Collins, Department of Earth Resources, Colorado State University, pp. 124-178.

Madsen, D. B., and D. R. Currey, 1979, Late Quaternary glacial and vegetation changes, Little Cottonwood Canyon Area, Wasatch Mountains, Utah: Quaternary Research, vol. 12, No. 2, pp. 254-270.

Mahaney, W. C., 1978, Late Quaternary stratigraphy and soils in the Wind River Mountains, western Wyoming, in Mahaney, W. C., ed., Quaternary Soils: Norwich, England, Geo Abstracts, pp 223-264.

Marcuson, W. F., A. G. Franklin, P. F. Hadala, 1980, Liquefaction potential of dams and foundations: U.S. Army Engineer Waterways Experiment Station, Research Report No. S-76-2, Report No. 7, 30 pp.

Mark, R. K., and M. G. Bonilla, 1977, Regression analysis of earthquake magnitude and surface fault length using the 1970 data of Bonilla and Buchanan: U.S. Geological Survey Open-file Report No. 77-614.

Martin, R. A. Jr., R. R. Weisser, and A. R. Nelson, 1983, Seismotectonic hazard evaluation of Upper Stillwater and Taskeech damsites, Central Utah Project: U.S. Bureau of Reclamation, Denver, Colorado, (being reviewed)

Matsuda, T., 1975, Magnitude and recurrence interval of earthquakes from a fault [in Japanese]: Earthquake, series 2, vol. 28, pp. 269-283.

Matthews, J. A., 1980, Some problems and implications of 14C dates from a podzol buried beneath an end moraine at Haugabreen, southern Norway: Geografiska Annaler, vol. 62A, pp. 185-208.

McCoy, W. D, 1981, Quaternary aminostratigraphy of the Bonneville and Lahontan basins, western U.S., with paleoclimatic implications [PH.D. thesis]: Boulder, University of Colorado, 157 pp.

McDonald, R. E., 1976, Tertiary tectonics and sedimentary rocks along the transition, Basin and Range Province to Plateau and Thrustbelt Province, Utah, in J. G. Hill, ed., Symposium of the Geology of the Cordilleran Hingeline: Rocky Mountain Association of Geologists, p. 281-317.

Miller, G. H., and P. E. Hare, 1980, Amino acid geochronology: Integrity of the carbonate matrix and potential of molluscan fossils, in, Hare, P. E., T. C. Hoering, and K. King Jr., eds., Biogeochemistry of Amino Acids: New York, John Wiley, pp. 415-443.

Miller, G. H., A. R. Nelson, W. McCoy, and A. L. Metcalf, 1979, Amino acid geochronology utilizing terrestrial gastropods from western U.S.: Geological Society of America, Abstracts with Programs, vol. 11, No. 6, pp. 280-281.

Miller, G. H., W. D. McCoy, and A. R. Nelson, 1982, Environmental controls in the amino acid racemization rate from continental-interior deposits: Geological Society of America, Abstracts with Programs, vol. 14, No. 7, p. 565.

Moore, J. G., 1960, Curvature of normal faults in the Basin and Range province of western United States: U.S. Geological Survey Professional Paper No. 400B, pp. B409-B411.

Mullens, T. E. and G. A. Izett, 1964, Geology of the Paradise quadrangle, Cache County, Utah: U.S. Geological Survey, Bulletin No. 1181-S.

Murdock, J. N., 1948, Reconnaissance geological report of the Soldier Creek Damsite: U.S. Bureau of Reclamation, Salt Lake City, Utah, Report No. G-40, 7 pp.

Nash, D. B., 1980, Morphologic dating of degraded normal fault scarps: Journal of Geology, vol. 88, pp. 353-360.

Nash, D. B., 1981, Fault: A fortran program for modeling the degradation of active normal fault scarps: Computers and Geosciences, vol. 7, pp. 249-266.

Nelson, A. R., 1982, Late Quaternary movement on the Strawberry fault, northeastern Utah: Geological Society of America, Abstracts with Programs, vol. 14, No. 2, pp. 219-220.

Nelson, A. R., and C. K. Krinsky, 1982, Late Cenozoic history of the upper Weber and Provo Rivers, NE. Utah: Geological Society of America, Abstracts with Programs, vol. 14, No. 3, p. 344.

Nelson, A. R., A. C. Millington, J. T. Andrews, and H. Nichols, 1979, Radiocarbon-dated upper Pleistocene glacial sequence, Fraser Valley, Colorado Front Range: Geology, vol. 7, pp. 410-414.

NOAA, 1980, Earthquake data file (through 1979): National Geophysical and Solar-terrestrial Data Center, Boulder, Colorado.

Nolan, T. B., 1943, The Basin and Range province in Utah, Nevada, and California: U.S. Geological Survey Professional Paper No. 197D, pp. 141-196.

Olsson, I. U., 1968, Modern C13 aspects of radiocarbon datings: Earth Science Reviews, vol. 4, pp. 203-218.

Osborn, G. D., 1973, Quaternary geology and geomorphology of the Uinta Basin and the south flank of the Uinta Mountains, Utah [Ph.D. thesis]: Berkeley, University of California, 266 pp.

Osborne, S. D., 1978, Late Cenozoic movement on the central Wasatch fault, Utah: Brigham Young University Geology Studies, vol. 25, pp. 99-114.

Osmond, J. C., 1960, Tectonic history of the Basin and Range Province in Utah and Nevada: Mining Engineer, vol. 12, pp. 251-265.

,1964, Tectonic history of the Uinta Basin, Utah: Intermountain Association Petroleum Geologists 13th Annual Field Conference Guidebook, pp. 47-58.

,1965, Geologic history of site of Uinta Basin, Utah: Bulletin American Association Petroleum Geologists, vol. 49, pp. 1957-1973.

Oyama, M. and Takehara, H., 1970, Revised Standard Soil Color Charts: Ministry of Agriculture and Forestry, Japan, 40 pp.

Packer, D. R., L. S. Cluff, P. L. Knuepfer, and R. J. Withers, 1977, Study of reservoir induced seismicity: U.S. Geological Survey Open-file Report No. 80-1092, 677 pp.

Peck, R. B., 1981, Review of Soldier Creek Dam, Bonneville Unit, Central Utah Project [Unpublished report for USBR dated May 18, 1981]: U.S. Bureau of Reclamation, Denver, Colorado.

Peterson, J. E., E. M. Baltzer, G. A. Teter, and J. T. Sullivan, 1982, Landsat image enhancement in support of seismotectonic studies in Utah: Proceedings of annual convention of the American Society of Photogrammetry, pp. 550-561.

Pierce, K. L., 1979, History and dynamics of glaciation in the northern Yellowstone National Park area: U.S. Geological Survey Professional Paper No. 729-F, 90 pp.

Pierce, K. L., J. D. Obradovitch, and I. Friedman, 1976, Obsidian hydration dating and correlation of Bull Lake and Pinedale glaciations near West Yellowstone, Montana: Geological Society of America Bulletin, vol. 87, pp. 703-710.

Porter, S. C., K. L. Pierce, and T. D. Hamilton, 1982, Mountain glaciation in the western United States, in, Porter, S. C., ed., Late Pleistocene environments in the United States: Minneapolis, Minnesota, University of Minnesota Press, (in press).

Proctor, P. D., 1959, Structural setting of Fivemile Pass and Northern Boulter Mountains area: Guidebook to the Geology of Utah, No. 14, pp. 188-197.

Proffett, J. M., Jr., 1977, Cenozoic geology of the Yerrington district, Nevada, and implications for the nature and origin of Basin and Range faulting: Geological Society America Bulletin, vol. 88, No. 2, pp. 247-266.

Randolph, P. E., 1974, Construction engineering geology report for Soldier Creek Dam: U.S. Bureau of Reclamation, Central Utah Project, Uinta Basin Construction Office, Duchesne, Utah, Report G295 [unpublished], 10 pp.

Richmond, G. M., 1965, Glaciation of the Rocky Mountains, in, Wright, H. E., Jr. and D. G. Frey, eds., The Quaternary of the United States: Princeton, Princeton University Press, pp. 217-230.

Roberts, R. J., P. E. Hotz, Gilluly, James, and H. G. Ferguson, 1958, Paleozoic rocks of north-central Nevada: American Association Petroleum Geologists Bulletin, vol. 20, part 3, pp. 2813-2857.

Roberts, R. J., M. D. Crittenden, Jr., E. W. Tooker, H. T. Morris, R. K. Hose, T. M. Cheney, 1965, Pennsylvanian and Permian in northwestern Utah, northeastern Nevada, and southcentral Idaho: American Association Petroleum Geologists Bulletin, vol. 49, pp. 1926-1956.

Royse, F., M. A. Warner, and D. L. Reese, 1975, Thrustbelt structural geometry and related stratigraphic problems: Wyoming-Idaho-Northern Utah, in, Rocky Moutain Association Geologists. Symposium on deep drilling frontiers in the Central Rocky Mountains, pp. 41-54.

Ryder, R. T., T. D. Fouch, and J. H. Elison, 1976, Early Tertiary sedimentation in the western Uinta Basin, Utah: Geological Society America Bulletin, vol. 87, pp. 496-512.

Scharpenseel, H. W., 1971, Radiocarbon dating of soils - problems, troubles, hopes, in, Yaalon, D. H., ed., Paleopedology: Origin, Nature, and Dating of Paleosols: International Society of Soil Science and Israel Universities Press, Jerusalem, pp. 77-88.

Scharpenseel, H. W., and H. Schiffmann, 1977, Radiocarbon dating of soils, a review: Zeitschrift fur Pflanzenernahrung Dungung und Bodenkunde, vol. 140, pp. 159-174.

Schroeder, R. A. and J. L. Bada, 1976, A review of the geochemical applications of the amino acid racemization reaction: Earth and Planetary Science Letters, vol. 12, pp. 347-391.

Scholz, C. H., Barazangi, Muawia, and M. L. Sbar, 1971, Late Cenozoic evolution of the Great Basin, western United States as an ensialic interarc basin: Geological Society America Bulletin, vol. 82, pp. 2979-2990.

Scott, W. E., 1980, New interpretations of Lake Bonneville stratigraphy and their significance for studies of earthquake-hazard assessment along the Wasatch Front: U.S. Geological Survey Open-file Report No. 80-801, pp. 548-576.

Scott, W. E., W. D. McCoy, R. R. Shroba, and R. D. Miller, 1980, New interpretations of the late Quaternary history of Lake Bonneville, western U.S.: American Quaternary Association, Abstracts of 6th Biennial Meeting, pp. 168-169.

Sherard, J. L., L. S. Cluff, and C. R. Allen, 1974, Potentially active faults in dam foundations: Geotechnique, vol. 24, pp. 367-428.

Shroba, R. R., 1980, Influence of parent material, climate, and time on soils formed in Bonneville-shoreline and younger deposits near Salt Lake City and Ogden, Utah: Geological Society of America, Abstracts with Programs, vol. 12, No. 6, p 304.

Shroba, R. R., 1982, Soil B-horizon properties as age indicators for late Quaternary deposits along the Wasatch Front, northcentral Utah: Geological Society of America, Abstracts with Programs, vol. 14, No. 4, p. 233.

Simpson, D. W., and S. K. Negmatulaev, 1981, Induced seismicity at Nurek Reservoir, Tadjikistan, U.S.S.R: Bulletin Seismological Society America, vol. 71, No. 5, pp. 1561-1586.

Singh, S. K., E. Bazan, and L. Esteva, 1980, Expected earthquake magnitude from a fault: Bulletin of Seismological Society of America, vol. 70, pp. 903-914.

Slemmons, D. B., 1977, Faults and earthquake magnitude: U.S. Army Enginer Waterways Experiment Station Miscellaneous Paper 5-73-1, 160 pp.

Smith, R. B., 1978, Seismicity, crustal structure, and intraplate tectonics of the interior of the Western Cordillera: Geological Society of America Memoir 142, pp. 111-144.

Smith, R. B. and W. J. Arabasz, 1979, Seismicity, tectonics, and crustal structure in Utah: important aspects from new data; in, Earthquake studies in Utah 1850 to 1978: Seismograph Stations, Salt Lake City, University of Utah, pp. 395-408.

Smith, R. B., and M. L. Sbar, 1974, Contemporary tectonics and seismicity of the western United States with emphasis on the intermountain seismic belt: Geological Society of America Bulletin, vol. 85, pp. 1205-1218.

Soil Survey Staff, 1975, Soil Taxonomy: U.S. Department of Agriculture, Agriculture Handbook No. 436, 754 pp.

Soil Survey Staff, 1981, Soil Survey Manual: Soil Conservation Service, U.S. Department of Agriculture (in review)

Spieker, E. M. and M. P. Billings, 1940, Glaciation in the Wasatch Plateau, Utah: Geological Society of America Bulletin, vol. 51, pp. 1173-1198.

Stepp, J. C., 1972, Analysis of the completeness of the earthquake sample in the Puget Sound area and its effect on statistical estimates of earthquake hazards, in, Proceedings, International Conference on Microzonation for Safer Construction, Research and Application, vol. 2, Seattle, Washington, Washington University, pp. 897-909.

Stewart, J. H., 1971, Basin and Range structure: a system of horsts and grabens produced by deep-seated extension: Geological Society America Bulletin, vol. 82, pp. 1019-1044.

Stewart, J. H., 1978, Basin-range structure in western North America: A review: Geological Society of America Memoir 152, pp. 1-32.

Stokes, W. L., 1976, What is the Wasatch Line?, in, J. G. Hill, Symposium on the Geology of the Cordilleran Hingeline: Rocky Mountain Association of Geologists, pp. 11-26.

Stokes, W. L. and J. H. Madsen, Jr., 1961, Geologic map of Utah - northeast quarter (1:250,000 scale): Utah State Land Commission and Utah Geological and Mineral Survey, Salt Lake City, Utah.

Sullivan, J. T., 1982, Late Cenozoic faulting in the back valleys of the Wasatch Mountains, northeastern Utah: Geological Society of America, Abstracts with Programs, vol. 14, No. 6, p. 351.

Sullivan, J. T., A. R. Nelson, R. A. Martin Jr., L. L. Foley, C. K. Krinsky, and E. M. Baltzer, 1983, Central Utah Regional Seismotectonic Study [unpublished report]: Denver, U.S. Bureau of Reclamation (in progress).

Survey Notes, 1977, Utah Geological and Mineral Survey, vol. 11, No. 4, November 1977, pp. 1 and 3.

Swan, F. H., III, D. P. Schwartz, and L. S. Cluff, 1980, Recurrence of moderate to large magnitude earthquakes produced by surface faulting on the Wasatch fault zone, Utah: Bulletin Seismological Society of America, vol. 70, No. 5, pp. 1431-1462.

Swan, F. H., III, K. L. Hanson, D. P. Schwartz, and P. L. Knuepfer, 1981, Study of earthquake recurrence intervals on the Wasatch fault, Utah - Little Cottonwood Canyon site: U.S. Geological Survey Open-file Report No. 81-450, 30 pp.

Szabo, B. J., 1980, Results and assessment of Uranium-series dating of vertebrate fossils from Quaternary alluviums in Colorado: Arctic and Alpine Research, vol. 12, No. 1, pp. 95-100.

Thenhaus, P. C. and C. M. Wentworth, 1981, Map showing regionalization of the Basin and Range according to ages to latest surface faulting and maximum estimated earthquake size: U.S. Geological Survey Open-file Report (unnumbered), 9 pp.

Thompson, F., 1965, Geology report for Soldier Creek Dam and Reservoir sites: U.S. Bureau of Reclamation, Central Utah Project, Salt Lake City, Utah, Report No. G-210 [unpublished], 10 pp.

Thompson, F., 1971, Construction Geologic Report, Water Hollow Tunnel: U.S. Bureau of Reclamation, Salt Lake City, Utah, Report No. G-275, 36 pp.

Tocker, D., 1958, Earthquake energy and ground breakage: Seismological Society of America Bulletin, vol. 48, pp. 147-153.

Toppozada, T. R., and C. Cramer, 1978, Ukiah earthquakes and Lake Mendocino, California: Geology, vol. 31, pp. 275-282.

Threet, R. L., 1959, Geomorphology of the Wasatch-Uinta Mountains junction, in, Guidebook to the Geology of the Wasatch and Uinta Mountains Transition Area: Intermountain Association of Petroleium Geologists, vol. 10, pp. 24-33.

U.S. Geological Survey, 1976, A study of earthquake losses in the Salt Lake City, Utah area: U.S. Geological Survey Open-file Report No. 76-89, 357 pp.

U.S. Geological Survey, 1977, Earthquakes in the United States, Geological Survey Circular 788-C, pp. 23-25.

University of Utah, 1982, Earthquake Data Tape for the Utah Region, 1850 through 1981: University of Utah Seismograph Stations, Salt Lake City, Utah

Van Arsdale, R. B., 1979a, Geology of Strawberry Valley and regional implications [Ph.D. thesis]: Salt Lake City, University of Utah, 65 pp.

Van Arsdale, R. B., 1979b, Geometry and most recent movement along Strawberry normal fault, Wasatch County, Utah: Geological Society America Abstracts with Programs, vol. 11, No. 7, pp. 531-532.

Wahler, W. A. and Associates, 1977, Review of design, construction, and operation of Soldier Creek Dam Project, Utah [unpublished report]: W. A. Wahler and Associates, Palo Alto, California, 64 pp.

Wallace, R. E., 1977, Profiles and ages of young fault scarps, north-central Nevada: Geological Society of America Bulletin, vol. 88, pp. 1267-1281.

Wallace, R. E., 1981, Active faults, paleoseismology, and earthquake hazards in the western United States, in, Simpson, D. W., and P. G. Richards, eds., Earthquake Prediction - An International Review: American Geophysical Union, Washington, D.C., pp. 209-216.

Walker, T. R., B. Waugh, and A. J. Crone, 1978, Diagenesis in first-cycle desert alluvium of Cenozoic age, southwestern United States and northwestern Mexico: Geological Society of America Bulletin, vol. 89, pp. 19-32.

Walkley, A., and I. A. Black, 1934, An examination of the Degtjareff method for determining soil organic matter, and a proposed modification of the chromic acid titration method: Soil Science, vol. 34, pp. 29-38.

Walton, P. T., 1959, Structure of the West Portal-Soldier Summit Area, Wasatch, Carbon, and Duchesne Counties, Utah: Intermountain Association Petroleum Geologists 10th Annual Field Conference Guidebook, pp. 150-152.

Wehmiller, J. F., 1977, Amino acid studies of the Del Mar, California, midden site: apparent rate constants, ground temperature models and chronological implications: Earth and Plantetary Science Letters, vol. 37, No. 2, pp. 184-196.

Wehmiler, J. F., K. R. Lajoie, K. A. Kvenvolden, E. Peterson, D. F. Belknap, G. L. Kennedy, W. O. Addicott, J. G. Vedder, and R. W. Wright, 1977, Correlation and chronology of Pacific coast marine terrace deposits of continental United States by fossil amino acid stereochemistry - technique evaluation, relative ages, kinetic model ages, and geologic implications: U.S. Geological Survey Open-file Report No. 77-680, 190 p.

Wehmiller, J. F. and D. F. Belknap, 1978, Alternative kinetic models for the interpretation of amino acid enantiomeric ratios in Pleistocene mollusks: examples from California, Washington, and Florida: Quaternary Research, vol. 9, No. 3, pp. 330-348.

Williams, K. M., and G. G. Smith, 1977, A critical evaluation of the application of amino acid racemization to geochronology and geothermometry: International Symposium on Origins of Life No. 8, Reidel Publishing Company, Dordrecht-Holland, pp. 91-144.

Woodward-Clyde Consultants, 1980, Seismic hazard evaluation, Grove Creek and Battle Creek Dams near Provo, Utah [report prepared for the U.S. Department of Agriculture Soil Conservation Service]: Woodward-Clyde Consultants, 39 pp.

Wyss, Max, 1979, Estimating maximum expectable magnitude of earthquakes from fault dimensions: Geology, vol. 7, pp. 336-340.

Wyss, M., and J. N. Brune, 1968, Seismic moment, stress, and source dimensions for earthquakes in the California-Nevada region: Journal Geophysical Research, vol. 73, pp. 4681-4694.

Appendix A
Soil Profile Descriptions

Soil Profile Description SC-1

Classification: Typic Paleboroll

Location: Co-op Creek Quadrangle; Station 15 in Co-op Creek trench 1; NW1/4, NW1/4, SE1/4, NW1/4, sec. 32, T. 2 S., R. 11 W.

Physiographic position: Upthrown surface 7 m from crest of 7-m-high scarp; 2440 m (8000 ft) elevation.

Topography: Smooth surface sloping 5° W.

Drainage: Well drained.

Vegetation: Grasses.

Parent material: Surface colluvium over alluvial fan stream and debris flow deposits with clasts of Tertiary conglomerate consisting of quartzites and sandstones with rare limestone.

Age: Bull Lake or younger (Pinedale).

Remarks: Percentages are visually estimated.

Sampled by: A. R. Nelson and C. K. Krinsky, July 31, 1981.

A1 0-10 cm. Dark brown (10YR 3/3) dry, brownish black (10YR 2/2 moist; loam; weak to moderate subangular blocky; slightly hard (dry), nonsticky (wet), nonplastic (wet); very slightly effervescent on clasts; 10% pebbles, 25% cobbles, 5% boulders by volume; abrupt wavy boundary.

A2 10-38 cm. Dark brown (10YR 3/3) dry, brownish black (10YR 2/2) moist; loam; weak fine subangular blocky; soft (dry), nonsticky (wet), nonplastic (wet); 10% pebbles, 25% cobbles, 5% boulders by volume; clear wavy boundary.

2E 38-60 cm. Orange (5YR 7/5) dry, bright reddish brown (5YR 5/7) moist; sandy loam; weak fine subangular blocky; hard (dry), nonsticky (wet), nonplastic (wet); 10% pebbles, 25% cobbles, 5% boulders by volume; abrupt wavy boundary.

2 Bt 60-114 cm. Bright brown (2.5YR 5/6) dry, reddish brown (2.5YR 4/6) moist; sandy clay loam; weak fine to medium angular blocky; hard (dry), slightly sticky (wet), very slightly plastic; few thin argillans line tubular or interstitial pores; many moderately thick argillans on clasts; continuous thin oriented argillan bridges; 5% grusified clasts; 10% pebbles, 20% cobbles, 2% boulders by volume; gradual wavy boundary.

2C 114-149 cm. Bright brown (2.5YR 5/6) dry, reddish brown (2.5YR 4/6) moist; sandy load; weak very fine to fine subangular blocky; slightly hard (dry), very slightly sticky (wet), nonplastic (wet); few thin argillan bridges; matrix slightly effervescent; 1% grusified clasts; some weak stratification; clear broken boundary.

2 Ckj 149-210 cm. Bright brown (2.5YR 5/7) dry, reddish brown (2.5YR 4/7) moist; sandy loam; single grain; loose (dry), nonsticky (wet), nonplastic (wet); few thin argillan bridges; matrix violently effervescent, clasts strongly effervescent, carbonate veins on clasts; carbonate stage I^-; 25% pebbles and 10% cobbles by volume; abrupt irregular boundary.

3 Ckj 210-273 cm. Orange (5YR 6/7) dry, bright brown (2.5YR 5/6) moist; loamy sand; single grain loose (dry), nonsticky (wet), nonplastic (wet); few thin argillan bridges, few thin argillans line tubular or interstitial pores (infiltrated); matrix violently effervescent, clasts strongly effervescent, carbonate light gray (5 YR 8/1) dry; carbonate stage I; 10% pebbles, 5% cobbles and 30% boulders by volume; clear wavy boundary.

4 Ckj 273-334 cm. Orange (5YR 6/7) dry, bright brown (2.5YR 5/6) moist; loamy sand; single grain; loose (dry), nonsticky (wet), nonplastic (wet); few thin argillans on clasts, few thin argillan bridges, few thin argillans in tubular or interstitial pores (infiltrated); clasts violently effervescent, carbonate light gray (5YR 8/1) dry, carbonate stage I^-; weakly stratified; 30% pebbles and 15% cobbles by volume.

Soil Profile Description SC-2

Classification: Cumulic Haploboroll

Location: Co-op Creek Quadrangle; Station 46 in Co-op Creek trench 1; NW1/4, NW1/4, SE1/4, NW1/4, sec. 32, T. 2 S., R. 11 W.

Physiographic position: Downthrown surface 13 m from base of 7-m-high scarp; 2440 m (8000 ft) elevation.

Topography: Smooth surface sloping 1° W.

Drainage: Well drained.

Vegetation: Grasses.

Parent material: Fine-grained distal colluvium over alluvium.

Age: Holocene.

Remarks: Percentages are visually estimated.

Sampled by: C. K. Krinsky, August 1, 1981.

A1 0-26 cm. Brown (7.5YR 4/3) dry, dark brown (7.5YR 3/3) moist; loam; very weak fine subangular blocky; soft (dry), nonsticky and nonplastic (wet); 5% pebbles by volume; abrupt wavy boundary.

A2 26-58 cm. Brown (7.5YR 4/3) dry, dark brown (7.5YR 3/3) moist; loam; weak to moderate fine to medium subangular blocky; slightly hard (dry), nonsticky and nonplastic (wet); 5% pebbles by volume; clear smooth boundary.

A3 58-80 cm. Brown (7.5YR 4/3) dry, dark brown (7.5YR 3/3) moist; loam; weak fine to medium subangular blocky; hard (dry), nonsticky and nonplastic (wet); 5% pebbles by volume; gradual irregular boundary.

E 80-110 cm. Dull brown (7.5YR 5/4) dry, brown (7.5YR 4/4) moist; sandy loam; very weak fine subangular blocky; loose (dry), nonsticky and nonplastic (wet); 1% pebbles by volume; abrupt smooth boundary.

2 Bw 110-155 cm. Dull orange (7.5YR 6/4) dry, dull brown (7.5YR 5/4) moist; sandy clay loam; weak fine to medium subangular blocky; hard (dry), very slightly sticky and nonplastic (wet); continuous thin argillans bridging grains, few thin argillans lining pores; 1% pebbles by volume; clear wavy boundary.

2C 155-230 cm. Dull orange (7.5YR 6/4) dry, dull brown (7.5YR 5/4) moist; loam; very weak fine subangular blocky; slightly hard (dry), nonsticky and nonplastic (wet); 1% pebbles by volume; abrupt wavy boundary.

3C 230-300+ cm. Dull orange (7.5YR 6/4) dry, dull brown (7.5YR 5/4) moist; sand to loam; single grain to strong medium subangular blocky; loose to hard (dry), nonsticky to slightly sticky and nonplastic to slightly plastic (wet); fragments, seams, and clast coatings of bright reddish brown (5YR 5/8) dry clay loam throughout horizon; 15% pebbles, 20% cobbles, and 5% boulders by volume, boulders near upper contact.

Soil Profile Description SC-3

Classification: Cumulic Haploboroll

Location: Co-op Creek Quadrangle; Station 19 in Co-op Creek trench 2; NW1/4, NE1/4, SE1/4, SW1/4, sec. 32, T. 2 S, R. 11 W.

Physiographic position: Downthrown surface at base of 5-m-high scarp; 2434 m (7980 ft) elevation.

Topography: Smooth surface sloping 2° W.

Drainage: Well drained.

Vegetation: Grasses.

Parent material: Distal and proximal colluvium over alluvial fan debris flow deposits.

Age: Holocene.

Remarks: Percentages are visually estimated.

Sampled by: A. R. Nelson, September 1, 1981.

A1 0-11 cm. Dull brown (7.5YR 5/4) dry, dark brown (7.5YR 3/4) moist; loam; weak coarse platy; weakly coherent (dry), nonsticky (wet), nonplastic (wet); 10% pebbles, and <1% cobbles by volume; abrupt smooth boundary.

A2 11-76 cm. Dull brown (7.5YR 5/4) dry, dark brown (7.5YR 3/4) moist; loam; weak medium prismatic to weak medium subangular blocky; slightly hard to weakly coherent (dry), nonsticky (wet), nonplastic (wet); 10% pebbles, and <1% cobbles by volume; clear smooth boundary.

A3 76-105 cm. Dull brown (7.5YR 5/4) dry, dark brown (7.5YR 3/4) moist; loam; very weak fine to medium subangular blocky; slightly hard (dry), slightly sticky (wet), nonplastic (wet); 10% pebbles,and <1% cobbles by volume; abrupt wavy boundary.

Bw 105-149 cm. Orange (7.5YR 6/6.5) and orange (5YR 6/6.5) dry, bright brown (7.5YR 4/6.5) and reddish brown (5YR 4/6.5) moist; loam; medium weak to moderate prismatic; slightly hard (dry), sticky (wet), plastic (wet); continuous thin argillan bridges, few thin argillans in tubular pores or interstitial pores, many thin argillans on clasts; 10-20% pebbles, 5% cobbles and 4% boulders by volume; clear wavy boundary.

2CB 149-183 cm. Dull orange (5YR 7/3) to orange (7.5YR 6/6) dry, bright reddish brown (5YR 5/6) to bright brown (7.5YR 5/6) moist; sand to sandy loam; single grain grading to weak fine subangular blocky; loose to weakly coherent (dry), nonsticky (wet), nonplastic (wet); common thin argillan bridges, common thin argillans on clasts; 20% pebbles, 10% cobbles, and <1% boulders by volume; clear wavy boundary.

2C1 183-204 cm. Orange (5YR 6/7) with pieces of 5YR 5/6, 5YR 7/5, 5YR 8/3, dry, bright reddish brown (5YR 5/7) with pieces of 5YR 6/4, moist; sandy loam; single grain with areas of weak fine subangular blocky; loose to weakly coherent (dry), nonsticky (wet), nonplastic (wet); 5-10% grusified clasts; 20% pebbles, 20% cobbles, and <1% boulders by volume; gradual wavy boundary.

2C2 204-279 cm. Bright brown (2.5YR 5/6) dry, dark reddish brown, (2.5YR 3/6) moist; sand to sandy clay loam; single grain to weak fine subangular blocky; loose to hard (dry), nonsticky to slightly sticky (wet), nonplastic to slightly plastic (wet); many moderately thick argillan bridges, common thin argillans in tubular or interstitial pores, many moderately thick argillans on clasts; common red clay seams; 5-10% grusified clasts; 20% pebbles, 20% cobbles and <1% boulders by volume; abrupt smooth boundary.

3C 279-360 cm. Reddish brown (2.5YR 5/6) with some orange (5YR 6/6) dry, reddish brown (2.5YR 4/6) with some reddish brown (5YR 4/8) to orange (5YR 6/8); sandy clay loam; massive; slightly sticky (wet); slightly plastic (wet); many moderately thick argillan bridges, common thin argillans in tubular or interstitial pores, many moderately thick argillans on clasts; common red clay seams; 1-10% pebbles and 0-20% cobbles by volume.

Soil Profile Description SC-4

Classification: Typic Ustochrept

Location: Deep Creek Canyon Quadrangle; NE1/4, NW1/4, NW1/4, SE1/4, sec. 7, T. 3 S., R. 9 W.

Physiographic position: Center of 28-m-high fluvial terrace; 2114 m (6930 ft) elevation.

Topography: Smooth surface, 0° slope.

Drainage: Well drained.

Vegetation: Scattered sage.

Parent material: Fluvial gravels with quartzite and sandstone clasts.

Age: Pinedale?

Remarks: Percentages are visually estimated.

Sampled by: A. R. Nelson, August 26, 1981.

A1 0-8 cm. Dull brown (7.5YR 5/3) dry, dark brown (7.5YR 3/3) moist; sandy loam; weak medium subangular blocky; soft (dry), nonsticky and nonplastic (wet); 40% pebbles, 15% cobbles, and 2% boulders by volume; clear wavy boundary.

A2 8-23 cm. Brown (7.5YR 4/4) dry, dark brown (7.5YR 3/4) moist; sandy loam; very weak fine to medium subangular blocky; soft (dry), nonsticky and nonplastic (wet); 40% pebbles, 15% cobbles, and 2% boulders by volume; gradual wavy boundary.

Bw 23-80 cm. Bright reddish brown (5YR 5/7) dry, reddish brown (5YR 4/7) moist; sandy loam; weak to moderate fine to medium subangular blocky; slightly hard (dry), very slightly sticky and nonplastic (wet); continuous colloidal stains on mineral grains, common thin argillans bridging grains and coating clasts; 40% pebbles, 15% cobbles, and 2% boulders by volume; clear wavy boundary.

Cwj1 80-122 cm. Bright brown (7.5YR 5/6) dry, brown (7.5YR 4/6) moist; sand+; very weak fine to medium subangular blocky; loose (dry), nonsticky and nonplastic (wet); common colloidal stains on mineral grains, few thin argillans bridging grains; 40% pebbles, 15% cobbles, and 2% boulders by volume; gradual wavy boundary.

Cwj2 122-140+ cm. Orange (7.5 YR 6/6) dry, brown (7.5YR 4/6) moist; sand; single grain; loose (dry), nonsticky and nonplastic (wet); few discontinuous carbonate coatings on lower half of clasts, coatings slightly effervescent; 40% pebbles, 15% cobbles, and 2% boulders by volume.

Appendix B

Auger and Bore Hole Logs

Auger hole 1

Depth (ft)	Texture (USDA)	Munsell color (dry)
2	sil	10-YR 3/3
4	sil	7.5-YR 5/3
6	sil	7.5-YR 5/4 to 7.5-YR 5/6
8	sicl	7.5-YR 5/6

Auger hole 2

Depth (ft)	Texture	Munsell color (dry)
2	l	10-YR 3/4
4	l	10-YR 4/4
6	l	10-YR 4/4
8	sicl	7.5-YR 6/4 to 7.5-YR 6/6
10	scl	7.5-YR 6/4 to 7.5-YR 6/6
12	scl	7.5-YR 6/4 to 7.5-YR 6/6
14	scl	7.5-YR 6/4

Auger hole 3

Depth (ft)	Texture	Munsell color (dry)
1	ls	10-YR 3/3
2	ls	10-YR 3/3
3	ls	10-YR 3/3
4	s	7.5-YR 5/3
5	s	7.5-YR 5/3
6	s	7.5-YR 6/4
7	scl	7.5-YR 6/6 and 5-YR 5/6
8	scl	5-YR 5/6

Auger hole 4

Depth (ft)	Texture	Munsell color (dry)
1	si	10-YR 4/4
2	sil	10-YR 4/4
3	sil	10-YR 4/6
4	sicl	5-YR 6/5
5	sicl	2.5-YR 6/5
6	sic	2.5-YR 5/6
7	sic	2.5-YR 5/6
8	sic	2.5-YR 5/6
9	sic	5-YR 5/6
10	sic	5-YR 5/6
11	sic	5-YR 5/6
12	sc	5-YR 5/6
13	sc	2.5-YR 5/6
14	sc	2.5-YR 5/6
15	sc	2.5-YR 5/6
16	sc	2.5-YR 5/6
17	sc	5-YR 5/6
18	sc	2.5-YR 5/6
19	sc	2.5-YR 5/6
20	sl	2.5-YR 5/6
21	sic	2.5-YR 5/6

Auger hole 5

Depth (ft)	Texture	Munsell color (dry)
1	ls	10-YR 3/3
2	ls	10-YR 3/3
4	s	7.5-YR 6/4
5	s	7.5-YR 6/4
6	s	5-YR 6/4

Auger hole 6

Depth (ft)	Texture	Munsell color (dry)
0	ls	10-YR 4/3
2	ls	10-YR 4/4
4	sl	10-YR 6/4
6	scl	5-YR 5/6
7	scl	5-YR 5/6
8	sc	5-YR 5/6
9	sc	5-YR 5/6
10	sc	5-YR 5/6
11	sc	5-YR 5/6
12	sc	5-YR 5/6

Auger hole 7

Depth (ft)	Texture	Munsell color (dry)
2	scl	7.5-YR 5/6
3	s	7.5-YR 7/6
4	si	15-YR 7/4
5	sil	15-YR 7/5
6	si	15-YR 6/4
9	si	15-YR 7/3
12	sil	15-YR 7/4
15	scl	7.5-YR 7/4

Bore hole 3

Depth (ft)	Texture	Munsell color (dry)
0	l	10-YR 5/2
1	sl	7.5-YR 6/3
2	sil	7.5-YR 6/4
3	sil	7.5-YR 6/4
4	sl	10-YR 6/4
5	sl	10-YR 6/4
8	sil	10-YR 7/4
10	sil	10-YR 7/3
12	si	2.5-Y 7/3
14	sicl	2.5-Y 6/2
20	scl	5-Y 6/2
22	sicl	5-Y 7/3
24	sicl	5-Y 7/3

Bore hole 4

Depth (ft)	Texture	Munsell color (dry)
1	l	10-YR 4/3
4	sil	10-YR 6/4
6	sil	10-YR 7/3
8	sl	2.5-Y 7/3
10	sl	10-YR 7/4
12	sl	10-YR 6/4
14	sl	10-YR 7/4
16	sil	10-YR 7/4
18	sil	7.5-YR 7/4
20	sil	10-YR 7/4
22	sil	10-YR 6/4
24	sl	2.5-Y 7/3
26	sl	10-YR 7/3

Appendix C

Indian Creek Core Logs

CORE 1

LOCATION Indian Creek alluvial plain

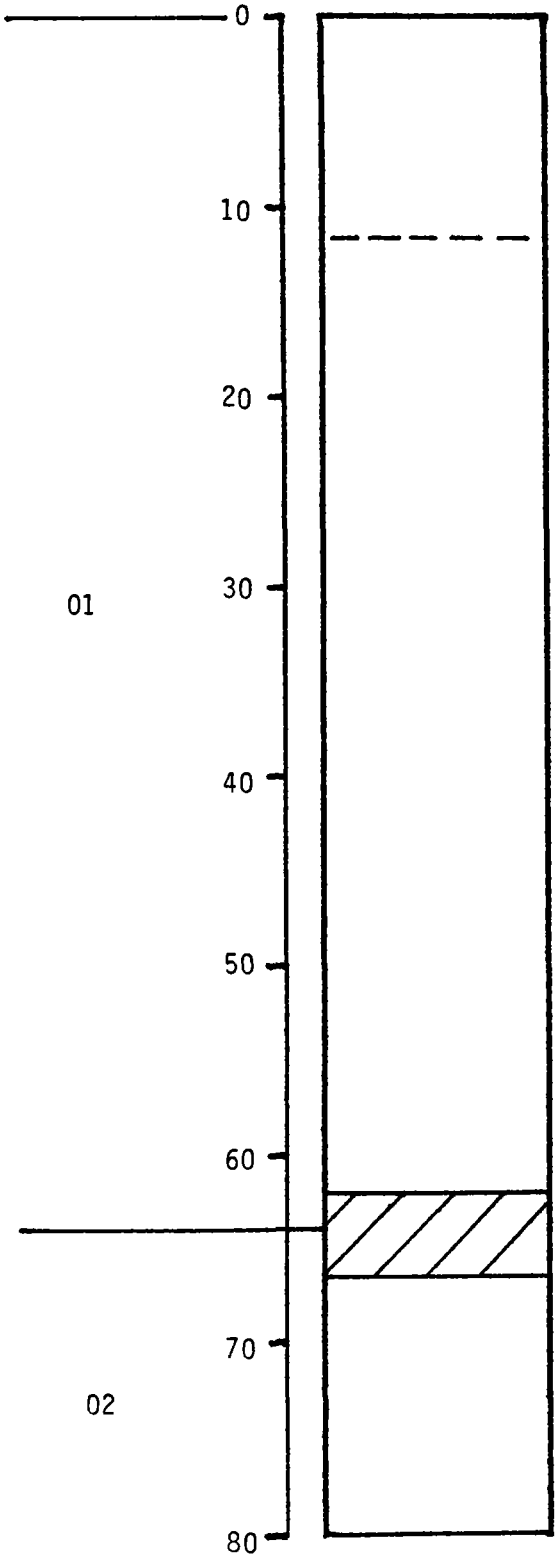

Texture	Structure	Moist Color	HCl reaction	Boundary thickness (cm)
sil	5,1,Sb many roots	10YR2/1.5	1	
				5
sil	3,3, Sb rare roots	10YR2/2	2	
			2	
				10
Sluff				
sil		10YR3/1	3	
			3	0.3

Descriptions follow Soil Survey Staff (1975).

CORE 1

LOCATION Indian Creek alluvial plain

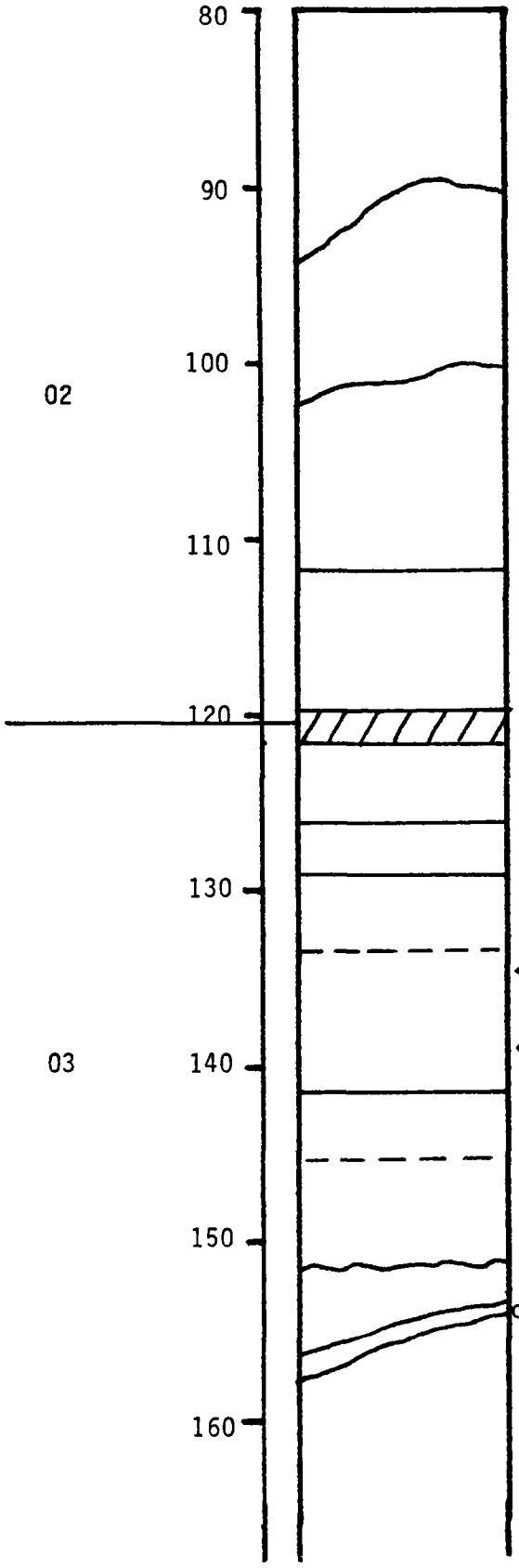

Core segment	Depth (cm)	Texture	Structure	Color	HCl reaction	Boundary thickness (cm)
						0.3
		sicl		10YR5/1	2	
						1
		sil	rare mottles 1 mm thick 10YR4/6	10YR7/2	3	
						broken 1.5
02			common 1 mm thick horz mottles			
		sl (vfs)	10YR7/2	10YR5/1.5	2	
			1 mm black horz streaks			
						0.1
		sl(fs)	mottles as above	10YR5/2	3-4	
		Sluff				
		sl(f)		10YR to 2.5Y6/3	2	
		sil(vfs)		2.5Y5/1	1	0.1
						0.2
		sl(fs)	rare 10YR7/2 streaks	2.5Y5/2	2	
						3
		sandy gravel max=1.5cm	rare streaks shell bed	2.5Y5/2	3	
03						0.3
		sil		2.5Y4/1	1	
						2
		sandy gravel	rare streaks	2.5Y5/1	1	
						0.2
		sil clsi	2.5Y3/1 streaks	2.5Y4/1	2	
						0.1
		cl		2.5Y5/1	1	

Descriptions follow Soil Survey Staff (1975).

CORE 1

LOCATION Indian Creek alluvial plain

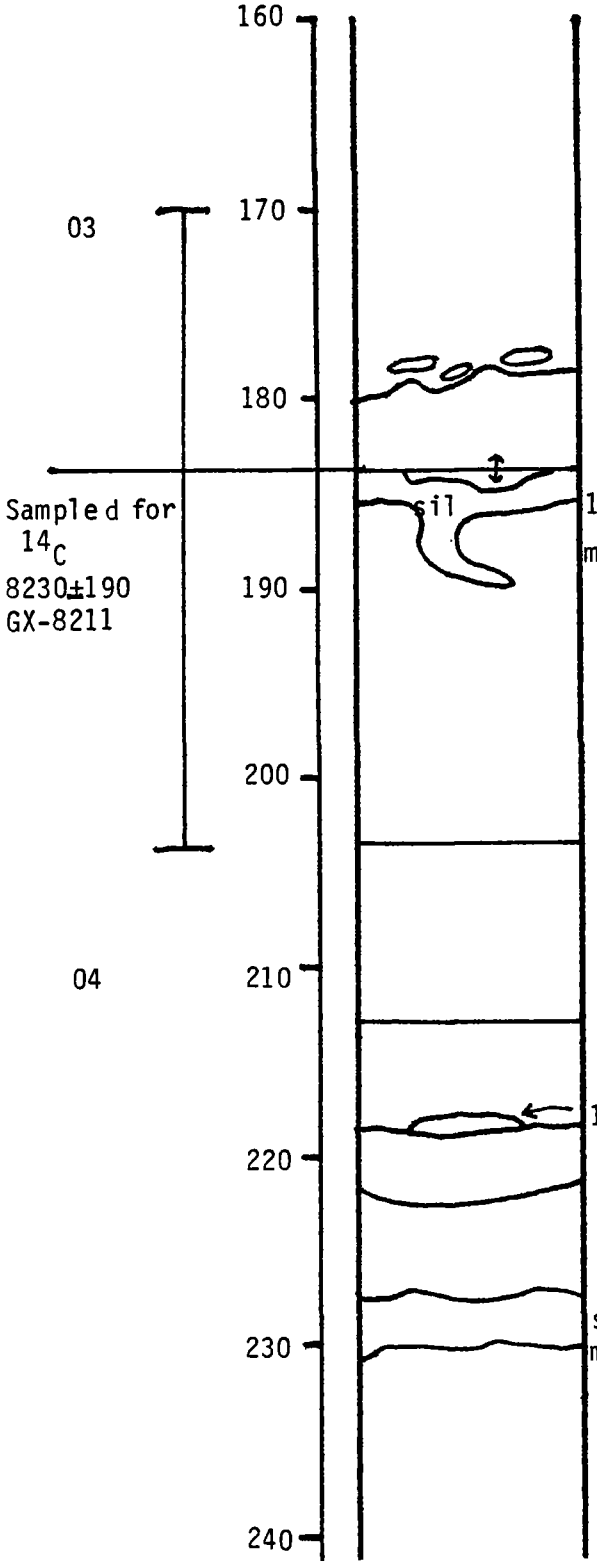

Core segment	Depth (cm)	Texture	Structure	Color	HCl reaction	Boundary thickness (cm)
			rare 1 mm 10YR7/2 streaks			
		cl		2.5Y5/1	1	
03	170		rare 10YR2/2 streaks			
				10YR3/2		1
	180	l	root holes & modern roots	10YR5/2 10YR1.7/1 2.5Y5/1	2	
		sil		10YR3/2		
			modern root hole			
	190	csi	rare 10YR2/2 root mottles rare 1 mm 10YR2/2 streaks	2.5Y5/1	1	
	200					0.2
		sil(vfs)		2.5Y4/1	2	
04	210					1
		sl(fs)		2.5Y4/1&3/1	2	
				10YR4/2		0.3
	220	l(vfs)		2.5Y4/1&3/1	2	0.1
		csi		2.5Y6/1	2	0.5
		sandy gravel max=2cm	3 mm black beds	2.5Y3/1to5/1	3	0.2
	230	sandy gravel	rare black streaks brown plant frags	2.5Y3/1		
	240					

Descriptions follow Soil Survey Staff (1975).

CORE 1

LOCATION Indian Creek alluvial plain

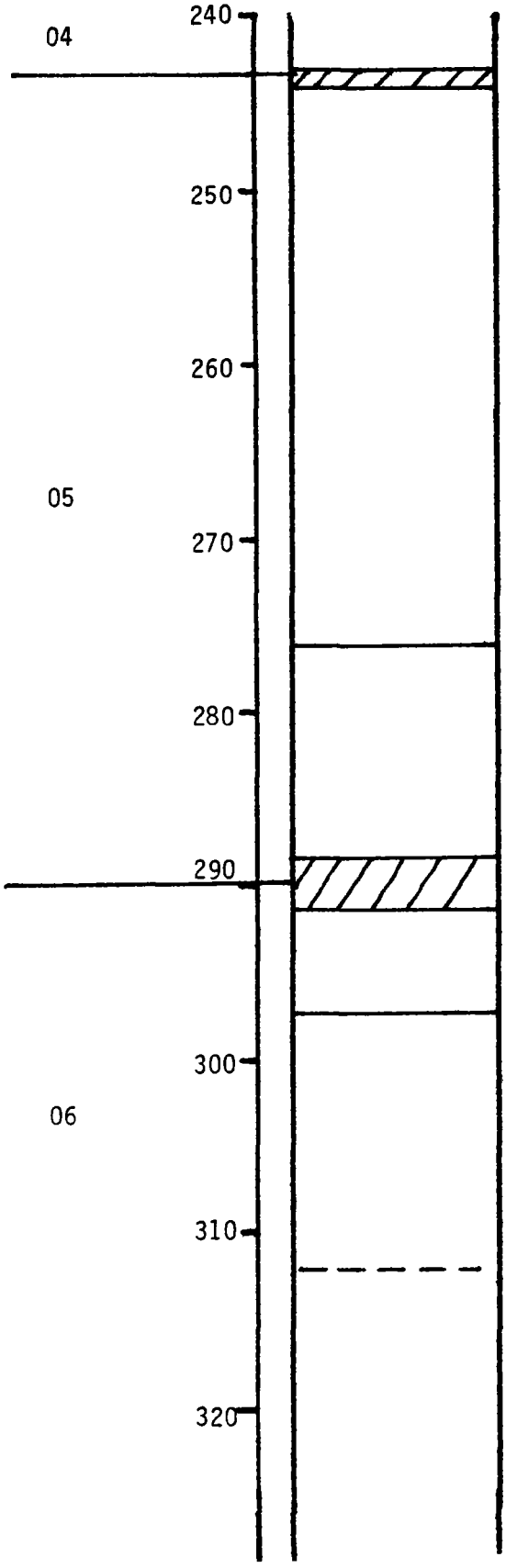

Core segment	Depth (cm)	Texture	Structure	Color	HCl reaction	Boundary thickness (cm)
04	240	sandy gravel	↑ gravels mostly subang and subrnd but some ang and rnd ↓ very rare mottles			
	250	sandy gravel		2.5Y4/1	2	
	260		some roots and plant frags			
05	270					0.5
	280	sl(f-ms)	horizontally bedded	2.5Y4/1	2	
	290	Sluff				
		sl	disturbed bedding	2.5Y4/1	2	1
	300	gravelly sand max=5mm		2.5Y4/1	2	
06	310					2
		gravel max=2cm		2.5Y4/1		
	320					

Descriptions follow Soil Survey Staff (1975).

CORE 1

LOCATION Indian Creek alluvial plain

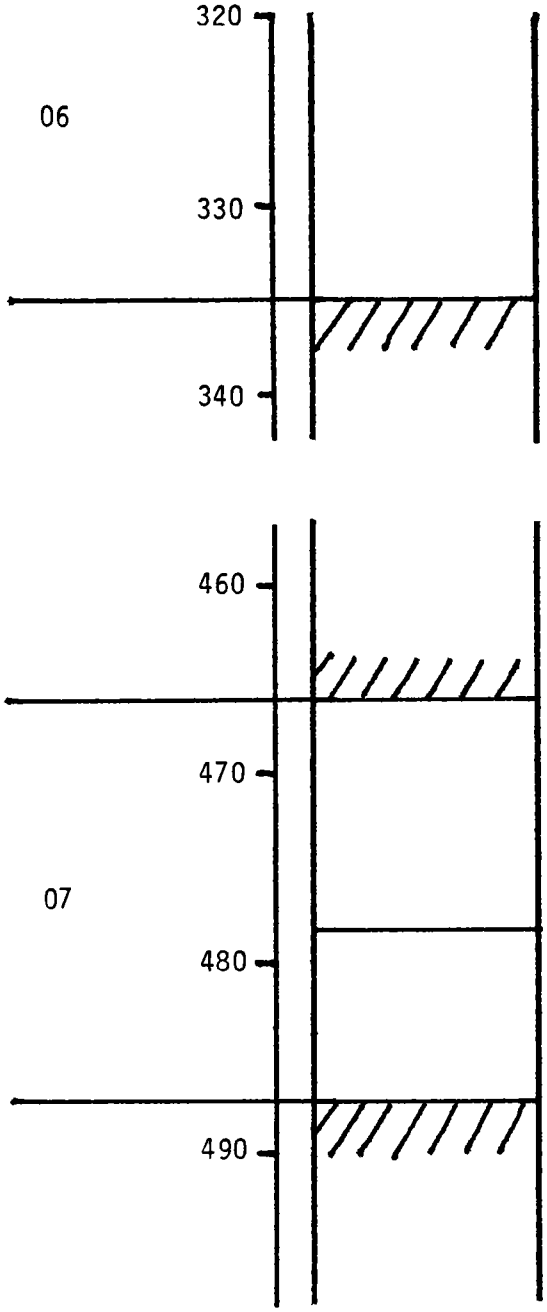

Core segment	Depth (cm)	Texture	Structure	Color	HCl reaction	Boundary thickness (cm)
06	320–330	gravel max=2cm		2.5Y4/1	2	
	330–340	Coarse gravel - No recovery				
	460–470	Coarse gravel - No recovery				
07	470–480	s(f-m)	somewhat disturbed	2.5Y5/2	2	0.3
	480–490	ls(c) gravelly max=4cm		2.5Y5/3	2	
	490	Coarse gravel - No recovery				

Descriptions follow Soil Survey Staff (1975).

CORE 1

LOCATION Indian Creek alluvial plain

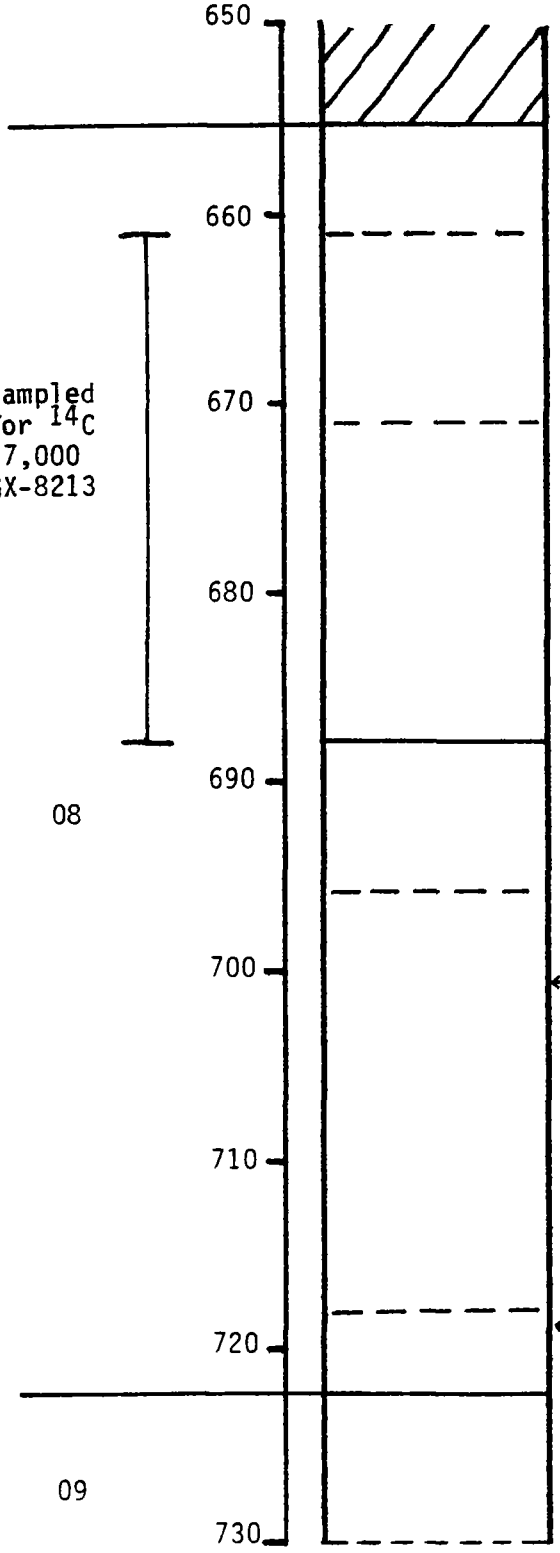

Core segment	Depth (cm)	Texture	Structure	Color	HCl reaction	Boundary thickness (cm)
	650	Coarse gravel - No recovery				
		Med pebbles				
		sil		10YR3/2	2	
	660					1.5
		sil		2.5Y4/2	2	
	670					2
			few black 1 mm flecks and streaks			
		cl		5Y4/1 to 2.5Y5/2	3	
	680					
						0.5
	690	sl(vf)		5Y4/1	3	
08						3
	700	←shell				
		cl	few 1-5 mm oval black mottles 5Y2/2	5Y4/1	2	
	710					
						1
	720	←shell				
		sic		5Y4/1	2	
		sic		5Y5/1	2	
09			patches of 2.5Y5/2			2
	730					

Descriptions follow Soil Survey Staff (1975).

CORE 1

LOCATION Indian Creek alluvial plain

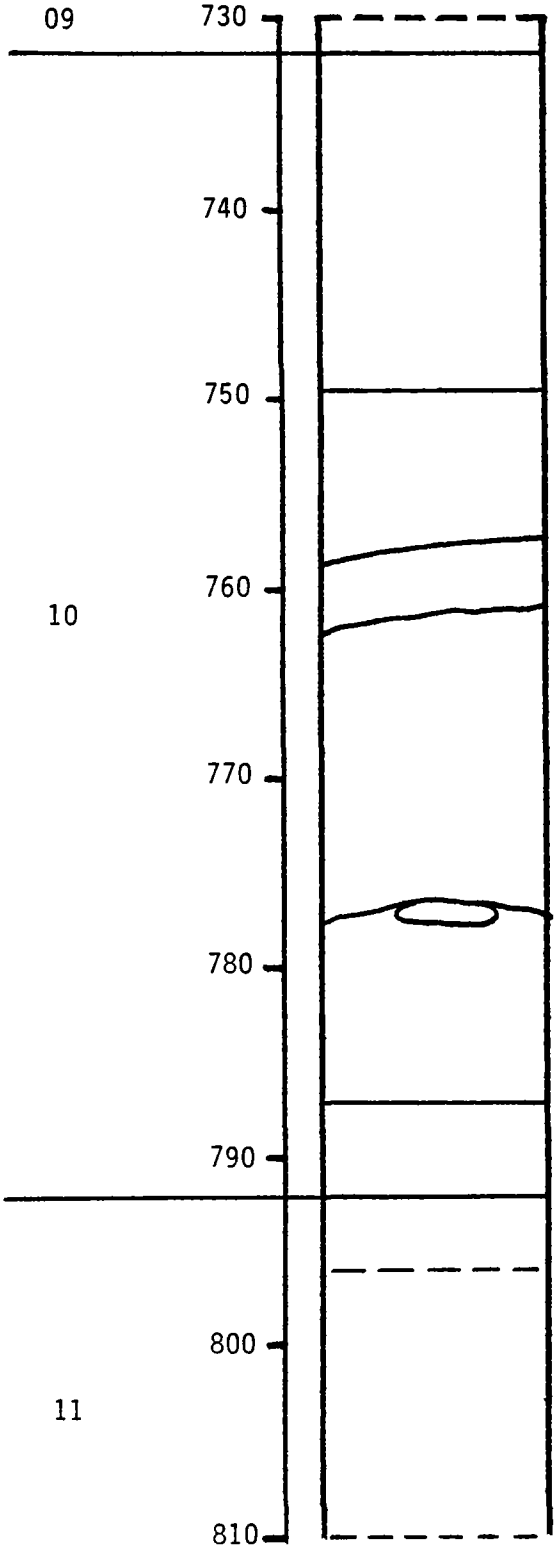

Core segment	Depth (cm)	Texture	Structure	Color	HCl reaction	Boundary thickness (cm)
09	730	cl		2.5Y5/2		
			zones of 5Y5/1			
	740	cl	rare 1 mm black flecks	2.5Y5/2 to 5Y5/2	2	
						1
	750	cl	few 1-3 mm mottles 2.5Y3/1	2.5Y4/2	2	
						0.5
		sil	3 mm beds	10YR5/2	1	
	760		10YR4/3			0.2
10						
		sl(vf)		10YR5/3	1	
	770		1-3 mm beds 10YR5/6 mottles in beds 2.5YR3/4			
		pebble				0.2
	780		upper 3 cm mottled 2.5YR3/4			
		sandy gravel max=3cm		10YR5/2	2	
						0.5
	790	fine gravelly sand		10YR5/2	2	
		fine gravelly sand				2
	800	gravelly sand max=3cm		10YR5/3	2	
11						
	810					2

Descriptions follow Soil Survey Staff (1975).

CORE 1

LOCATION Indian Creek alluvial plain

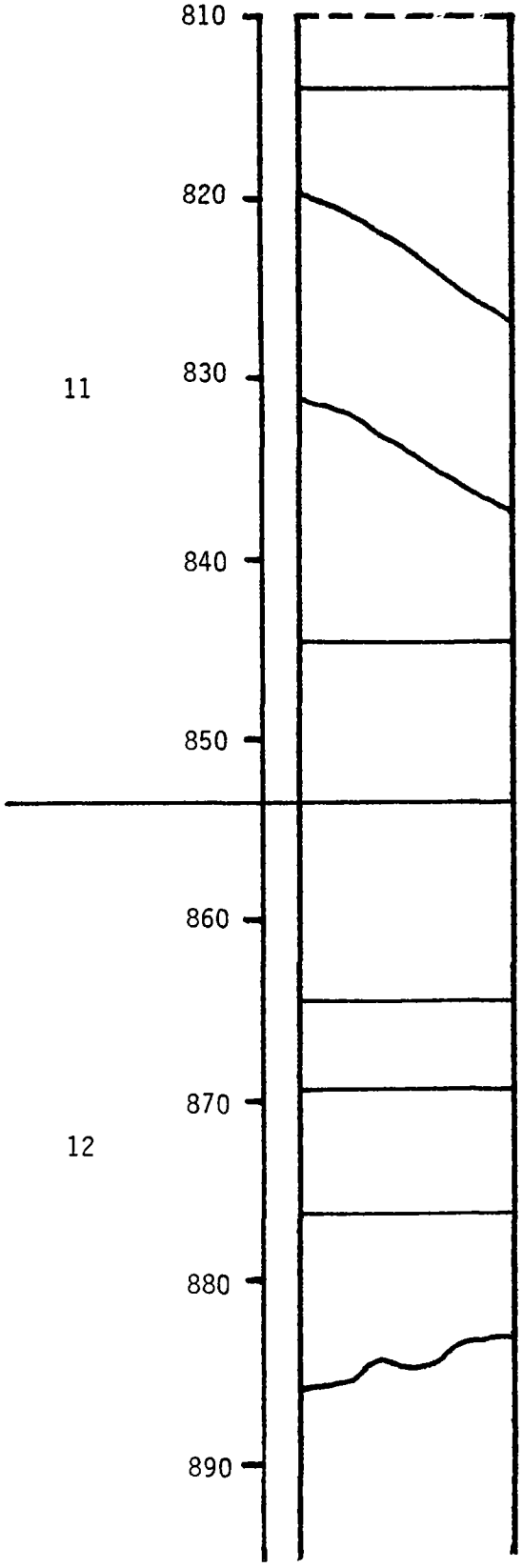

Core segment	Depth (cm)	Texture	Structure	Color	HCl reaction	Boundary thickness (cm)
						2
		ls(co)		10YR5/2	2	1
		sandy gravel max=1.5cm		10YR5/3	2	0.3
11	830	sl	mottles 2-4 mmm beds 10YR5/6 and 5YR3/7	10YR5/2	2	0.2
	840	sandy gravel	rare Mn? stain on clasts	5YR3/7	2	
	850	ls(f-m)	few 1-3 mm mottles 5YR3/7	2.5Y5/2		
		gravelly sand	rare mottles 5YR3/7	10YR5/3	2	
	860	ls(vf-f)	minor 7.5YR5/8 stains	2.5Y6/2	1	0.2
	870	sl(f-co)		10YR5/2		0.2
12		fine gravelly sand	5YR3/7 mottles	2.5Y6/3	2	0.1
	880	gravelly clay max=2cm	common 1-3 mm mottles 5YR3/7	5GY5/1	2	0.3
	890					

Descriptions follow Soil Survey Staff (1975).

CORE 1

LOCATION Indian Creek alluvial plain

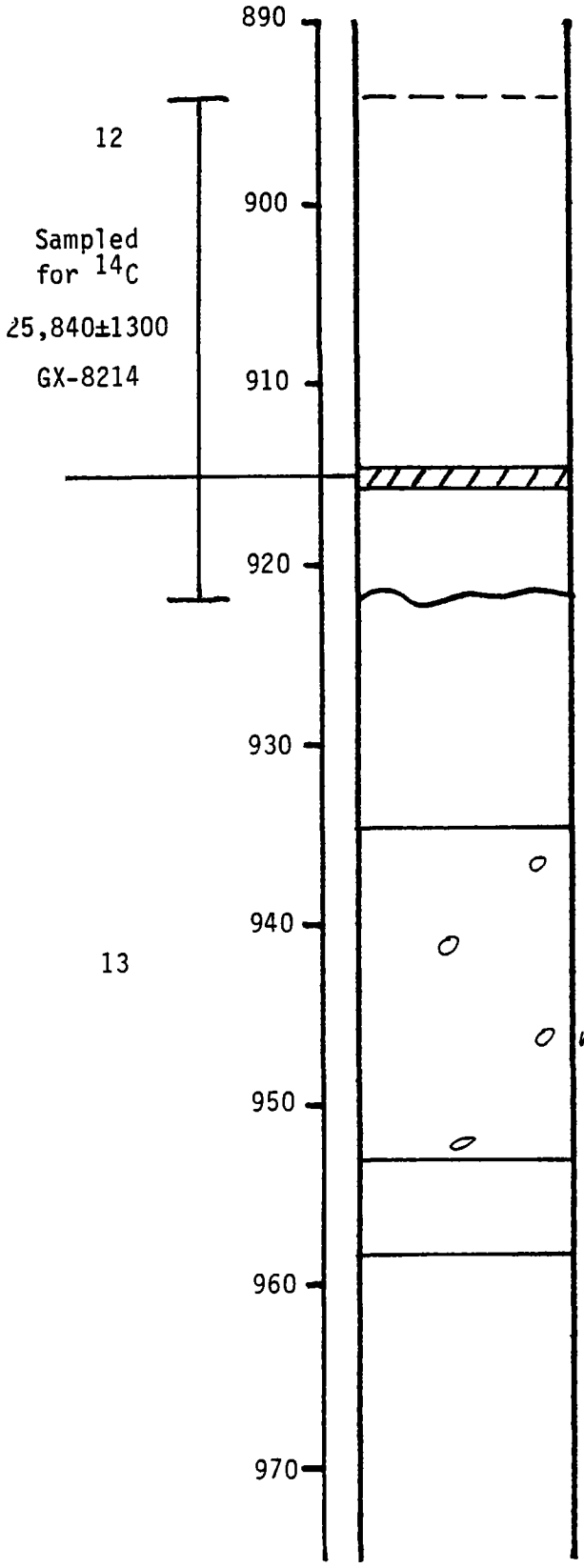

Core segment	Depth (cm)	Texture	Structure	Color	HCl reaction	Boundary thickness (cm)
	890					2
12		sic	rare 10YR1/1 1-3 mm decomposed roots	10Y6/1	1	
Sampled for ^{14}C 25,840±1300 GX-8214	900					
	910	sic		10Y6/1	1	
	920					0.1
		ls(f-m)	rare pebbles to 2 cm	2.5Y5/3	2	
	930					1
13	940	ls(f-m)	0.5-1 cm 7.5Y4/7 mottles	10YR5/3-6/3	2	
	950	c	rare 1-3 mm black mottles	2.5GY6/1	1	0.1
						<0.1
	960	cl	1 mm black streaks	2.5Y6/1	2	
	970					

Descriptions follow Soil Survey Staff (1975).

CORE 1

LOCATION Indian Creek alluvial plain

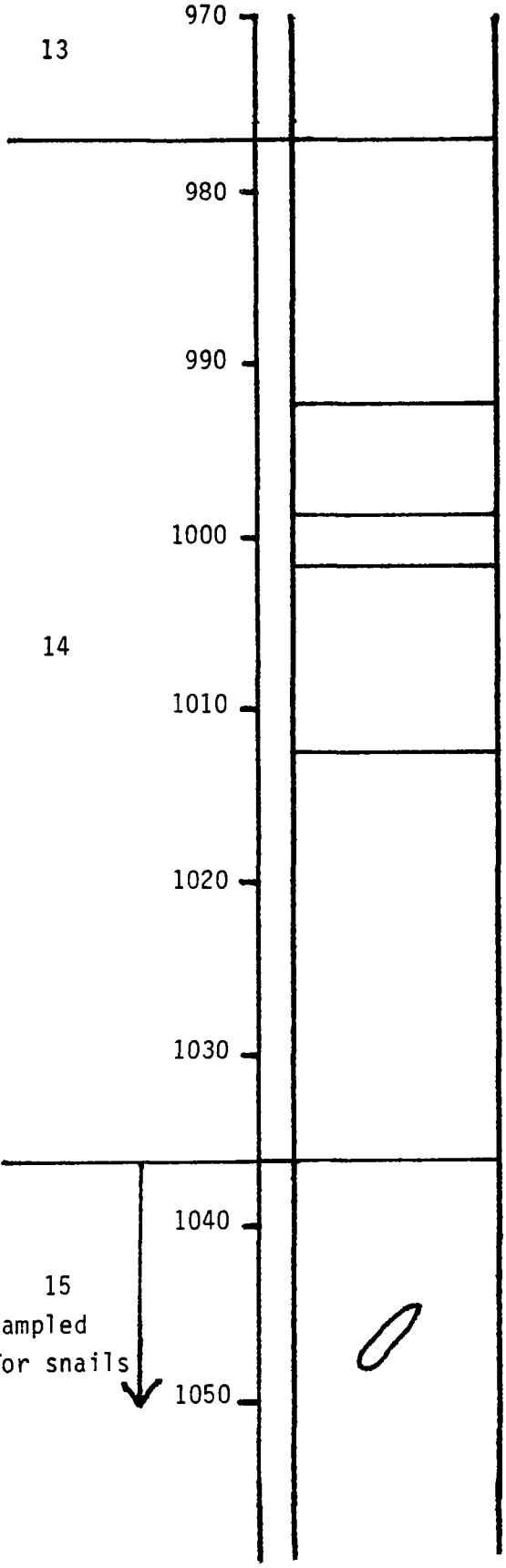

Core segment	Depth (cm)	Texture	Structure	Color	HCl reaction	Boundary thickness (cm)
13	970	sic		2.5Y5/2	1	
						1
	980	sic		2.5Y4/1	1	
	990					1
		sic		2.5Y5/1	1	
						1
	1000	20% black	streaks	2.5Y5/2	1	
						1
14		sic				
	1010					0.1
			5-10% 1 mm black streaks and blotches, concentrated in beds in upper ½			
	1020	sic		2.5Y5/1	1	
	1030					
	1040	sic		2.5Y5/1	1	
15 Sampled for snails	1050	pebble				

Descriptions follow Soil Survey Staff (1975).

CORE 1

LOCATION Indian Creek alluvial plain

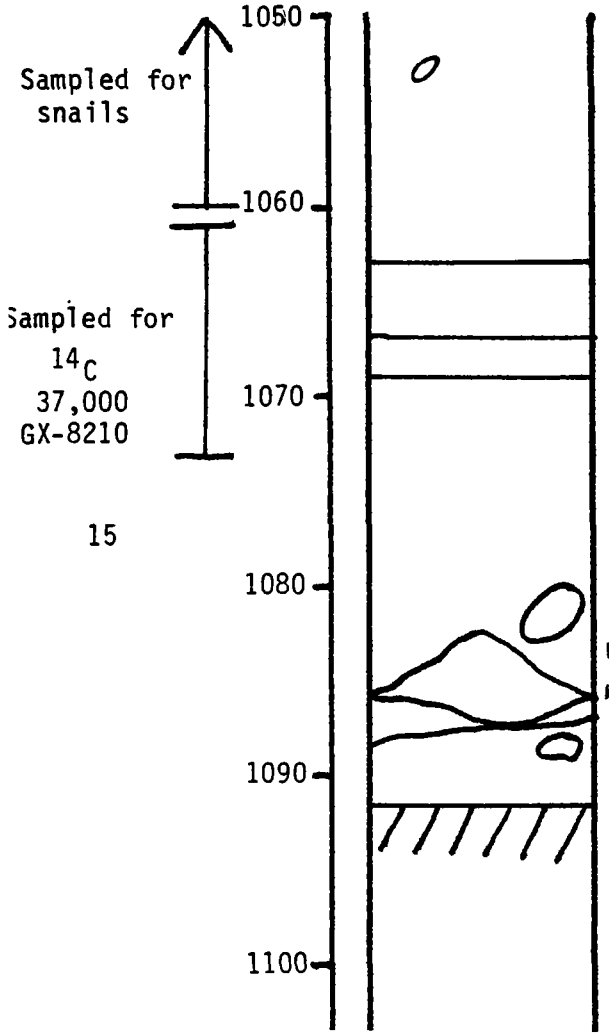

Texture	Structure	Color	HCl reaction	Boundary thickness (cm)
pebble				
sic		2.5Y5/1	1	
				0.1
fiberous clayey peat		2.5Y3/1-2/1	1	
				0.1
cl				0.1
gravelly sand		2.5Y3/2-4/1	2	
pebbles				
gravelly sand	some mottled beds 5YR3/8 to 2.5Y6/8	2.5Y6/3	2	0.1
Coarse gravel - No recovery				

Descriptions follow Soil Survey Staff (1975).

CORE 2

LOCATION Indian Creek alluvial plain

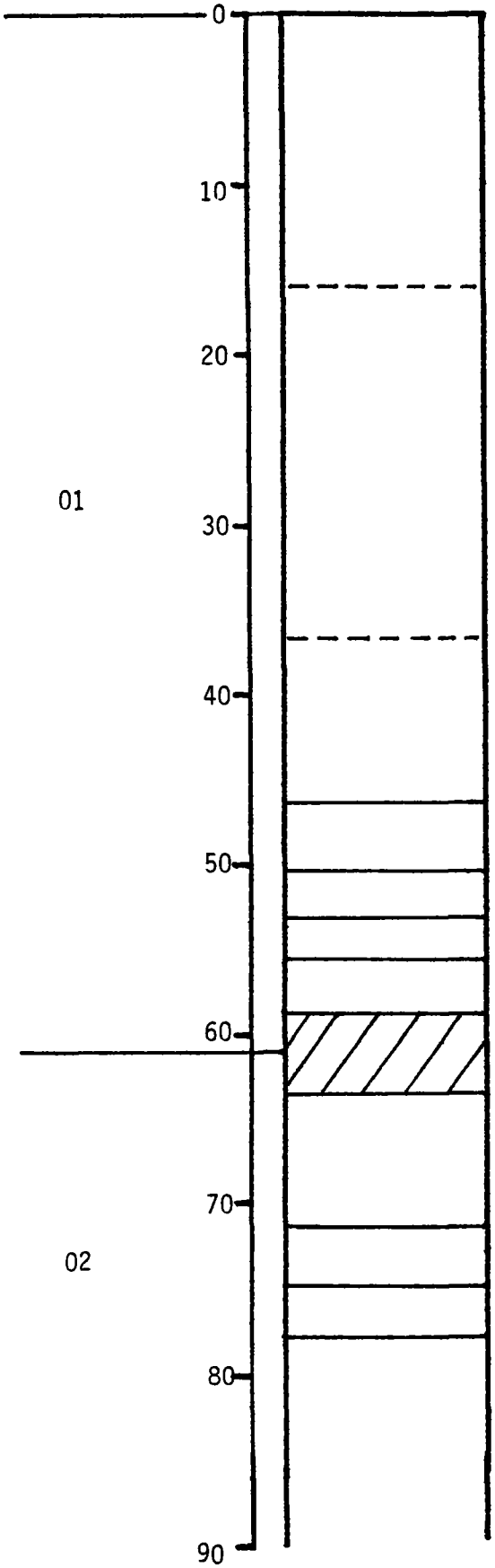

Texture	Structure	Moist Color	HCl reaction		Boundary thickness (cm)
sil	granular	7.5YR2/2	3		
	medium-sized roots				4
sl		10YR2/3	3		
					2
ls(vf-f)	large roots	10YR4/2	2		
					0.2
l		10YR4/2	1		0.1
ls(f)		2.5YR5/3	2	5mm	ottles 5YR4/6
sl(vf)		10YR4/2	2		0.2
ls(f)		2.5YR5/2	3		0.2
Sluff					
sl(f)		2.5Y5/2	3		
					0.5
sl(vf)		10YR4/2	2		
					0.5
sl(f)		2.5Y5/2	3		
					0.3
sl		2.5Y5/1	3		

Descriptions follow Soil Survey Staff (1975).

CORE 2

LOCATION Indian Creek Alluvial plain

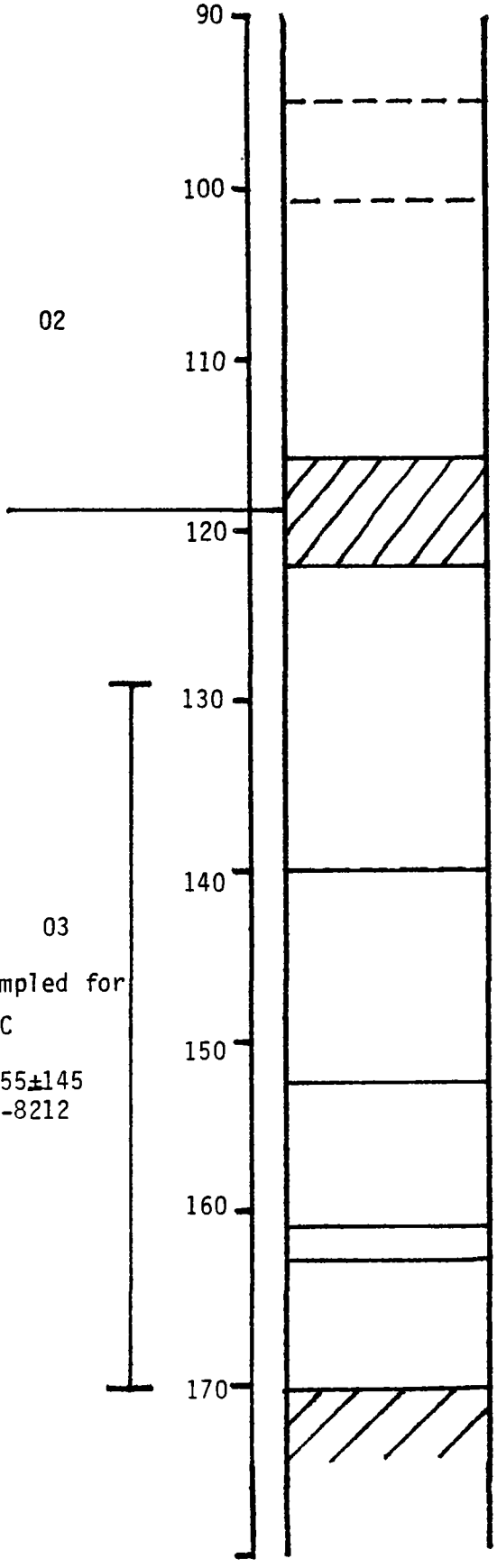

Core segment	Depth (cm)	Texture	Structure	Moist Color	HCl reaction	Boundary thickness (cm)
	90	fine gravelly sl		2.5Y5/1	3	
		max clast=1cm				1
		ls	stains on clasts 7.5YR3/7	2.5Y5/1	3	
	100					1
02		ls		2.5Y4/1	3	
	110	max clast=2cm				
	120	Sluff				
	130	gravelly coarse s		2.5Y4/1	3	
		max clast=1.5cm				
	140					0.5
03		sl(f)		2.5Y4/1	3	
Sampled for ^{14}C 2955±145 GX-8212	150					0.2
		ls(f)	← shell sample	2.5Y4/1	3	
	160					0.3
		l		10YR2/2	2	0.2
		sandy gravel max=1cm		2.5Y4/1	3	
	170	Coarse gravel - No recovery				
		Bedrock at 2.6 m				

Descriptions follow Soil Survey Staff (1975).

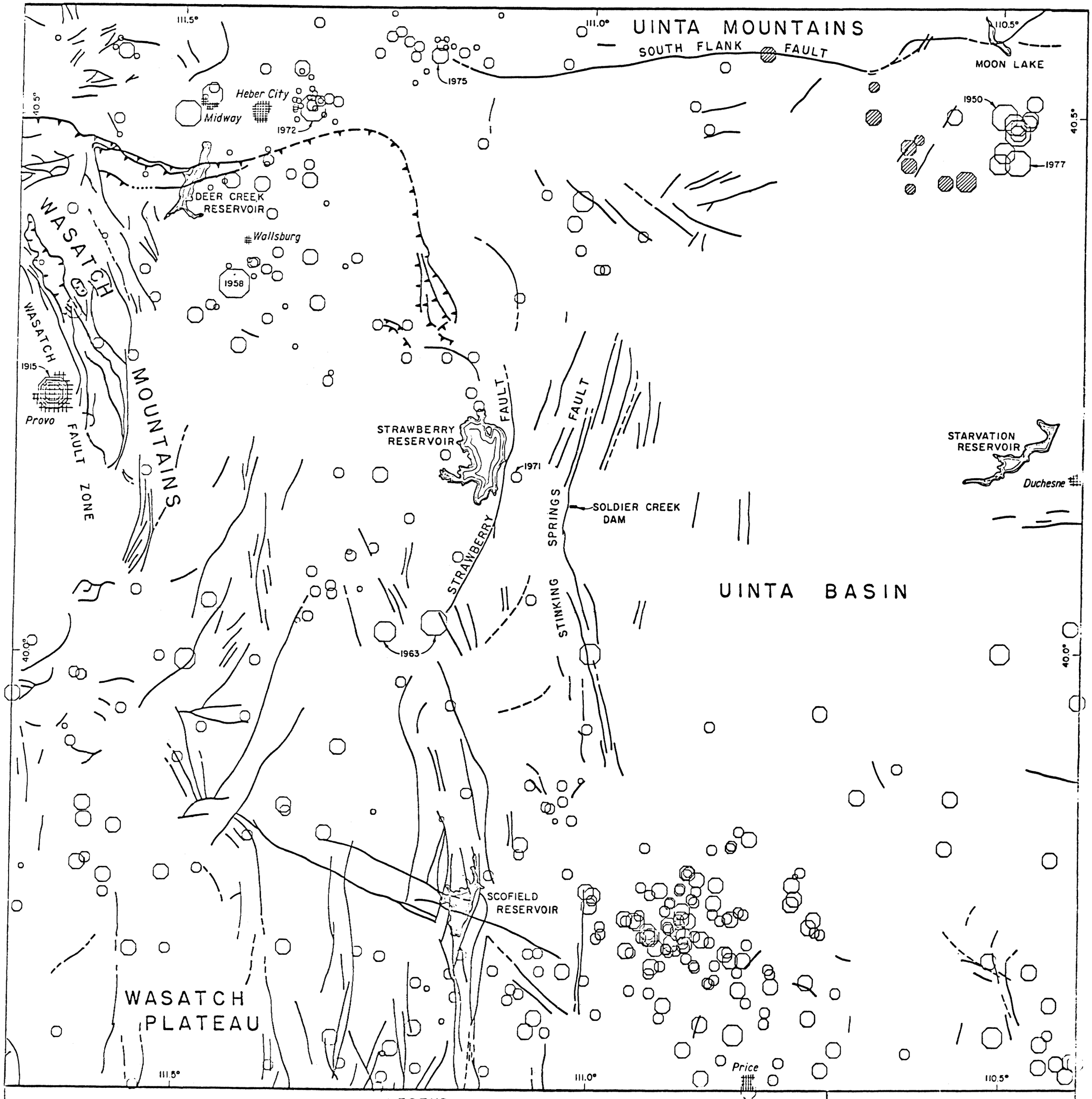

LEGEND

EARTHQUAKE MAGNITUDE SCALE (M_L)

<1.0 | 1.0–1.9 | 2.0–2.9 | 3.0–3.9 | 4.0–4.9 | 5.0–5.9

SCALE = 1:250,000

5 0 5 10 15 Km

TRANSVERSE MERCATOR PROJECTION

Faults-dashed where approximately located

Earthquake epicenter

Presumed mislocated aftershocks of the 9/30/77 earthquake

SOLDIER CREEK SEISMOTECTONIC STUDY

HISTORICAL SEISMICITY (1850-1981) AND FAULT MAP OF THE STRAWBERRY VALLEY REGION

PLATE 1

111° W

ASHLEY NATIONAL FOREST

40° N

AREA OF FIGURE 414

AREA OF FIGURE 415

CURRANT CREEK DAM

SOLDIER CREEK DAM

STRAWBERRY FAULT

STINKING SPRINGS FAULT

CO-OP CREEK TRENCHES

INDIAN CREEK CORE SITE

FIFTH WATER DAMSITE (PROP.)

THE NARROWS

TWIN PEAKS

TABBY MOUNTAIN

GRAY WOLF MOUNTAIN

CEDAR MOUNTAIN

RASPBERRY KNOLL

BIG DRY HOLLOW

LAYOUT CANYON

BIG HORN KNOLL

SOLDIER CREEK

CURRANT CREEK

STRAWBERRY RES.

DUCHESNE COUNTY

WASATCH COUNTY

EXPLANATION

- Previously mapped faults, good field evidence
- Previously mapped faults, limited or ambiguous evidence
- Previously mapped faults, inferred
- Additional faults, good field evidence
- Additional probable faults, limited field evidence
- Overthrust faults, hachures on overthrust sheet
- Pipeline - proposed and existing
- A — Faults and pediments referred to in text

SCALE 1:125,000

0 2 4 6 8 10 12 KILOMETERS

CONTOUR INTERVAL 200 FEET

Base maps 1:250,000 USGS 2° maps, Salt Lake City, Utah; and Price, Utah.

Area to be covered by proposed reservoirs

SOLDIER CREEK DAM

SEISMIC HAZARD EVALUATION

FAULT MAP OF STRAWBERRY RESERVOIR AREA

PLATE 2

UNIT DESCRIPTIONS

ALLUVIAL FAN DEPOSITS

1 Fine gravelly alluvial facies-orange (2.5 YR 6/7)
- 1a Well-stratified sandy loam
- 1b Sandy loam
- 1c Bouldery loamy sand

2 Gravelly debris flow facies-bright brown (2.5 YR 5/7)
- 2a Loamy sand
- 2b Bouldery loamy sand
- 2c Loamy sand

3 Cobbly alluvial facies-orange (2.5 YR 6/7)
- 3a Sandy gravel
- 3b Gravelly sandy loam
- 3c Loamy sand

4 Coarse gravelly alluvial facies-orange (2.5 YR 6/7) loamy sand

5 Bouldery debris flow facies-carbonate-rich orange (2.5 YR 6/7) loamy sand

6 Gravelly alluvial facies-dull orange (5 YR 6/4) well-stratified loamy sand

7 Cobbly debris flow facies-bright brown (2.5 YR 5/6) sandy loam
- 7B Argillic B soil horizon-bright brown (2.5 YR 5/8) sandy clay loam
- 7E Elluvial soil horizon-dull orange (5 YR 7/5) sandy loam

UNIT DESCRIPTIONS (Continued)

STREAM – REWORKED COLLUVIUM AND FAN DEPOSITS

8 Well-stratified gravelly facies- orange (2.5 YR 6/8) sandy loam

STREAM – REWORKED ALLUVIUM

10 Gravelly sand facies
- 10a Dull orange (5 YR 7/4) loamy sand
- 10b Dull orange (5 YR 7/4) loose loamy sand
- 10E Elluvial soil horizon-dull orange (7.5 YR 7/4) loamy sand

SCARP-DERIVED COLLUVIUM

9 Proximal gravelly sand facies-dull orange (5 YR 7/4)

11 Proximal sand facies
- 11a Orange (5 YR 6/8) loamy sand with clay mottles
- 11b Dull orange (7.5 YR 7/4) cobbly loamy sand

12 Distal fine-grained facies-dull orange (7.5 YR 6/4) silt loam
- 12B Cambic B soil horizon-dull orange (7.5 YR 6/4) sandy clay loam

13 Graben-fill sandy facies.
- 13a Bright brown (2.5 YR 5/6) cobbly sandy loam
- 13b Orange (2.5 YR 6/7) sandy loam

14 Graben-fill gravelly sand facies-orange (5 YR 7/5) sandy loam

15 Loose cobbly sand facies-dull yellowish brown (10 YR 5/3) loamy sand

NEAR-SURFACE COLLUVIUM

16 Thin slopewash and elluvial horizons on older units-dull orange (5 YR 7/4) to dull orange (7.5 YR 7/3) sandy loam

17 Modern A soil horizon-dark brown (10 YR 3/3) loam

EXPLANATION

- Lithologic and soil horizon contacts, dashed where less distinct or gradational
- Lateral facies changes; dashed where less distinct; width of tongues indicates zone over which facies change
- Inferred contacts covered by shoring
- Buried free-face of fault scarp
- Fault; arrows indicate relative sense of displacement
- B soil horizon
- Tertiary conglomerate

NOTES

n1 Zone that was backfilled immediately after excavation; apparently units 1 and 2, but fault not recognized.
n2 Fault strikes 3°, dips 63°; several imbricated cobbles.
n3 Fault strikes 5°, dips 88°.
n4 Zone that was back-filled immediately after excavation; apparently unit B to base of excavation.
n5 Probable buried free-face of fault scarp.

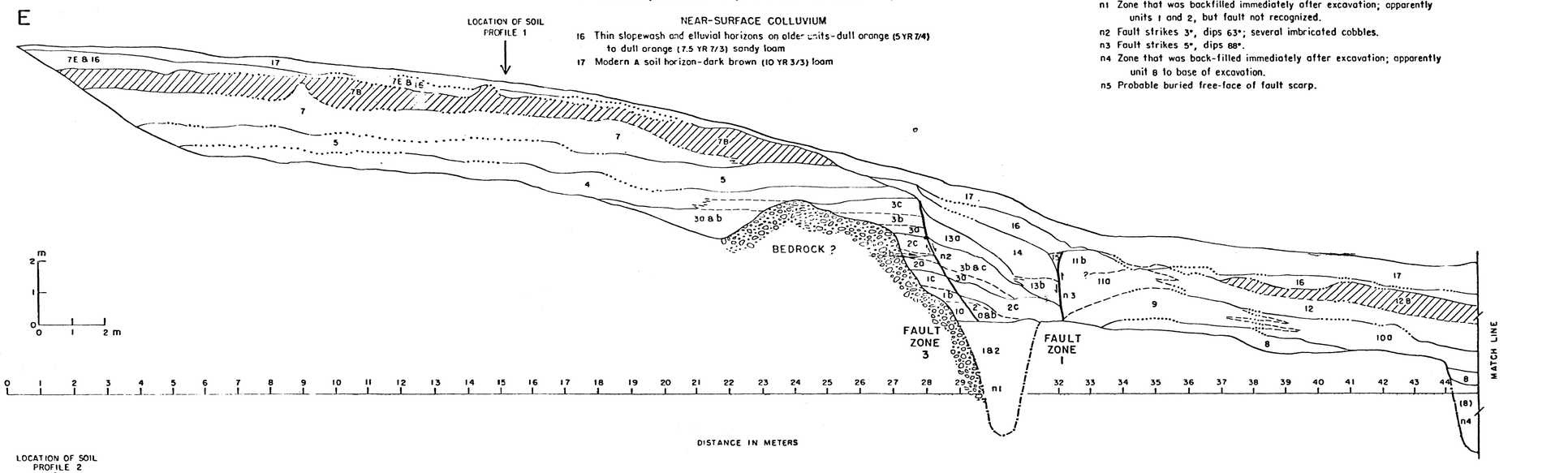

SOLDIER CREEK
SEISMOTECTONIC STUDY

LOG OF CO-OP CREEK
TRENCH 1

PLATE 3

UNIT DESCRIPTIONS

ALLUVIAL FAN DEPOSITS

1 Mudflow facies
- 1a Reddish brown (2.5 YR 4/8) silty clay
- 1b Carbonate-rich silty clay

2 Debris flow facies
- 2a Carbonate-rich clay loam
- 2b Bright brown (2.5 YR 5/6) clay loam
- 2B Argillic B soil horizon-bright brown (2.5 YR 6/8) clay loam
- 2E Elluvial soil horizon-dull orange (5 YR 6/5) sandy loam

SCARP-DERIVED COLLUVIUM

3 Proximal colluvium
- 3a Bright reddish brown (5 YR 5/8) gravelly sandy loam
- 3b Dull orange (5 YR 7/4) gravelly sandy loam
- 3c Orange (7.5 YR 7/5) gravelly loamy sand
- 3d Orange (5 YR 6/6) gravelly sandy loam

4 Distal colluvium-dull orange (5 YR 7/3) sandy loam
- 4B Cambic B soil horizon-dull orange (5 YR 7/4) loam

5 Proximal colluvium-dull orange (5 YR 7/4) loamy sand

NEAR-SURFACE COLLUVIUM

6 Modern A soil horizon-dull brown (7.5 YR 5/4) loam

EXPLANATION

- Lithologic and soil horizon contacts; dashed where less distinct or gradational
- Lateral facies changes; dashed where less distinct; width of tongues indicates zone over which facies change
- Inferred contacts covered by shoring
- Fault; arrows indicate relative sense of displacement
- B soil horizon

NOTES

n1, n2, n3, n4 Location of 3-6 cm diameter infillings of organic-rich sediment. Combined sample from n1, n2, n3 14C dated at 3135 ± 205 yr B.P. (GX-8208).

n5 Location of 5 X 12 cm burrow infilling 14C dated at 2990 ± 650 yr B.P. (GX-8209).

n6 Area disturbed during excavation; dashed line shows original ground surface.

n7 Fault plane strikes 147°, dips 42°-72°.

n8 1cm-thick clay seams show fault drag.

E W

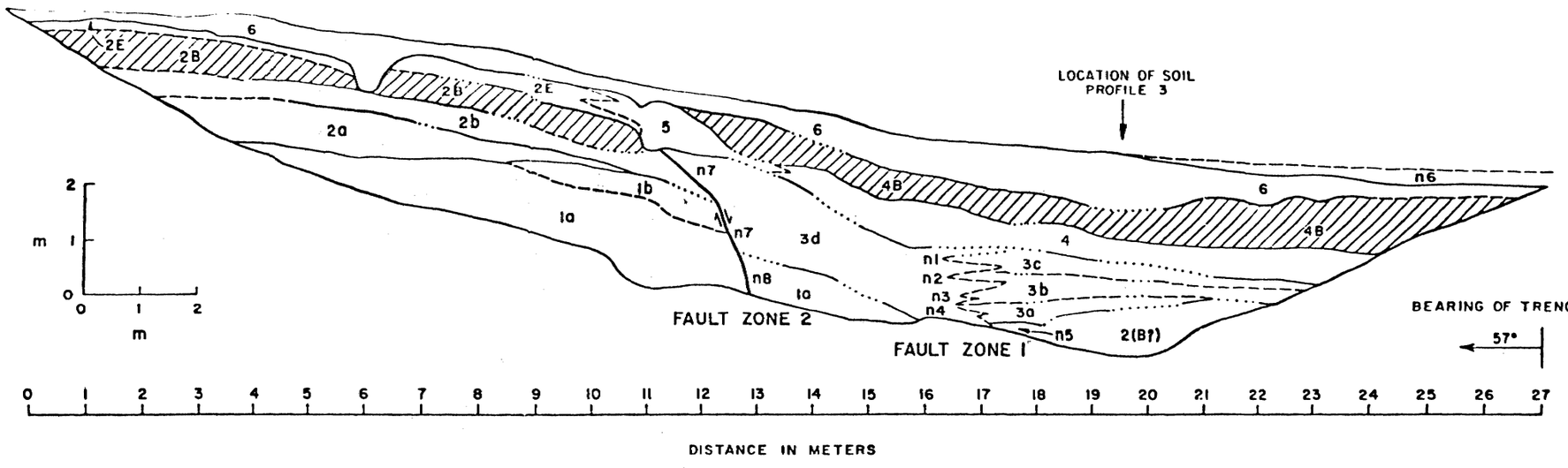

SOLDIER CREEK SEISMOTECTONIC STUDY

LOG OF CO-OP CREEK TRENCH 2

PLATE 4